2018

Assembly and Ecological Function of the Root Microbiome across Angiosperm Plant Species

Connor R. Fitzpatrick, Julia Copeland, Pauline W. Wang, David S. Guttman, Peter M. Kotanen, and Marc T. J. Johnson

Classification: Biological Sciences | Ecology

Assembly and ecological function of the root microbiome across angiosperm plant species

Connor R. Fitzpatrick[1,2], Julia Copeland[3], Pauline W. Wang[3,4], David S. Guttman[3,4], Peter M. Kotanen[1,2] & Marc T. J. Johnson[1,2]

[1]Department of Ecology & Evolutionary Biology, University of Toronto, Toronto, ON, Canada, M5S 3B2
[2]Department of Biology, University of Toronto Mississauga, Mississauga, ON, Canada L5L 1C6
[3]Centre for the Analysis of Genome Evolution & Function, University of Toronto ON, Canada, M5S 3B2
[4]Department of Cell & Systems Biology, University of Toronto, Toronto, ON, Canada, M5S 3B2

Corresponding author:
Connor Fitzpatrick
Department of Biology, University of Toronto Mississauga, Mississauga, ON, Canada L5L 1C6. (1) 416-834-8270. connor.fitzpatrick@mail.utoronto.ca

Keywords: root microbiome | plant-soil feedback | plant drought | host-microbial ecology

Number of pages: 36
Number of figures: 5
Number of references: 68

Abstract:

Across plants and animals, host-associated microbial communities play fundamental roles in host nutrition, development, and immunity. The factors that shape host-microbiome interactions are poorly understood, yet essential for understanding the evolution and ecology of these symbioses. Plant roots assemble two distinct microbial compartments from surrounding soil – the rhizosphere (microbes surrounding roots) and the endosphere (microbes within roots). Root-associated microbes were key for the evolution of land plants and underlie fundamental ecosystem processes. However, it is largely unknown how plant evolution has shaped root microbial communities, and in turn, how these microbes affect plant ecology, such as the ability to mitigate biotic and abiotic stressors. Here we show that variation among 30 angiosperm species, which have diverged for up to 140 million years, affects root bacterial diversity and composition. Greater similarity in root microbiomes between hosts leads to negative effects on plant performance through soil feedback, with specific microbial taxa in the endosphere and rhizosphere potentially affecting competitive interactions among plant species. Drought also shifts the composition of root microbiomes, most notably by increasing the relative abundance of the Actinobacteria. However, this drought response varies across host plant species and host-specific changes in the relative abundance of endosphere *Streptomyces* are associated with host drought tolerance. Our results emphasize the causes of variation in root microbiomes and their ecological importance for plant performance in response to biotic and abiotic stressors.

Significance:

Microbial communities living on and within plants and animals contribute to host function. How host evolution shapes associated microbial communities, and in turn, how these microbes affect the ecology of their hosts is relatively unknown. Here, we demonstrate that evolution occurring across plant species affects root microbial diversity and composition. Greater similarity in root microbiota among host plant species leads to reduced plant performance through negative soil-feedbacks. Additionally, drought shifts the composition of root microbiomes, where changes in the relative abundance of specific bacterial taxa are associated with increased drought tolerance of plants. Our work highlights the potential role of host-associated microbial communities in mediating interactions between hosts and their biotic and abiotic environment.

The discovery that macroscopic organisms host unique assemblages of microorganisms has the potential to transform our understanding of ecology and evolution (1). In plants and animals, associated microbiomes contribute to host nutrition, development, and immunity (2-4), yet how they scale up to influence host ecological function and performance is largely unknown. For example, associated microbiota may alter the interactions between hosts and their environment. Here, we address how host plant evolution over macroevolutionary timescales shapes the assembly of root microbiomes, and in turn, how root microbiota mitigate biotic and abiotic environmental stressors experienced by host plants.

Land plants have formed symbioses with microorganisms since their colonization of terrestrial environments (5). Interactions between plants and microbes continue to benefit plants by increasing the acquisition of nutrients, producing growth hormones, and defending against enemies (6). Root microbiota can also reduce plant performance by competing for limited nutrients and attacking plants as pathogens (7). Recent work (8, 9) shows that plant roots assemble two distinct microbial compartments (i.e., microbiomes) from the pool of soil microbial diversity – the rhizosphere (microbes surrounding roots) and the endosphere (microbes within roots). Root microbiome assembly is a multistep process shaped by both soil type and host differences (6, 10). However, our understanding of how variation among host species shapes endosphere and rhizosphere assembly remains limited (6, 11-13), yet is essential for understanding how root microbiota contribute to the ecology and performance of their hosts.

Plants must contend with numerous environmental stressors throughout their lifetime. Competition between plants for shared resources is an important biotic stressor

87 shaping both ecological and evolutionary outcomes (14, 15). Soil microbes have long
88 been recognized as key components to plant competition (16, 17). For example, plants
89 can indirectly compete with one another through recruitment of soil microbes (18), where
90 microbial recruitment by one plant can feed back to affect the performance of a second
91 plant. Competitive interactions among plant species mediated by these so-called "plant-
92 soil feedbacks" (PSF) are known to affect fundamental terrestrial ecosystem processes
93 such as community assembly and succession, plant invasions, and primary productivity
94 (19-22). The biotic drivers of PSF are not well understood but likely include the
95 recruitment of assemblages of root microbiota across host plant species.
96 Drought represents one of the most important abiotic stressors that plants face in
97 both natural and managed systems, negatively affecting plant growth and productivity
98 worldwide (23-25). Due to their sessile nature, plants must employ a broad repertoire of
99 phenotypic mechanisms to mitigate drought stress including life-history, morphological,
100 physiological, and molecular changes (26, 27). Emerging evidence suggests that soil
101 microbes may play an important yet poorly understood role in plant drought tolerance.
102 For example, soil microbes can intercept hormones in plants leading to a dampened stress
103 response to drought (28, 29), and drought-induced shifts in soil microbial communities
104 can reduce the negative fitness effects of drought (30). Recent work shows that drought
105 also shifts the composition of root microbial communities in numerous grass species (31,
106 32). However, whether variation in the diversity or composition of host plant root
107 microbiota contributes to plant drought tolerance is unknown.
108 Here, we perform a comparative root microbiome study, characterizing the
109 assembly of the endosphere and rhizosphere compartments of the root microbiome across

phylogenetically diverse angiosperm species. We coupled our comparative study with manipulative experiments to understand the ecological function of the root microbiome. Specifically, we investigated how the root microbiome across a diverse set of host plant species mitigates biotic and abiotic stressors (*SI Appendix*, Fig. S1). Our study sought to answer four questions: 1) How do endosphere and rhizosphere microbiomes differ in diversity and composition across 30 phylogenetically diverse host plant species? 2) Does evolutionary divergence among host plant species affect the assembly of the endosphere and rhizosphere microbiome? 3) Does variation in the root microbiome between host plant species affect indirect competitive interactions between plant species via plant-soil feedbacks? 4) Does the root microbiome influence drought tolerance across host plant species? Our results provide some of the first evidence of how evolution over long timescales shapes the root microbiome, and how root microbiota influence plant performance in response to variation in biotic and abiotic components of the environment.

Results

Endosphere and rhizosphere microbiomes differ in diversity and composition across host plant species. We grew 30 plant species that have diverged for up to 140 MYR (Fig. 1*A*, *SI Appendix*, Table S1). Plants were grown from surface-sterile seeds in a live soil inoculum collected from a naturalized field site where all species co-occur (Koffler Scientific Reserve, ON, Canada). We measured a suite of morphological, physiological and performance traits from every plant (N = 10/species, *SI Appendix,* Table S2). After 16 weeks, we partitioned root samples from each plant into endosphere and rhizosphere

compartments (8, 9), extracted total DNA, and characterized the bacterial community by sequencing the V4 region of the 16S rRNA gene using Illumina MiSeq (*SI Appendix*, Fig. S1). We assembled quality-filtered reads into error-corrected amplicon sequence variants (ASVs) using DADA2 v.1.4.0 (33), which represent unique bacterial taxa. We analyzed the effects of host plant species and root compartment on the diversity and composition of bacterial communities, as well as the abundance of individual bacterial taxa.

Across plant species, the rhizosphere exhibited higher diversity and greater evenness in abundance than the endosphere (Simpson's D^{-1} mean ± standard error (SE): rhizosphere, 202 ± 1.8, endosphere, 38 ± 8.2, $F_{1,56} = 64.62$, $P < 0.001$; evenness: rhizosphere, 0.32 ± 0.01, endosphere, 0.13 ± 0.01, $F_{1,56} = 73.89$, $P < 0.001$; Fig. 1*A*, *SI Appendix*, Fig. S2 and Table S3). We quantified microbiome community composition using weighted UniFrac distances with principal coordinates analysis and found clear differences in the composition of endosphere and rhizosphere compartments (*SI Appendix*, Fig. S3 and Table S4). Nearly 90% of bacterial phyla and 55% of bacterial ASVs exhibited significant differential abundance between endosphere and rhizosphere compartments (GLM: $P_{FDR} < 0.05$ after FDR correction, *SI Appendix*, Fig. S4*A*). In the endosphere, Actinobacteria and Bacteroidetes exhibited higher relative abundance, while Acidobacteria were significantly reduced (Fig. 1*B*). Additionally, we found a higher number of ASVs that were unique to the endosphere (65 ASVs), versus those that were only found in the rhizosphere (46 ASVs) or live bulk soil (8 ASVs) (*SI Appendix*, Fig. S5).

Our comparative framework uncovered larger effects of host plant species on endosphere than rhizosphere compartments (Fig. 1*C*, 1*D*, *SI Appendix*, Fig. S6, S7, and

Table S3, S4). Host species varied much more in their endosphere (Simpson's D^{-1} range: 6-87; SE: 8.2) than rhizosphere diversity (range: 111-315; SE: 1.8; Levene's test: $F_{1,58} = 18.55$, $P < 0.001$; Fig. 1*C*, *SI Appendix*, Table S3). Similarly, host plant species explained 40% of the total variation in endosphere composition (PERMANOVA: pseudo-$F_{1,29} = 7.57$, $P < 0.001$), but only 17% in rhizosphere composition (PERMANOVA: pseudo-$F_{1,29} = 1.90$, $P < 0.001$). Consequently, large proportions of bacterial taxa at all taxonomic ranks in the endosphere varied significantly in abundance among host plant species (bacterial phyla: 65%; ASVs: 12%), whereas far fewer taxa in the rhizosphere were affected (bacterial phyla: 19%; ASVs: 1%) (GLM: $P_{FDR} < 0.05$; Fig. S4*D*). Additionally, only a fraction of the responsive bacterial taxa in the endosphere were also influenced by host plant species in the rhizosphere (bacterial phyla: 36%; ASVs: 17%). Several phyla in particular were strongly affected by variation among host plant species, including Proteobacteria, Actinobacteria, and Bacteroidetes (GLM: $P_{FDR} < 0.05$; Fig. 1*D*). Across host plant species, we found little correlation between endosphere and rhizosphere diversity (Simpson's D^{-1}: $r = 0.06$, $P = 0.09$), despite a significant correlation between endosphere and rhizosphere community composition (weighted UniFrac distances: $r_{Mantel} = 0.26$, $P = 0.04$). Finally, we identified 133 endosphere and 334 rhizosphere ASVs found in all host plant species (*SI Appendix*, Dataset S1), suggesting the existence of a prevalent core microbial assemblage despite tremendous variability occurring among host plant species. 59% of these ASVs in the endosphere and 40% in the rhizosphere that make up the core microbiome were found at intermediate (2-3 individuals/host species) or high prevalence (5 individuals/host species).

Evolutionary divergence among host plant species affects the assembly of the endosphere and rhizosphere microbiome. To understand how plant evolution has shaped root microbial communities, we tested whether close relatives share similar endosphere and rhizosphere microbiomes. Microbial diversity in the endosphere (Blomberg's $K = 1.08$, $P = 0.001$), but not the rhizosphere (Blomberg's $K = 0.67$, $P = 0.94$), exhibited significant phylogenetic signal (Fig. 1*C* and *SI Appendix*, Table S6). We used Mantel tests of phylogenetic relatedness versus root microbial community similarity among plant species to understand whether plant evolution shapes the community composition of the root microbiome. Again, endosphere similarity ($r_{Mantel} = 0.15$, $P = 0.004$), but not rhizosphere ($r_{Mantel} = 0.05$, $P = 0.15$), was positively correlated with phylogenetic relatedness between plant species (Fig. 1*D* and *SI Appendix*, Table S7). We used phylogenetic generalized least-squares regression (PGLS) to investigate the relationship between experimentally measured plant traits and root microbial diversity and composition (*SI Appendix*, Table S8). Root microbial diversity was associated with numerous host plant traits, however the importance of individual traits varied between endosphere and rhizosphere compartments (*SI Appendix*, Table S8). Endosphere diversity was positively associated with increasing root hair density, while rhizosphere diversity was positively associated with host plant productivity and negatively associated with root length (PGLS: $P_{FDR} < 0.05$). Endosphere and rhizosphere composition were also associated with numerous plant traits including host plant productivity, physiology, and root architectural traits (*SI Appendix*, Table S8; PGLS: $P_{FDR} < 0.05$).

Variation in the root microbiome between host plant species affects indirect competitive interactions between plant species via plant-soil feedbacks. Using a multi-generation plant-soil feedback experiment, we investigated how patterns of root microbial recruitment among host plant species can feed back to affect competitive interactions (*SI Appendix*, Fig. S1). In the first generation, we grew each of the 30 plant species in a homogenous soil mixture collected from the same field site as our comparative microbiome study. In the second generation, we grew replicate individuals of 5 focal species, representative of our host plant phylogenetic diversity, in bulk and rhizosphere soil collected and preserved from each of the 30 plant species from the previous generation. The net effect of soil conditioning in the first generation on plant performance in the second generation is the plant-soil feedback (PSF). PSF can be caused by modification to both biotic and abiotic soil properties including the alteration of soil bacterial communities as well as the depletion of soil nutrients. We calculated the PSF as: $\log_e$ ((focal species biomass in heterospecific soil)/(focal species biomass in conspecific soil)); positive values indicate that a focal species performed better in soil conditioned by a different species from the focal plant relative to soil conditioned by the same species as the focal plant, whereas negative values indicate the opposite (34). We observed strong positive and negative soil feedback occurring among pairs of plant species.

We sought to understand how root microbiota assembled by different plant species contributes to their experimentally measured PSF (Fig. 2*A*). We correlated the root microbiome similarity (weighted and unweighted UniFrac distances) between host plant species with their PSF measured in our multi-generation experiment. Remarkably, the effect of inoculation with soil conditioned by heterospecific plants depended on the

223 degree of similarity between the root microbiomes assembled by the focal and soil-
224 conditioning plant species. On average, highly dissimilar microbiomes had more positive
225 effects on focal plant growth than highly similar ones (Fig. 2*B*, 2*C*, and *SI Appendix*, Fig.
226 S8). This pattern was consistent for both the endosphere and rhizosphere, though
227 depended on the particular measure of community similarity used.
228 Next, we investigated how specific bacterial taxa contributed to the effect of the
229 root microbiome on PSF. First, we used generalized linear models to calculate the $\log_2$-
230 fold change (i.e. doublings) of each taxon abundance between all pairs of focal and soil-
231 conditioning host plant species (35). We identified bacterial taxa across all taxonomic
232 ranks that exhibited significant differential abundance across host plant species in either
233 the endosphere or rhizosphere (e.g. Fig. 3*A*, 3*B*). We correlated the differential
234 abundance between host plant species of each bacterial taxon with the experimentally
235 measured host plant pairs' PSF (*SI Appendix*, Dataset S2).
236 Numerous bacterial taxa were strongly associated with positive and negative PSF
237 occurring between plant species (hereafter, PSF-related taxa), including a number of
238 endosphere and rhizosphere ASVs found across all host species (representative taxa
239 shown in Fig. 3*C*, 3D; for full list see *SI Appendix*, Dataset S2). Differential abundance of
240 particular ASVs explained up to 15% of the total variation in the measured PSF between
241 host plant species (e.g. Fig. 3*C*, and *SI Appendix*, Dataset S2). Though bacterial phyla
242 such as Proteobacteria, Bacteroidetes, and Actinobacteria are well represented in the list
243 of PSF-related taxa in both the endosphere and rhizosphere, we found little overlap at
244 lower taxonomic ranks (*SI Appendix*, Dataset S2). In general, when the abundance of a
245 bacterial taxon in the focal host species was less than the soil-conditioner host species,

we observed enhanced growth of the focal plant. By contrast, when the abundance of the bacterial taxon was greater in the focal host species than the soil-conditioner plant species, we observed reduced growth of the focal plant (e.g. Fig. 3*D* and *SI Appendix*, Dataset S2: r values < 0, unshaded rows). However, we noticed that for some microbial taxa the association was reversed (e.g. Fig. 3*C* and *SI Appendix*, Dataset S2: r values > 0, blue-shaded rows). Furthermore, of the microbial taxa significantly related to PSF, a greater proportion in the endosphere (35% of taxa) versus the rhizosphere (12% of taxa) exhibited this opposite association (Fig. 3*E,* 3*F*; Fisher's exact test for the difference in proportion: $P = 0.01$; *SI Appendix*, Dataset S2: r values > 0, blue-shaded rows).

The root microbiome is associated with drought tolerance across host plant species. During our comparative root microbiome study we imposed a chronic drought treatment on replicate individuals from each host plant species, which resulted in a 4-fold difference in soil moisture compared to well-watered control plants. We investigated how this abiotic stressor affects the diversity and composition of the root microbiome across 30 host plant species. We also included pots without plants that were filled with the same soil mixture in each watering treatment and identically treated, non-living structures (bamboo toothpicks) that were analogous to plant roots (9). Comparing the bacterial communities in living roots to non-living root analogues allowed us to understand the host-mediated effects of drought on the root microbiome.

Drought reduced microbial diversity in the endosphere and rhizosphere by 15% and 27%, respectively ($F_{1,53} = 5.56$, $P_{FDR} = 0.06$; Fig. 4*A*). Drought also caused large changes in bacterial community composition (Fig. 4*B*, 4*C*, and *SI Appendix*, Table S3).

Surprisingly, the effect of drought was stronger on the endosphere than the rhizosphere microbiome, suggesting large indirect effects of drought through changes in host plant physiology or immune status (26, 27, 36). Consistent with this result, drought caused changes in the relative abundance of 65% of bacterial phyla in the endosphere versus only 43% in the rhizosphere (GLM: $P_{FDR} < 0.05$; *SI Appendix*, Fig. S4*C*). In particular, the abundance of Actinobacteria in the drought endosphere increased over 2-fold, whereas the abundance of Proteobacteria decreased nearly 2.5-fold (GLM: $P_{FDR} < 0.05$; Fig. 4*B* and *SI Appendix*, Fig. S9 and Dataset S3). However, host plants varied in the magnitude of the shift in their endosphere microbiome during drought (drought X host species: $\chi^2 = 7.15$, $P_{FDR} = 0.03$, *SI Appendix*, Table S4), which included the enrichment/depletion of bacteria found in well-watered plants and the recruitment of new taxa into their roots (*SI Appendix*, Fig. S5, S7). The drought-induced changes in the microbiota of living plant roots were distinct from those occurring in the microbiota of root analogues and soil (*SI Appendix*, Fig. S15, Table S9, Dataset S3).

We sought to understand whether drought-induced shifts in the root microbiome were related to drought tolerance across plant species. This question was motivated by the prediction that plastic responses in the root microbiome may maintain host functions and ultimately plant fitness in response to stress (37, 38). We measured drought tolerance as the proportional difference in total biomass between drought and well-watered conditions. On average, plants exhibited a 35% reduction in total biomass in response to drought, however species varied between an 80% reduction to a 127% increase in biomass in response to drought (Fig. 5*A* and *SI Appendix*, Fig. S10). We found no evidence of phylogenetic signal in drought tolerance across the plant phylogeny. Changes

292 in overall root microbiome composition or diversity under drought were not associated
293 with drought tolerance. However, coarse estimates of overall composition have a poor
294 ability to detect the ecological effects of particular bacterial clades or ASVs.
295 To further examine whether the root microbiome affects drought tolerance, we
296 investigated how individual bacterial taxa were related to drought tolerance across plant
297 species. First, for each host plant species, we used generalized linear models to calculate
298 the $\log_2$-fold change of each drought-responsive taxon between watering treatments (35).
299 We identified bacterial taxa at all taxonomic ranks in the endosphere and rhizosphere that
300 were differentially abundant between well-watered and drought conditions. Next, we
301 correlated patterns of differential abundance for each bacterial taxon with drought
302 tolerance across host plant species. We detected two striking results. First, the
303 Streptomycetaceae (all ASVs combined, three of which were found in the endosphere of
304 every host plant species), exhibited a 3-fold increase abundance within the endosphere,
305 but not rhizosphere, under drought (*SI Appendix*, Fig. S11). However, the magnitude of
306 Streptomycetaceae enrichment varied between 0 to 4-fold across plant species (Fig. 5*B*
307 and *SI Appendix*, Fig. S13). Second, the relative enrichment of one *Streptomyces* ASV,
308 found in the endosphere of every host plant in the experiment, explained nearly 40% of
309 the variation in drought tolerance among host plant species (Fig. 5*C* and *SI Appendix*,
310 Dataset S4). A number of other endosphere taxa exhibited strong correlations ($r > 0.4$)
311 with host drought tolerance, including another *Streptomyces* ASV at high host prevalence
312 (*SI Appendix*, Dataset S4). However, with the exception of the *Streptomyces* ASV
313 depicted in Fig. 5*C*, these correlations were non-significant after multiple test correction
314 (*SI Appendix*, Dataset S4). Importantly, after examination of the non-living wood

315 samples, all of the endosphere ASVs related to drought tolerance in living roots were not
316 enriched in the endosphere of these root analogues under drought (*SI Appendix,* Dataset
317 S3).
318
319 **Discussion**
320 We demonstrate that plant evolution over long timescales shapes root microbiome
321 assembly, which in turn influences how host plants respond to biotic and abiotic
322 environmental stressors. Our results successfully address our four research questions.
323 First, the diversity and composition of the root microbiome was markedly different
324 between the endosphere and rhizosphere compartments across host species. Second, host
325 plant species explained much of the variation in the diversity and composition of the root
326 microbiome. Variation in the endosphere microbiome exhibited strong correspondence
327 with the underlying host plant phylogeny, though this was not the case for the
328 rhizosphere. Third, patterns of root microbial recruitment among host plants in both the
329 endosphere and rhizosphere influence indirect competitive interactions among plant
330 species through plant-soil feedbacks. Fourth, under drought stress the root endosphere
331 dynamically responds, and these changes correspond to variation in host plant tolerance
332 to drought. Below, we discuss how these results inform our understanding of the factors
333 that shape root microbiomes, and their ecological importance.
334 **Root microbiome assembly across angiosperm species.**
335 Our results provide clear insight into how host plants affect the assembly of root
336 microbiomes. Large differences in endosphere and rhizosphere diversity and composition
337 (Fig. 1*A* and *B*) are likely a conserved feature in plants, reflecting general rules for the

assembly of root microbiomes across angiosperm species. For example, we found a significant correlation between endosphere and rhizosphere community composition, indicating that the host-specific factors shaping composition, but not diversity, are at least partly shared between endosphere and rhizosphere compartments. Despite a broad conservation of root microbiome assembly, we also uncovered tremendous variation in microbiome communities occurring across host plant species. Plant species varied much more in their endosphere diversity (Fig. 1*C*) and composition (Fig. 1*D*), than the rhizosphere microbiome compartment, which supports the idea of greater host plant importance in the assembly of the endosphere microbiome (6). Several plant lineages exhibited pronounced differences in their endosphere microbiota including the Fabaceae, which have an elevated proportion of Proteobacteria, and the Poaceae, which are enriched in Actinobacteria.

We find support for the emerging view that plant evolution influences the root microbiome (12, 31, 39). Pronounced effects of host plant species in the face of recruitment of microbiota from the surrounding environment suggest that plants have evolved traits that govern root microbiome assembly. We found a particularly strong association between host plant evolutionary relatedness and endosphere diversity and composition, which indicates that host traits underlying endosphere assembly covary with phylogenetic relatedness among hosts. By contrast, rhizosphere assembly exhibited no clear relationship with host plant phylogeny (Fig. 1*C* and *D*, *SI Appendix,* Table S6, S7), despite host plant species having a strong effect on the rhizosphere microbiome (*SI Appendix,* Table S3, S4, S5). This result suggests that the plant traits which shape the rhizosphere compartment are themselves uncorrelated with host plant phylogeny.

Our analysis of plant traits revealed that plant productivity and physiology are associated with variation in root microbiome diversity and composition, similar to a recent study of leaf bacterial communities in tropical tree species (40). These physiological traits are often correlated with broad resource acquisition strategies employed across plant species (41), suggesting that plant resource consumption and turnover are correlated with root microbiota. Several host traits were associated with microbial composition in both the endosphere and rhizosphere, however this was not the case for microbial diversity (*SI Appendix,* Table S8). These results support our previous finding that host plant factors associated with root microbial composition, but not diversity, are partially shared between endosphere and rhizosphere compartments. We speculate that finer insight into how host plant variation and evolution affects root microbiome assembly, particularly the endosphere compartment, will require characterization of root metabolites and exudates as well as the microbial-triggered immune responses across plant species (4, 42-44).

The ecological importance of the plant root microbiome.

Plants evolved the ability to colonize land at a time when the terrestrial environment already contained microorganisms. Interactions between plants and soil microbes were key to the colonization and persistence of land plants (5), and they continue to play essential roles in host plant evolution and ecology. How assemblages of root microbiota contribute to the interaction between host plants and their biotic and abiotic environment is poorly understood and was a central focus of our study.

Root microbiota and plant-soil feedback. Biotic interactions via plant-soil feedbacks are a form of plant competition that have far-reaching importance for terrestrial

384 ecosystems (19, 20, 22). Soil microbes are generally recognized as the main factors
385 driving PSF, but beyond this, general theories addressing how microbial taxa contribute
386 to the strength of PSF among plants remain limited (45, 46). Our results lead to several
387 important and novel conclusions. First, the PSF between host plants depends on overall
388 compositional differences of root microbiota (Fig. 2). On average, highly similar root
389 microbiomes lead to negative PSF between host plant species. Increasing root microbial
390 similarity between plant species could directly reduce plant performance due to shared
391 pathogenic bacteria transferred through soil. If host immunity shapes associated-
392 microbiota (4, 42, 43), or if host-microbiota affect immunity (43, 47), then host plants
393 with similar root microbiomes may exhibit increased susceptibility to, and co-infection
394 with, the same pathogens. This hypothesis is indirectly supported by studies reporting
395 higher co-infectivity rates of pathogens between close versus distant plant relatives,
396 presumably driven by variation in pathogen-specific resistance across the plant
397 phylogeny (48). Alternatively, root microbiota may influence plant-plant interactions
398 through soil resource partitioning. In our PSF experiment the major source of mineral
399 nutrients for focal plants was the inoculum from soil conditioned in the previous
400 generation. Differential association with particular soil microorganisms is thought to
401 increase soil resource partitioning between plant species (16). Focal plants with similar
402 root microbiota to soil-conditioning plants may exhibit reduced growth due to a shared
403 microbial mutualist, involved in the acquisition of a limiting soil resource depleted during
404 generation one. Future work is required to understand the relative importance of
405 antagonistic versus beneficial microorganisms in driving the correlation between root
406 microbial similarity and PSF.

PSF between host plant species also depended on the differential abundance of particular root bacterial taxa (Fig. 3). This suggests a dynamic interplay between the root microbiota of interacting host plant species. In general, a higher abundance of PSF-related taxa in the rhizosphere of soil-conditioning host plants led to increased focal plant performance (e.g. Fig. 3*D*, 3*F; SI Appendix*, Dataset S2: unshaded rows). Greater abundance of mutualistic bacterial taxa in the rhizosphere of a host plant could enhance soil quality for future generations of plants by increasing abundance of the bacterial mutualist or through a fertilization effect (46). In the endosphere, we observed a high proportion of bacterial taxa exhibiting the opposite association, whereby increased abundance in the endosphere of the soil-conditioning host plant lead to reduced focal plant performance (e.g. Fig. 3*C*, 3*E; SI Appendix*, Dataset S2: blue shaded rows). This opposing association suggests that greater abundance of specific bacterial taxa in the endosphere reduces soil quality for the next generation of plants. This pattern is consistent with root bacteria recruited by a tolerant host plant acting as a plant pathogen in subsequent generations, but could also be driven by the depletion of mutualistic bacteria from the soil environment reducing subsequent host plant performance (46, 49).

The opposing effects of differential abundance illustrate that microbial members of either the endosphere or rhizosphere may have very different roles in plant competitive interactions mediated through soil-feedback, potentially related to their relative importance as either pathogens or mutualists. Additionally, the effects of root microbiota on PSF include compositional differences of entire root microbial compartments and the unique effects of individual bacterial taxa. Overall, our results raise the possibility that patterns of root microbial recruitment among plant species, through their effects on PSF,

may contribute to fundamental terrestrial ecology, such as the mechanisms underlying species coexistence (50) and ecosystem processes (21).

Drought and the root microbiome. In natural and managed ecosystems water availability is a strong determinant of plant performance. We investigated how drought shapes the root microbiome and whether or not drought-induced changes in root microbiota are associated with drought tolerance across host plant species. Drought substantially altered the composition of the root microbiome and marginally reduced microbial diversity, with larger effects on the endosphere than the rhizosphere microbiome (Fig. 4). Our results suggest that the effects of drought on microbiota are indirectly mediated by host plant responses (*SI Appendix,* Fig. S13, Table S9, and Dataset S3). A number of drought-induced plant responses, including physiological and molecular changes, could be responsible for these effects of plants on the endosphere microbiome. Interestingly, one of the chief regulators of drought stress response in plants is the hormone abscisic acid (ABA), which exhibits negative crosstalk with a number of defense hormones (36). A dampening of host plant immunity during drought could facilitate large shifts in endosphere colonization by microorganisms, otherwise restricted by the plant immune system (42). Indeed, a number of bacterial pathogens exploit this crosstalk by producing metabolites that mimic ABA (51). Two recent studies have shown that drought alters the root microbiome of cereal crop species (31, 32). Our findings extend these results to a wider phylogenetic diversity of plant species and demonstrate that large effects of host plants on the root endosphere under drought is a general pattern shared among angiosperms.

We found compelling evidence that increases in endosphere Actinobacteria, and especially members of the Streptomycetaceae, are associated with increased drought tolerance (Fig. 5). The Streptomycetaceae exhibit traits of potential benefit to host plants including the production of anti-microbial compounds, thick-walled spores resilient to environmental perturbation and inducible exploratory behavior (52), all of which may increase colonization rates of plant tissue under stressful environments. Another study investigating *Streptomyces* isolated from wheat roots found a potential benefit to host plants under drought stress, possibly through production of plant hormones and biochemical activity that help mitigate water stress (53). Members of the Actinobacteria were also enriched in root analogues (toothpicks) under drought, but these were not the same ASVs associated with drought tolerance in living host plants (*SI Appendix,* Dataset S3). Moreover, the ASVs enriched in the endosphere of root analogues under drought represented only 3% of the total ASVs enriched in living plant roots. Surprisingly, we failed to find any rhizosphere taxa that were related to host drought tolerance, despite numerous reports of drought-related rhizobacteria (54). While features of the Actinobacteria make them particularly suited to persist in stressful abiotic conditions like drought, our findings and others' point to the existence of lineages enriched only in roots of living plants under drought (31).

Our results present the intriguing hypothesis that changes in the host-microbiome under abiotic stress may be adaptive for the host (37, 38). If true, this would represent a form of adaptive phenotypic plasticity mediated by a plant's extended microbial community. More work is required to unravel the genetic and physiological mechanisms underlying host plant effects on the root microbiome, as well as any fitness benefits of

475 increased Streptomycetaceae abundance under drought. Recent findings may provide
476 some insight into possible mechanisms regulating adaptive host-microbiome interactions.
477 This work suggests that hosts modify their associated microbiota through regulating
478 innate immunity (e.g. 4), or by interfering with quorum sensing in bacteria (55, 56). How
479 animal and plant hosts modify their associated microbiota in response to environmental
480 perturbations, and whether these modifications represent adaptations, are important
481 questions for understanding the ecological and evolutionary importance of host
482 microbiota.

483 The examination of both biotic and abiotic stressors in our study uncovered
484 several important findings. Different compartments of the root microbiome (endosphere
485 and rhizosphere) are uniquely associated with a plant's response to environmental stress.
486 For example, while the endosphere and rhizosphere microbiome were both associated
487 with PSF, different taxa in each compartment were related to the strength of PSF (*SI*
488 *Appendix*, Dataset S2). By contrast, only the endosphere compartment was related to
489 drought tolerance (*SI Appendix*, Dataset S4). We also found three bacterial ASVs in the
490 root endosphere that were strongly associated with plant responses to both biotic and
491 abiotic host plant stress (*SI Appendix*, Dataset S2 and S4: green, orange, and purple
492 shaded ASVs). We speculate that some members of the root microbiome may benefit
493 host plants across a wide range of biotic and abiotic stressors. Finally, many of the PSF-
494 related and drought-related endosphere ASVs were found in all host plant species (*SI*
495 *Appendix*, Dataset S2 and S4), which points to the importance of widespread root
496 bacterial symbionts for plant ecology.

497 **Caveats**

Linking ecological functions across host plant species with root microbial diversity and composition derived from deep-amplicon sequencing data has several important limitations. First, though strongly suggestive of an important role for root bacterial communities in mitigating interactions between host plants and their biotic and abiotic environment, our results are correlative. Future research requires controlled experiments using synthetic communities or single inoculations to understand the mechanisms underlying the patterns uncovered here. Second, measures of relative abundance are unable to detect absolute increases in bacterial abundance. Using qPCR, Naylor et al. (31) recently confirmed that relative increases in Actinobacteria abundance in plant roots reflect absolute increases. Thus, the results from our drought study likely reflect absolute changes in the abundance of Streptomycetaceae. Third, characterization based on the 16S rRNA gene yields little functional information about microbial communities. Genomic analyses of root microbiota in addition to ecological assays of individual taxa or synthetic communities will elucidate the functional importance of root microbiota (57-59). Despite these limitations, our results reveal important effects of plant evolution and stress on root microbiota, and how the root microbiome is tightly related to the ecological response of plants to environmental stressors.

Conclusions

Host-associated microbiota are essential for nutrition, development, and immunity across plant and animal hosts (2), yet our understanding of their broader ecological importance remains limited. Our study provides some of the first evidence of the causes of variation in the host microbiome across a wide range of host plant species, as well as the general ecological importance of this variation for biotic and abiotic stressors. This study may

521 also inform future efforts to engineer the root microbiome in diverse agricultural systems
522 to increase plant performance in the face of competition and drought stress (60, 61).
523
524 **Materials and Methods**
525 To understand the assembly and ecological function of the angiosperm root bacterial
526 microbiome we combined a comparative study of 30 phylogenetically diverse plant
527 species with manipulative experiments (Fig. 1*A*, *SI Appendix*, Table S1). First, we
528 characterized the endosphere and rhizosphere microbiome of replicate individuals grown
529 from surface-sterile seeds in a common environment. Seeds were planted in a live soil
530 inoculum collected from a naturalized field site where all species co-occur (Koffler
531 Scientific Reserve, ON, Canada). We measured a suite of morphological, physiological
532 and performance traits from every plant (*SI Appendix*, Table S2). After 16 weeks, we
533 partitioned standard root samples from each plant into endosphere and rhizosphere
534 compartments (8, 9) and extracted total DNA. We characterized the bacterial community
535 by sequencing amplicons of the V4 region of the 16S rRNA gene using Illumina MiSeq
536 (*SI Appendix*, Fig. S1). To reduce host contamination, we used peptide nucleic acids
537 designed to block amplification of host plant plastid and mitochondrial sequences (62).
538 We assembled quality-filtered reads into error-corrected amplicon sequence variants
539 (ASVs) using DADA2 v.1.4.0 (33), which represent unique bacterial taxa. ASVs exhibit
540 fewer false positive taxa and reveal cryptic diversity, otherwise undetected by traditional
541 OTU approaches (33). In total, we profiled 271 endosphere communities, 255
542 rhizosphere communities and 58 soil and control samples (*SI Appendix*, Table S1) and
543 assembled 56,063 ASVs.

544 Assembled ASVs were assigned taxonomy (phylum to genus) using the RDP
545 naïve Bayesian classifier (implemented in DADA2) and the 'RDP training set 14' (63).
546 We used PASTA to align ASV sequences and build a maximum likelihood phylogenetic
547 tree (64). Next, using the R package 'phyloseq' (65), we removed any ASVs without a
548 bacterial phylum assignment, assigned to Archaea, chloroplast, or mitochondrial origin.
549 To simplify downstream analyses, we applied a prevalence and abundance threshold for
550 bacterial ASVs, where taxa were kept only if they were found in 1% of samples (7
551 samples) and at a frequency of 25 reads per sample. This yielded 2,799 ASVs, which
552 accounted for 94% of the total number of sequences in the dataset (*SI Appendix*, Fig.
553 S14). For downstream composition analyses, we performed proportional abundance
554 normalization (relative abundance) on this common set of ASVs, where the sequencing
555 reads for an ASV in a given sample were divided by the total number of sequencing reads
556 in that sample (66). As an additional set of analyses, we used the traditional approach of
557 rarefaction (to 800 reads) to normalize our full dataset prior to any threshold, which
558 yielded approximately 13,000 ASVs and accounted for less than 2% of the total read
559 count (*SI Appendix*, Fig. S14). Both methods (rarefaction on the full dataset and relative
560 abundance normalization on the simplified dataset) yielded qualitatively identical results,
561 we therefore present the non-rarefied data because it retained a larger portion of our data.
562 We investigated the ecological importance of root microbiota for both biotic and
563 abiotic stressors. As a biotic stressor, we measured how patterns of root microbial
564 recruitment among host plant species can feed back to affect indirect competitive
565 interactions via plant-soil feedbacks (*SI Appendix*, Fig. S1). In the first generation of our
566 plant-soil feedback experiment, we grew each of our 30 plant species in a homogenous

soil mixture collected from the same field site as our comparative microbiome study. Pots were filled with 800 mL of sterilized soil (mixture of potting soil and sand [2:3 V/V]) and 200 mL of live inoculum collected from KSR. We preserved bulk and rhizosphere soil collected and pooled from 5 individuals from each of the 30 plant species and used it to inoculate replicate individuals of 5 focal species, representative of our host plant phylogenetic diversity. In this second generation, we mixed live soil inoculum preserved from the previous generation with the same sterile soil mix in the same ratio as the first generation. The effect of soil conditioning in the first generation on plant performance in the second generation is the plant-soil feedback (PSF). Operationally, we measured the PSF as: $\log_e$ ((focal species biomass in heterospecific soil)/(focal species biomass in conspecific soil)); positive values indicate that a focal species performed better in soil conditioned by a different species from the focal plant relative to soil conditioned by the same species as the focal plant, whereas negative values indicate the opposite (34).

As an abiotic stressor, we manipulated drought and measured how water limitation affected patterns of root microbial recruitment among host plant species and host plant drought tolerance. We used a drip irrigation system to impose a chronic drought stress on replicate individuals from each host plant species during the comparative root microbiome study, as well as an equal number of well-watered control plants. Our manipulation resulted in a 4-fold difference in soil moisture and a mean biomass reduction of 35% across host plant species in the drought treatment compared to the control, though host plant species varied widely in their tolerance to drought. Alongside living plants we also included bare soil pots and pots planted with structurally similar root analogues (toothpicks). Differences in drought responses between living root

590 microbial communities and root analogues or soil indicate the effects of living host plants
591 on microbial dynamics.

592 We analyzed the effects of host plant species, root compartment and watering
593 treatment on the diversity (observed ASV richness, Simpson's D^{-1}, and evenness [Simpson's D^{-1}/ observed ASV richness]), and composition (weighted UniFrac

594
595 dissimilarity (67)) of bacterial communities using linear mixed models (*SI Appendix,*
596 Table S3 and S4). We also analyzed the effects of host plant species, root compartment,
597 and watering treatment on the differential abundance of bacterial taxa using DESeq2
598 (35). DESeq2 uses negative binomial models and ASV read counts to test whether
599 individual bacterial taxa are differentially abundant across experimental factors. To
600 understand how plant evolution has shaped root microbial communities, we calculated
601 phylogenetic signal (Blomberg's K and Pagel's λ) present in diversity estimates and used
602 Mantel tests to determine the correlation between host plant evolutionary relatedness and
603 root microbial compositional similarity (*SI Appendix,* Table S6 and S7). Finally, we used
604 phylogenetic generalized least-squares regression (PGLS) to determine the relationship
605 between plant traits and root microbial diversity and composition (*SI Appendix,* Table
606 S8).

607 We investigated the ecological importance of root microbiota by correlating
608 patterns of root microbial composition and differential abundance among host plant
609 species with experimentally measured PSF and drought tolerance. Correlations between
610 root microbial composition and ecological processes indicate an importance of broad
611 patterns of root microbiome assembly, whereas correlations with individual taxa indicate
612 particular individual bacterial taxa are associated with host plant performance. First, we

analyzed how endosphere and rhizosphere compositional differences (weighted and unweighted UniFrac dissimilarity) among pairs of host plant species was correlated with PSF. Next, we identified those bacterial taxa that were differentially abundant among host plant species and correlated their log_2-fold change between focal and soil-conditioning plant species with the experimentally measured PSF (*SI Appendix,* Dataset S2). In the drought experiment, we correlated endosphere and rhizosphere compositional differences (weighted and unweighted UniFrac dissimilarity) between watering treatments within a host plant species with their measured drought tolerance. To understand the potential role of individual taxa, we first identified drought-responsive bacterial taxa and correlated their log_2-fold change between watering treatments within a host plant species with host species' drought tolerance (*SI Appendix,* Dataset S4). All analyses were carried out in R v.3.3.3 (68). For detailed materials and methods see *SI Appendix, Materials and Methods.* Sequence files associated with individual samples are available on the NCBI Sequence Read Archive (PR####). All data and R code used in the analyses are available on Dryad digital repository.

Acknowledgements

We thank M. Kalich and B. Pitton for greenhouse support. A. Chen, K. Cory, D. Filice, L. Gehant, J. Lee, A. Longley, M. Middleton, L. Rawofi, H. Sekhon, A. Severino, K. Vigmond, and members of the Centre for the Analysis of Genome Evolution and Function (CAGEF), provided assistance with experiments and data collection. We also thank members of the Johnson and Guttman labs, J. L. Dangl, D. S. Lundberg, J. R. Stinchcombe, and M. R. Wagner for helpful discussion. The editor and two anonymous

reviewers provided thoughtful evaluation, which greatly improved the manuscript. This work was supported by OGS and QEII awards to C.R.F., and funding from U. Toronto, UTM OVPR and NSERC to D.S.G., P.M.K., and M.T.J.J.

Footnotes

Author Contributions: C.R.F., D.S.G., P.M.K. and M.T.J.J. designed the project, C.R.F. performed research. C.R.F, J.C. and P.W.W. optimized PCR and performed sequencing. C.R.F. and M.T.J.J. wrote the manuscript with input from J.C., P.W.W., P.M.K., and D.S.G.

References

1. McFall-Ngai M, et al. (2013) Animals in a bacterial world, a new imperative for the life sciences. *Proc Natl Acad Sci U S A* 110(9):3229–3236.

2. Hacquard S, et al. (2015) Microbiota and Host Nutrition across Plant and Animal Kingdoms. *Cell Host Microbe* 17(5):603–616.

3. Chung H, et al. (2012) Gut immune maturation depends on colonization with a host-specific microbiota. *Cell* 149(7):1578–1593.

4. Castrillo G, et al. (2017) Root microbiota drive direct integration of phosphate stress and immunity. *Nature* 543(7646):513–518.

5. Field KJ, Pressel S, Duckett JG, Rimington WR, Bidartondo MI (2015) Symbiotic options for the conquest of land. *Trends Ecol Evol* 30(8):477–486.

6. Bulgarelli D, Schlaeppi K, Spaepen S, van Themaat EVL, Schulze-Lefert P (2013) Structure and functions of the bacterial microbiota of plants. *Annu Rev Plant Biol* 64(1):807–838.

7. Berendsen RL, Pieterse CMJ, Bakker PAHM (2012) The rhizosphere microbiome and plant health. *Trends Plant Sci* 17(8):478–486.

8. Lundberg DS, et al. (2012) Defining the core *Arabidopsis thaliana* root microbiome. *Nature* 488(7409):86–90.

9. Bulgarelli D, et al. (2012) Revealing structure and assembly cues for *Arabidopsis* root-inhabiting bacterial microbiota. *Nature* 488(7409):91–95.

10. Edwards J, et al. (2015) Structure, variation, and assembly of the root-associated microbiomes of rice. *Proc Natl Acad Sci U S A* 112(8):E911–20.

11. Schlaeppi K, Dombrowski N, Oter RG, van Themaat EVL, Schulze-Lefert P (2014) Quantitative divergence of the bacterial root microbiota in *Arabidopsis thaliana* relatives. *Proc Natl Acad Sci U S A* 111(2):585–592.

12. Bouffaud M-L, Poirier M-A, Muller D, Moënne-Loccoz Y (2014) Root microbiome relates to plant host evolution in maize and other Poaceae. *Environ Microbiol* 16(9):2804–2814.

13. Zgadzaj R, et al. (2016) Root nodule symbiosis in *Lotus japonicus* drives the establishment of distinctive rhizosphere, root, and nodule bacterial communities. *Proc Natl Acad Sci U S A* 113(49):E7996–E8005.

14. Thorpe AS, Aschehoug ET, Atwater DZ, Callaway RM (2011) Interactions among plants and evolution. *J Ecol* 99(3):729–740.

15. Tilman D (1982) *Resource competition and community structure* (Princeton University Press, Princeton NJ).

16. Bever JD, et al. (2010) Rooting theories of plant community ecology in microbial interactions. *Trends Ecol Evol* 25(8):468–478.

17. Hodge A, Fitter AH (2012) Microbial mediation of plant competition and community structure. *Funct Ecol* 27(4):865–875.

18. Bever JD (1994) Feedback between plants and their soil communities in an old field community. *Ecology* 75(7):1965–1977.

19. Kardol P, Bezemer TM, van der Putten WH (2006) Temporal variation in plant-soil feedback controls succession. *Ecol Lett* 9(9):1080–1088.

20. Klironomos JN (2002) Feedback with soil biota contributes to plant rarity and invasiveness in communities. *Nature* 417(6884):67–70.

21. Schnitzer SA, et al. (2011) Soil microbes drive the classic plant diversity-productivity pattern. *Ecology* 92(2):296–303.

22. Callaway RM, Thelen GC, Rodriguez A, Holben WE (2004) Soil biota and exotic plant invasion. *Nature* 427(6976):731–733.

23. Choat B, et al. (2012) Global convergence in the vulnerability of forests to drought. *Nature* 491(7426):752–755.

24. Siepielski AM, et al. (2017) Precipitation drives global variation in natural selection. *Science* 355(6328):959–962.

25. Farooq M, Wahid A, Kobayashi N, Fujita D (2009) Plant drought stress: effects, mechanisms and management. *Agron Sustain Dev* 29(1):185–212.

26. Shinozaki K, Yamaguchi-Shinozaki K (2006) Gene networks involved in drought stress response and tolerance. *J Exp Bot* 58(2):221–227.

27. Brunner I, Herzog C, Dawes MA, Arend M, Sperisen C (2015) How tree roots respond to drought. *Front Plant Sci* 6(e1000492):932–16.

28. Timmusk S, Wagner EG (1999) The plant-growth-promoting rhizobacterium *Paenibacillus polymyxa* induces changes in *Arabidopsis thaliana* gene expression: a possible connection between biotic and abiotic stress responses. *MPMI* 12(11):951–959.

29. Mayak S, Tirosh T, Glick BR (2004) Plant growth-promoting bacteria that confer resistance to water stress in tomatoes and peppers. *Plant Science* 166(2):525–530.

30. Lau JA, Lennon JT (2012) Rapid responses of soil microorganisms improve plant

712 fitness in novel environments. *Proc Natl Acad Sci U S A* 109(35):14058–14062.

713 31. Naylor D, DeGraaf S, Purdom E, Coleman-Derr D (2017) Drought and host
714 selection influence bacterial community dynamics in the grass root microbiome.
715 *ISME J* 11(12):2691-2704.

716 32. Santos-Medellín C, Edwards J, Liechty Z, Nguyen B, Sundaresan V (2017)
717 Drought stress results in a compartment-specific restructuring of the rice root-
718 associated microbiomes. *mBio* 8(4):e00764–17–15.

719 33. Callahan BJ, et al. (2016) DADA2: High-resolution sample inference from
720 Illumina amplicon data. *Nat Meth* 13(7):581–583.

721 34. Pernilla Brinkman E, van der Putten WH, Bakker E-J, Verhoeven KJF (2010)
722 Plant-soil feedback: experimental approaches, statistical analyses and ecological
723 interpretations. *J Ecol* 98(5):1063–1073.

724 35. Love MI, Huber W, Anders S (2014) Moderated estimation of fold change and
725 dispersion for RNA-seq data with DESeq2. *Genome Biology* 15(12):31–21.

726 36. Robert-Seilaniantz A, Grant M, Jones JDG (2011) Hormone crosstalk in plant
727 disease and defense: more than just jasmonate-salicylate antagonism. *Annu Rev*
728 *Phytopathol* 49(1):317–343.

729 37. Alberdi A, Aizpurua O, Bohmann K, Zepeda-Mendoza ML, Gilbert MTP (2016)
730 Do vertebrate gut metagenomes confer rapid ecological adaptation? *Trends Ecol*
731 *Evol* 31(9):689–699.

732 38. Goh C-H, Veliz Vallejos DF, Nicotra AB, Mathesius U (2013) The impact of
733 beneficial plant-associated microbes on plant phenotypic plasticity. *J Chem Ecol*
734 39(7):826–839.

735 39. Yeoh YK, et al. (2017) Evolutionary conservation of a core root microbiome
736 across plant phyla along a tropical soil chronosequence. *Nature Communications*
737 8(1):215 doi: 10.1038/s41467-017-00262-8.

738 40. Kembel SW, et al. (2014) Relationships between phyllosphere bacterial
739 communities and plant functional traits in a neotropical forest. *Proc Natl Acad Sci*
740 *U S A* 111(38):13715–13720.

741 41. Comas LH, Eissenstat DM (2004) Linking fine root traits to maximum potential
742 growth rate among 11 mature temperate tree species. *Funct Ecol* 18(3):388–397.

743 42. Lebeis SL, et al. (2015) Salicylic acid modulates colonization of the root
744 microbiome by specific bacterial taxa. *Science* 349(6250):860–864.

745 43. Hacquard S, Spaepen S, Garrido-Oter R, Schulze-Lefert P (2017) Interplay
746 between innate immunity and the plant microbiota. *Annu Rev Phytopathol* 55:565-

589.

44. van Dam NM, Bouwmeester HJ (2016) Metabolomics in the rhizosphere: tapping into belowground chemical communication. *Trends Plant Science* 21(3):256–265.

45. van der Putten WH, et al. (2013) Plant-soil feedbacks: the past, the present and future challenges. *J Ecol* 101(2):265–276.

46. Bever JD, Platt TG, Morton ER (2012) Microbial population and community dynamics on plant roots and their feedbacks on plant communities. *Annu Rev Microbiol* 66(1):265–283.

47. Vogel C, Bodenhausen N, Gruissem W, Vorholt JA (2016) The *Arabidopsis* leaf transcriptome reveals distinct but also overlapping responses to colonization by phyllosphere commensals and pathogen infection with impact on plant health. *New Phytol* 212(1):192–207.

48. Gilbert GS, Parker IM (2016) The evolutionary ecology of plant disease: a phylogenetic perspective. *Annu Rev Phytopathol* 54(1):549–578.

49. Bever JD, Mangan SA, Alexander HM (2015) Maintenance of plant species diversity by pathogens. *Annu Rev Ecol Evol Syst* 46(1):305–325.

50. Chung YA, Rudgers JA (2016) Plant-soil feedbacks promote negative frequency dependence in the coexistence of two aridland grasses. *Proc Biol Sci* 283(1835):20160608–10.

51. Mine A, et al. (2017) Pathogen exploitation of an abscisic acid- and jasmonate-inducible MAPK phosphatase and its interception by *Arabidopsis* immunity. *Proc Natl Acad Sci U S A* 114(28):7456–7461.

52. Jones SE, et al. (2017) *Streptomyces* exploration is triggered by fungal interactions and volatile signals. *eLife* 6:e21738.

53. Yandigeri MS, et al. (2012) Drought-tolerant endophytic Actinobacteria promote growth of wheat (*Triticum aestivum*) under water stress conditions. *Plant Growth Regul* 68(3):411–420.

54. Yang J, Kloepper JW, Ryu C-M (2009) Rhizosphere bacteria help plants tolerate abiotic stress. *Trends Plant Science* 14(1):1–4.

55. Pietschke C, et al. (2017) Host modification of a bacterial quorum-sensing signal induces a phenotypic switch in bacterial symbionts. *Proc Natl Acad Sci U S A* 114(40):E8488-E8497.

56. Gao M, Teplitski M, Robinson JB, Bauer WD (2003) Production of substances by *Medicago truncatula* that affect bacterial quorum sensing. *MPMI* 16(9):827–834.

781 57. Bai Y, et al. (2015) Functional overlap of the *Arabidopsis* leaf and root microbiota.
782 *Nature* 528(7582):364–369.

783 58. Cole BJ, et al. (2017) Genome-wide identification of bacterial plant colonization
784 genes. *PLoS Biol* 15(9):e2002860–24.

785 59. Haney CH, Samuel BS, Bush J, Ausubel FM (2015) Associations with rhizosphere
786 bacteria can confer an adaptive advantage to plants. *Nature Plants* 1(6):15051.

787 60. Finkel OM, Castrillo G, Herrera Paredes S, Salas González I, Dangl JL (2017)
788 Understanding and exploiting plant beneficial microbes. *Curr Opin Plant Biol*
789 38:155–163.

790 61. Meena KK, et al. (2017) Abiotic stress responses and microbe-mediated mitigation
791 in plants: the omics strategies. *Front Plant Sci* 8:172 doi:10.3389/fpls.2017.00172

792 62. Lundberg DS, Yourstone S, Mieczkowski P, Jones CD, Dangl JL (2013) Practical
793 innovations for high-throughput amplicon sequencing. *Nat Meth* 10(10):999–1002.

794 63. Wang Q, Garrity GM, Tiedje JM, Cole JR (2007) Naive bayesian classifier for
795 rapid assignment of rRNA sequences into the new bacterial taxonomy. *Appl*
796 *Environ Microbiol* 73(16):5261–5267.

797 64. Mirarab S, et al. (2015) PASTA: ultra-large multiple sequence alignment for
798 nucleotide and amino-acid sequences. *J Comput Biol* 22(5):377–386.

799 65. McMurdie PJ, Holmes S (2013) phyloseq: an R package for reproducible
800 interactive analysis and graphics of microbiome census data. *PLoS ONE*
801 8(4):e61217–11.

802 66. McMurdie PJ, Holmes S (2014) Waste not, want not: why rarefying microbiome
803 data is inadmissible. *PLoS Comput Biol* 10(4):e1003531–12.

804 67. Lozupone C, Knight R (2005) UniFrac: a new phylogenetic method for comparing
805 microbial communities. *Appl Environ Microbiol* 71(12):8228–8235.

806 68. R Core Team (2012) R: A Language and Environment for Statistical Computing
807 (R Found Stat Comput, Vienna).

Figure captions

Fig. 1

The diversity and composition of endosphere and rhizosphere compartments across plant species. (*A*) The endosphere exhibited less than one-quarter of the diversity found in the rhizosphere ($F_{1,56} = 64.62$, $P_{FDR} < 0.001$, *P*-value adjusted using the false discovery rate). (*B*) The abundance of bacterial phyla were significantly affected (GLM: $P_{FDR} < 0.05$) by compartment (black star) and host plant species (green star = endosphere, yellow star = rhizosphere). (*C*) Endosphere diversity exhibited greater variation across host plants than rhizosphere diversity ($\chi^2 = 17.72$, $P_{FDR} < 0.001$). Endosphere diversity was also correlated with the underlying plant phylogeny, while rhizosphere diversity was not. (*D*) Plant species varied more in the composition of their endosphere versus rhizosphere compartments ($\chi^2 = 20.06$, $P_{FDR} < 0.001$). Mantel tests revealed a significant correlation between endosphere (but not rhizosphere) compositional similarity and phylogenetic relatedness.

Fig. 2

Root microbial composition is related to plant-soil feedbacks (PSF). (*A*) PSF occurs when the soil microbes recruited by one plant influence the growth of other plants. Positive values indicate that a focal species performed better in soil conditioned by a heterospecific plant relative to a conspecific plant, whereas negative values indicate the opposite. (*B*) Plants exhibit enhanced growth when inoculated with soil conditioned by a heterospecific species with dissimilar endosphere (measured as weighted UniFrac distance) and (*C*) rhizosphere compartments (measured as unweighted UniFrac distance).

Fig. 3

Differential abundance of root bacterial taxa and PSF. Host plant species exhibit differential abundance for numerous root bacterial taxa in either the endosphere or rhizosphere, including (*A*) an endosphere Streptomyces ASV and (*B*) the genus *Pseudoxanthomonas* found in the rhizosphere (GLM: $P_{FDR} < 0.05$). We estimated the log_2-fold change of differentially abundant root bacterial taxa among all unique pairs of focal and soil-conditioning host plant species and correlated this with their measured PSF. Negative log_2-fold changes indicate a higher taxon abundance in soil-conditioning host plant species, while positive values indicate a higher taxon abundance in focal host plant species. (*C*) The differential abundance of the endosphere *Streptomyces* ASV between focal and soil-conditioning host plant species was positively related to their PSF. (*D*) However, the differential abundance of rhizosphere *Pseudoxanthomonas* between focal and soil-conditioning host plant species was negatively related to their PSF. (*E* and *F*) PSF between host plant species was significantly associated with the differential abundance of 66 endosphere taxa and 33 rhizosphere taxa. (*E*) In the endosphere, we observed a high proportion (35%) of PSF-related taxa exhibiting the association depicted in panel *C* (green lines illustrate significant trend lines between differential abundance of endosphere taxa and PSF at $P_{FDR} < 0.05$). (*F*) While in the rhizosphere, a greater proportion (88%) of taxa exhibited the association depicted in panel *D* (yellow lines illustrate significant trend lines between rhizosphere taxa and PSF at $P_{FDR} < 0.05$). See *SI Appendix*, Dataset S2 for a full list of PSF-related taxa.

Fig. 4

The effects of drought on root microbial communities. (*A*) The drought treatment (denoted by T) caused small reductions in the diversity of the endosphere and rhizosphere compartments (denoted by C), and (*B*) had large effects on the relative abundance of major bacterial phyla; starred phyla were significantly affected (GLM: $P_{FDR} < 0.05$) by drought (green = endosphere, orange = rhizosphere). (*C*) Drought also had strong effects on the overall composition of the endosphere and rhizosphere microbiomes, though endosphere compartments exhibited a greater response. Inset: plants under drought experienced four-fold lower soil moisture than well-watered plants.

Fig. 5

The relationship between drought tolerance and Streptomycetaceae**.** (*A*) On average the drought treatment (denoted by T) caused a 35% reduction in biomass compared to well-watered conditions ($F_{1,44} = 17.37$, $P < 0.001$), and plant species (denoted by S) varied significantly in their response to drought (represented by dots connected by individual lines). (*B*) Drought caused a 6-fold increase in the mean relative abundance of endosphere Streptomycetaceae (Actinobacteria), but this effect varied among plant species. (*C*) Plant species with greater relative increases in an endosphere *Streptomyces* ASV under drought conditions had greater drought tolerance. See *SI Appendix*, Dataset S4 for a full list of drought-related taxa.

A

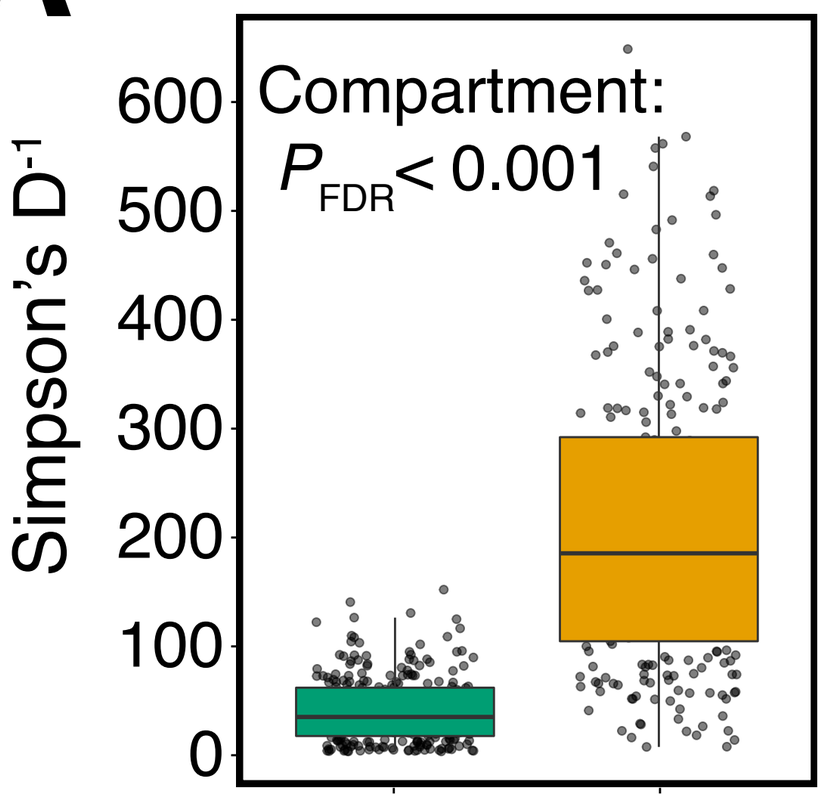
Simpson's D-1
600
500
400
300
200
100
0
Compartment:
PFDR< 0.001
Endo
Rhizo

B

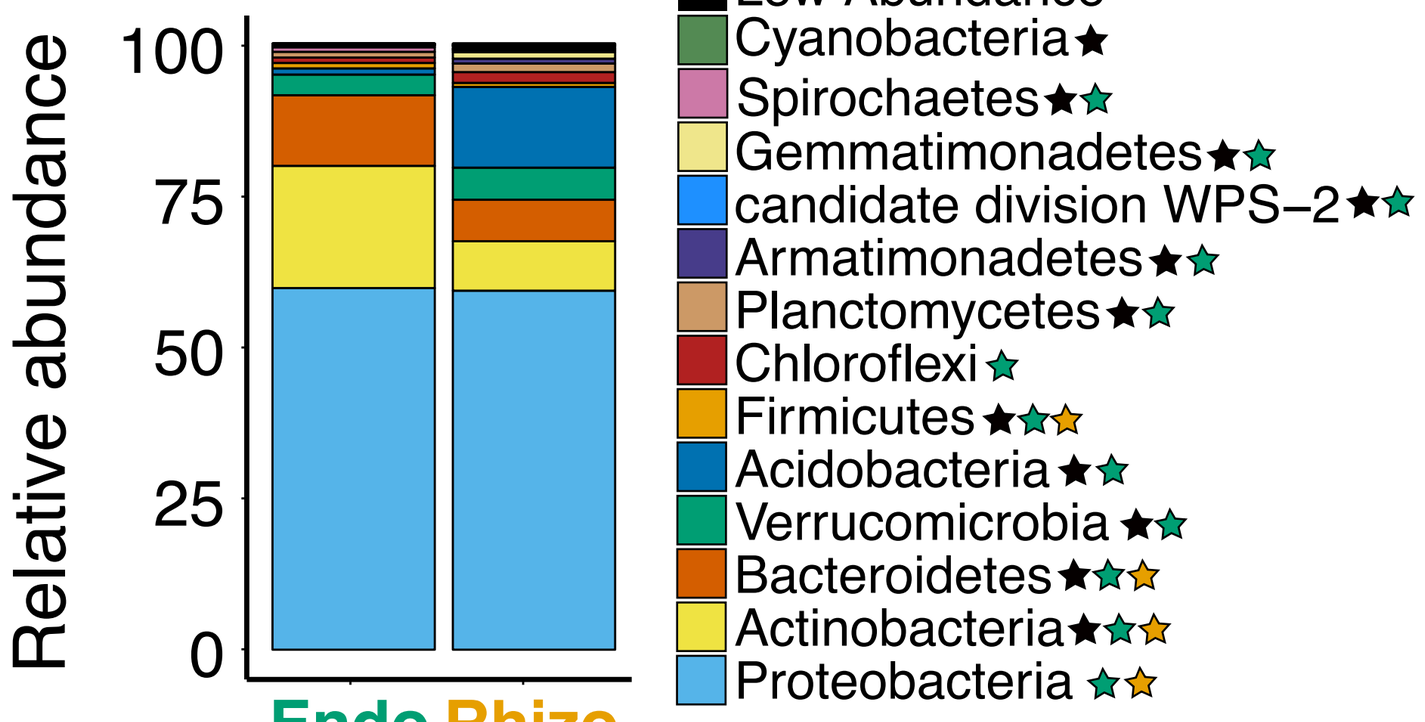
Relative abundance
100
75
50
25
0
Endo Rhizo
Bacterial phylum
Low Abundance
Cyanobacteria
Spirochaetes
Gemmatimonadetes
candidate division WPS–2
Armatimonadetes
Planctomycetes
Chloroflexi
Firmicutes
Acidobacteria
Verrucomicrobia
Bacteroidetes
Actinobacteria
Proteobacteria

C

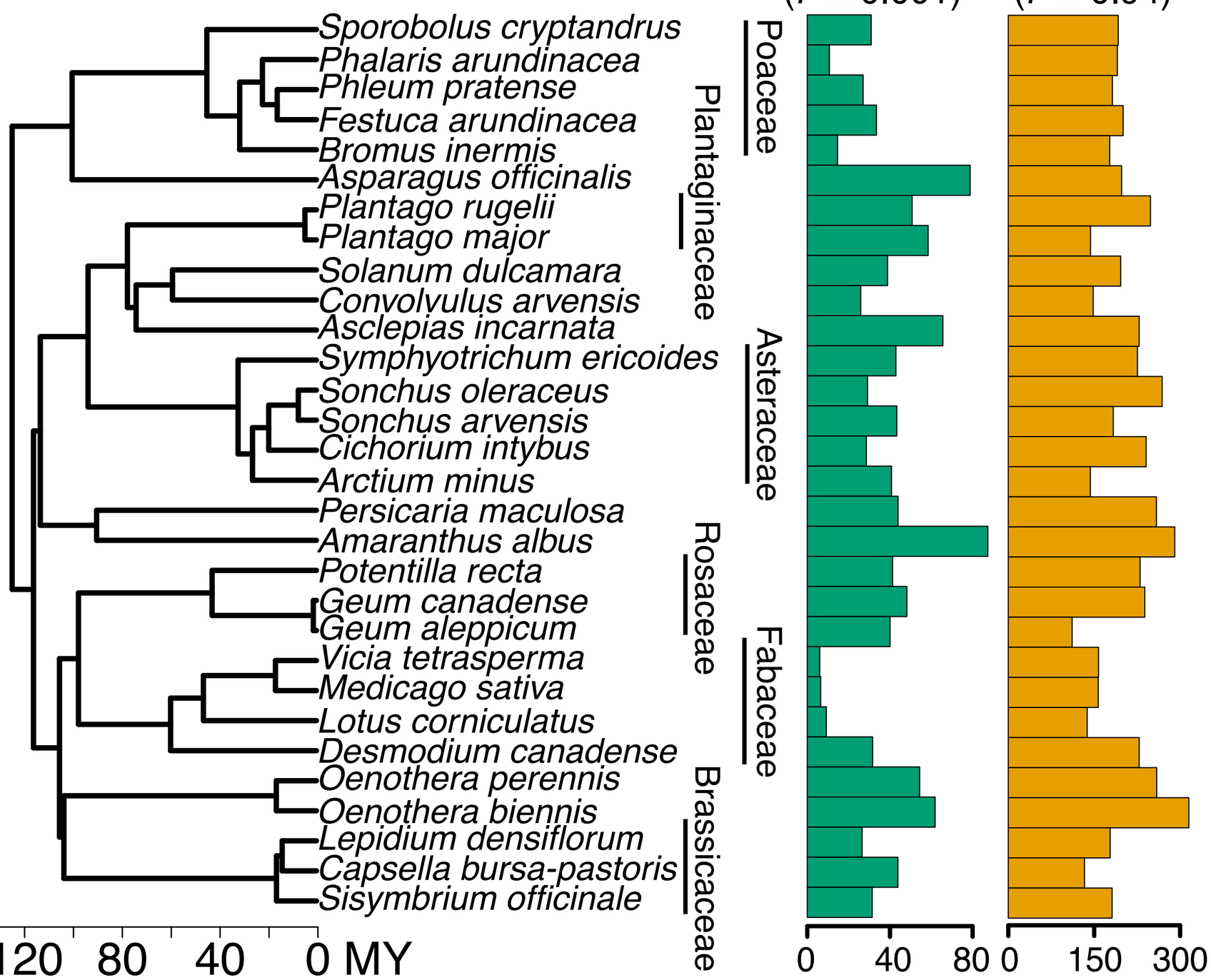
Endo
Rhizo
Phylogenetic signal K*
1.09
(P = 0.001)
0.67
(P = 0.94)
Sporobolus cryptandrus
Phalaris arundinacea
Phleum pratense
Festuca arundinacea
Bromus inermis
Asparagus officinalis
Plantago rugelii
Plantago major
Solanum dulcamara
Convolvulus arvensis
Asclepias incarnata
Symphyotrichum ericoides
Sonchus oleraceus
Sonchus arvensis
Cichorium intybus
Arctium minus
Persicaria maculosa
Amaranthus albus
Potentilla recta
Geum canadense
Geum aleppicum
Vicia tetrasperma
Medicago sativa
Lotus corniculatus
Desmodium canadense
Oenothera perennis
Oenothera biennis
Lepidium densiflorum
Capsella bursa-pastoris
Sisymbrium officinale
Poaceae
Plantaginaceae
Asteraceae
Rosaceae
Fabaceae
Brassicaceae
120 80 40 0 MY
0 40 80
0 150 300
Simpson's D-1

D

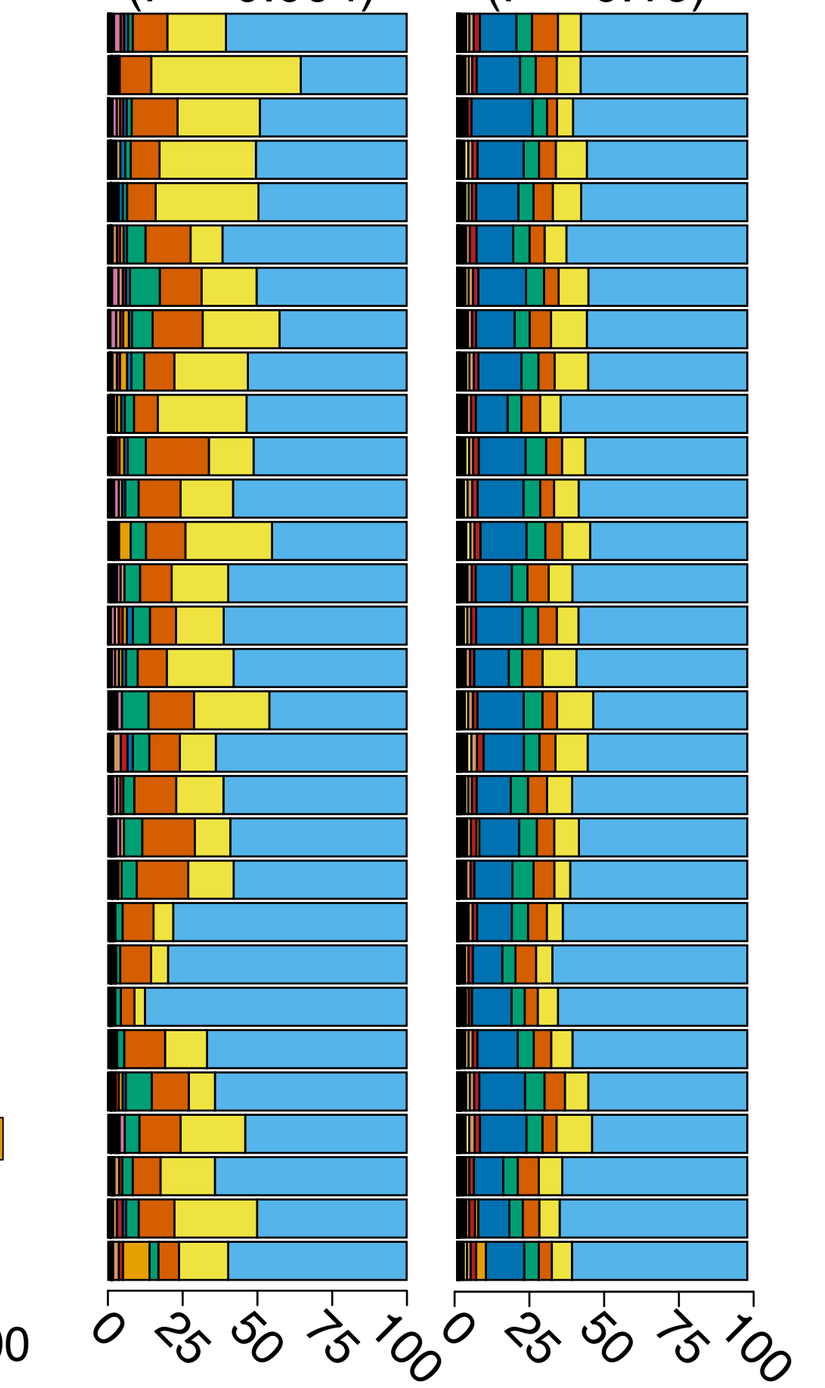
Endo
Rhizo
Mantel's r
0.15
(P = 0.004)
0.05
(P = 0.16)
0 25 50 75 100
0 25 50 75 100
Relative abundance

A

Focal species

Soil conditioning species

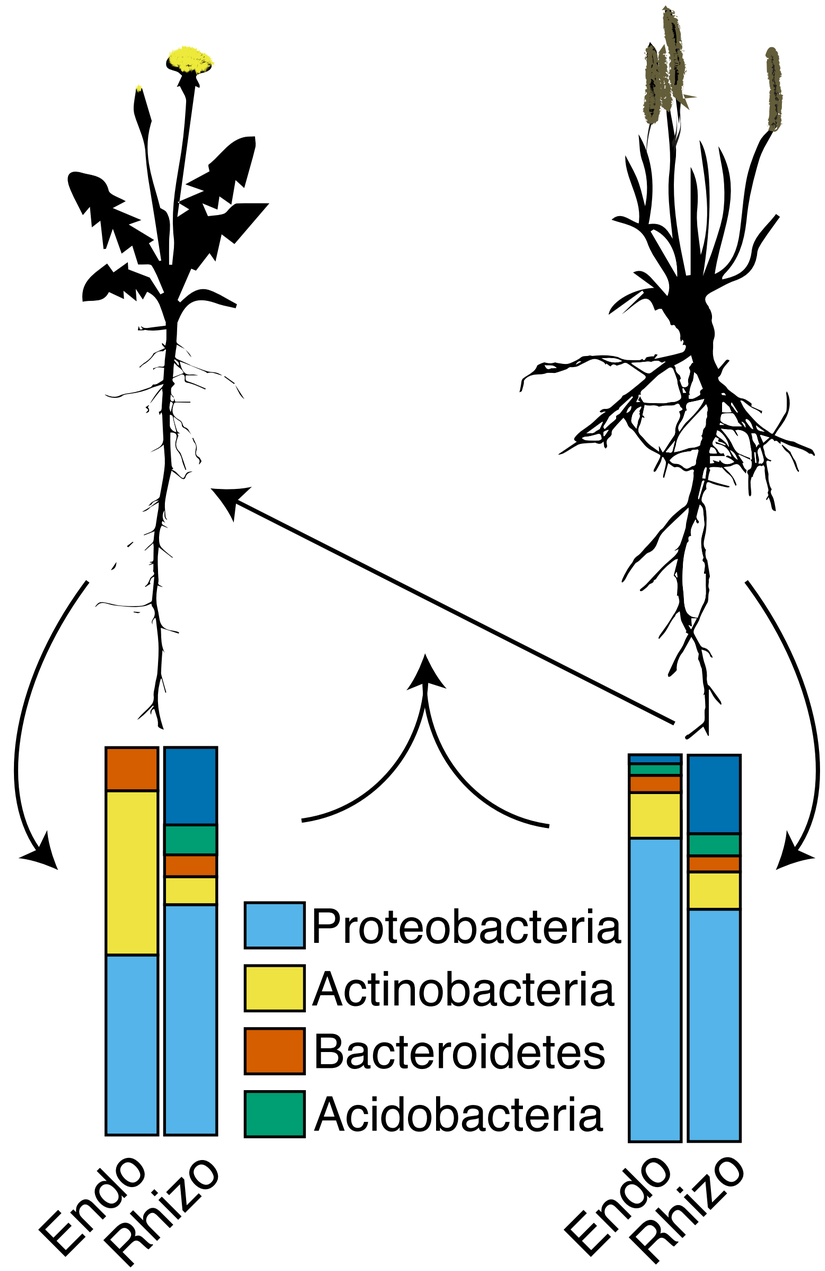

$$\text{Plant–soil feedback} = \ln\left(\frac{\text{mean biomass of focal species in heterospecific soil}}{\text{mean biomass of focal species in conspecific soil}}\right)$$

B

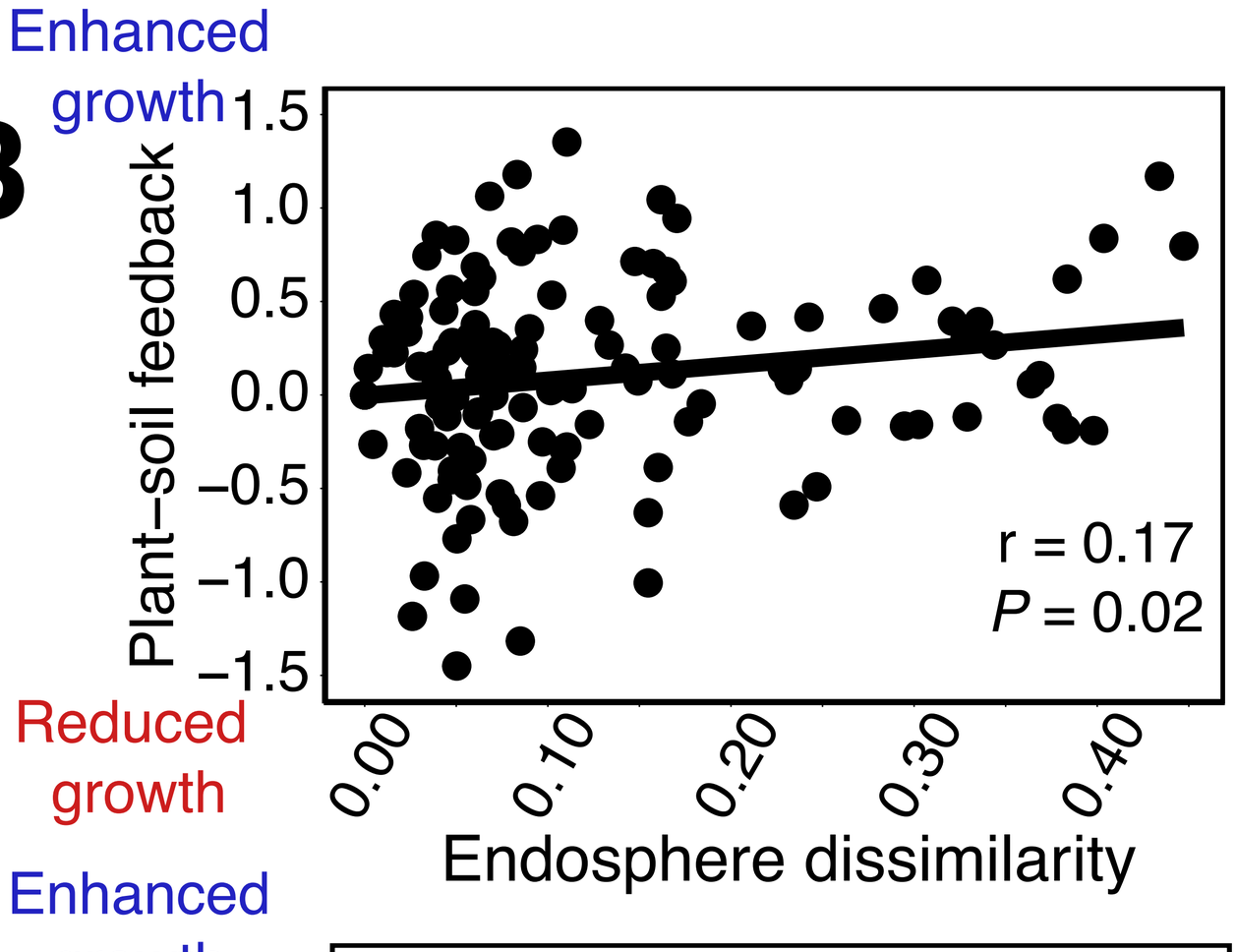

C

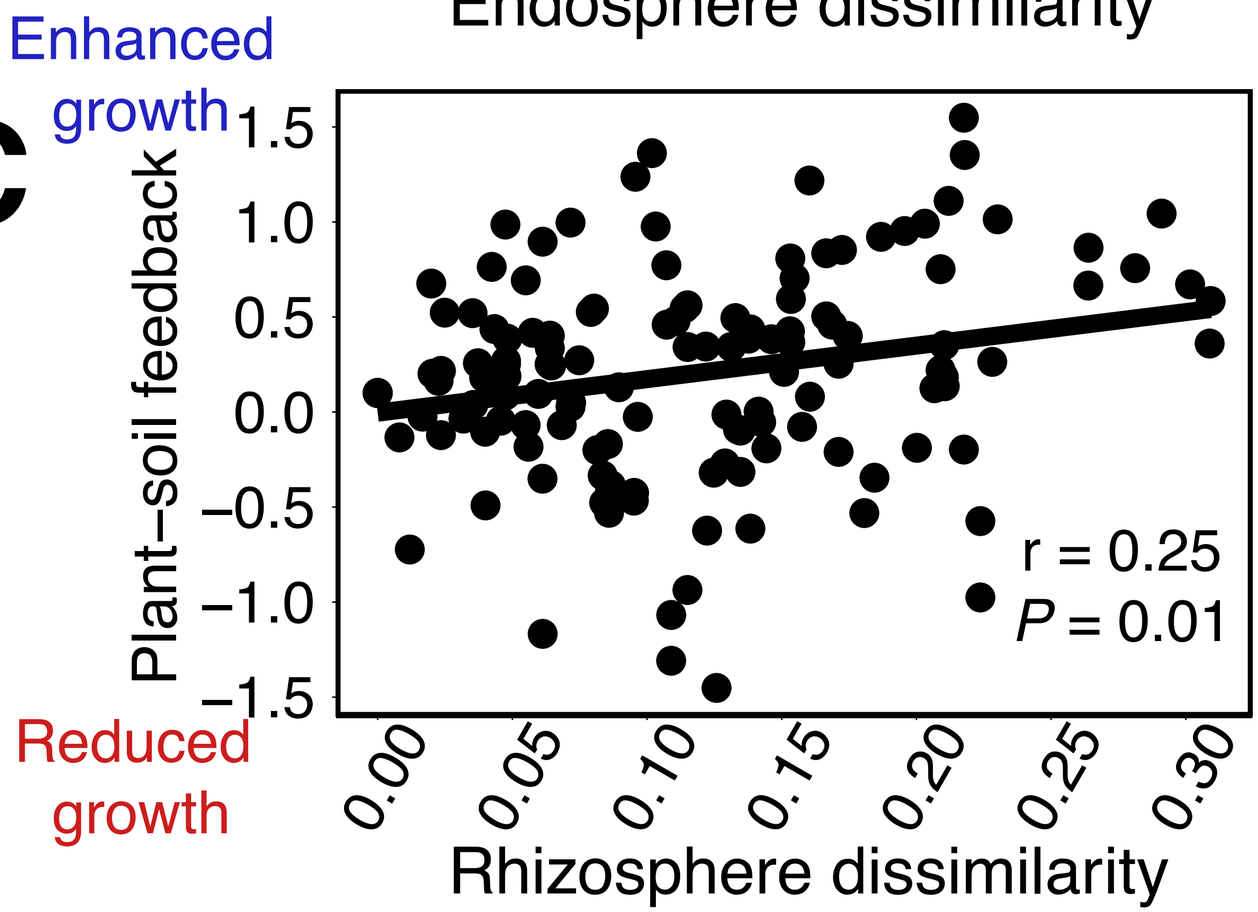

A

Endosphere

Streptomyces ASV1

B

Rhizosphere

Pseudoxanthomonas

Sporobolus cryptandrus
Phalaris arundinacea
Phleum pratense ✱
Festuca arundinacea
Bromus inermis
Asparagus officinalis
Plantago rugelii ✱
Plantago major
Solanum dulcamara
Convolvulus arvensis
Asclepias incarnata
Symphyotrichum ericoides
Sonchus oleraceus
Sonchus arvensis
Cichorium intybus
Arctium minus
Persicaria maculosa
Amaranthus albus
Potentilla recta
Geum canadense ✱
Geum aleppicum
Vicia tetrasperma
Medicago sativa
Lotus corniculatus
Desmodium canadense
Oenothera perennis
Oenothera biennis ✱
Lepidium densiflorum ✱
Capsella bursa-pastoris
Sisymbrium officinale

0 5 10 15 20 25 30

Relative abundance (%)

0 1 2 3 4

Relative abundance (%)

C

D

Enhanced growth

Plant–soil feedback

Reduced growth

r = 0.32
P_{FDR} = 0.005

r = - 0.35
P_{FDR} = 0.004

1.5 1.0 0.5 0.0 −0.5 −1.0 −1.5

−5.0 −2.5 0 2.5

−4 −2 0 2 4

Streptomyces ASV1
$\log_2$-fold change

Pseudoxanthomonas
$\log_2$-fold change

E

F

Enhanced growth

Plant–soil feedback

Reduced growth

$P_{FDR} > 0.05$

$P_{FDR} < 0.05$
$r < 0$: 43 taxa
$r > 0$: 23 taxa

$P_{FDR} > 0.05$

$P_{FDR} < 0.05$
$r < 0$: 29 taxa
$r > 0$: 4 taxa

0.8 0.4 0.0 −0.4 −0.8

−5 −4 −3 −2 −1 0 1 2 3 4 5

Endosphere taxon
$\log_2$-fold change

Rhizosphere taxon
$\log_2$-fold change

Root taxon abundance

Focal

Soil-conditioner

A

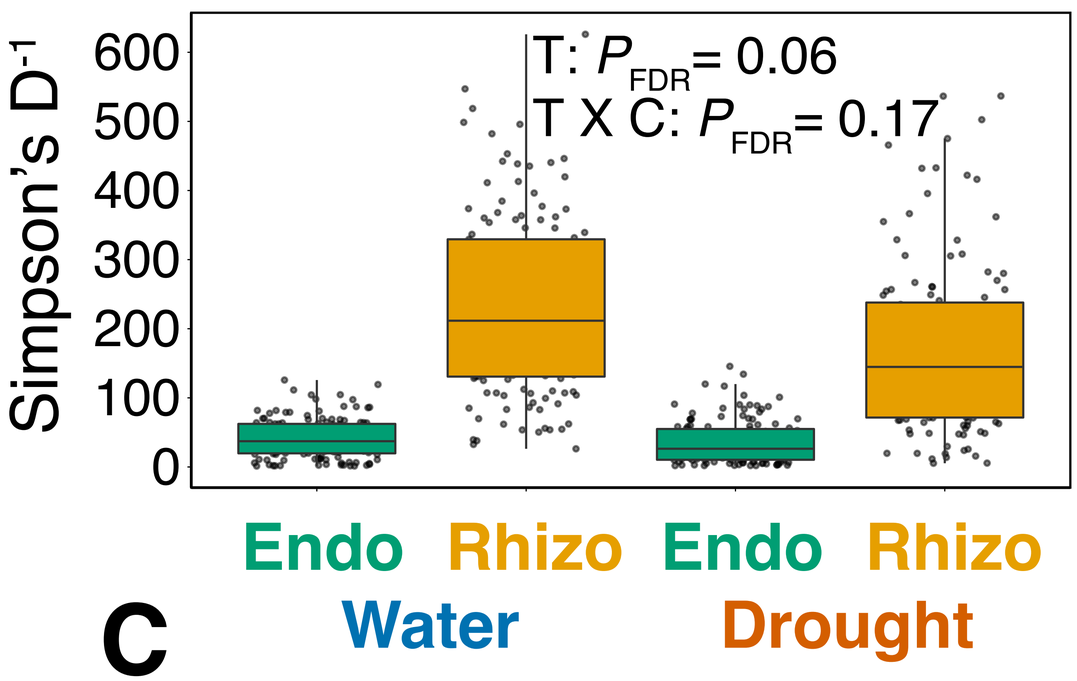
Simpson's D-1
600
500
400
300
200
100
0
T: P_{FDR}= 0.06
T X C: P_{FDR}= 0.17
Endo
Rhizo
Endo
Rhizo
Water
Drought

B

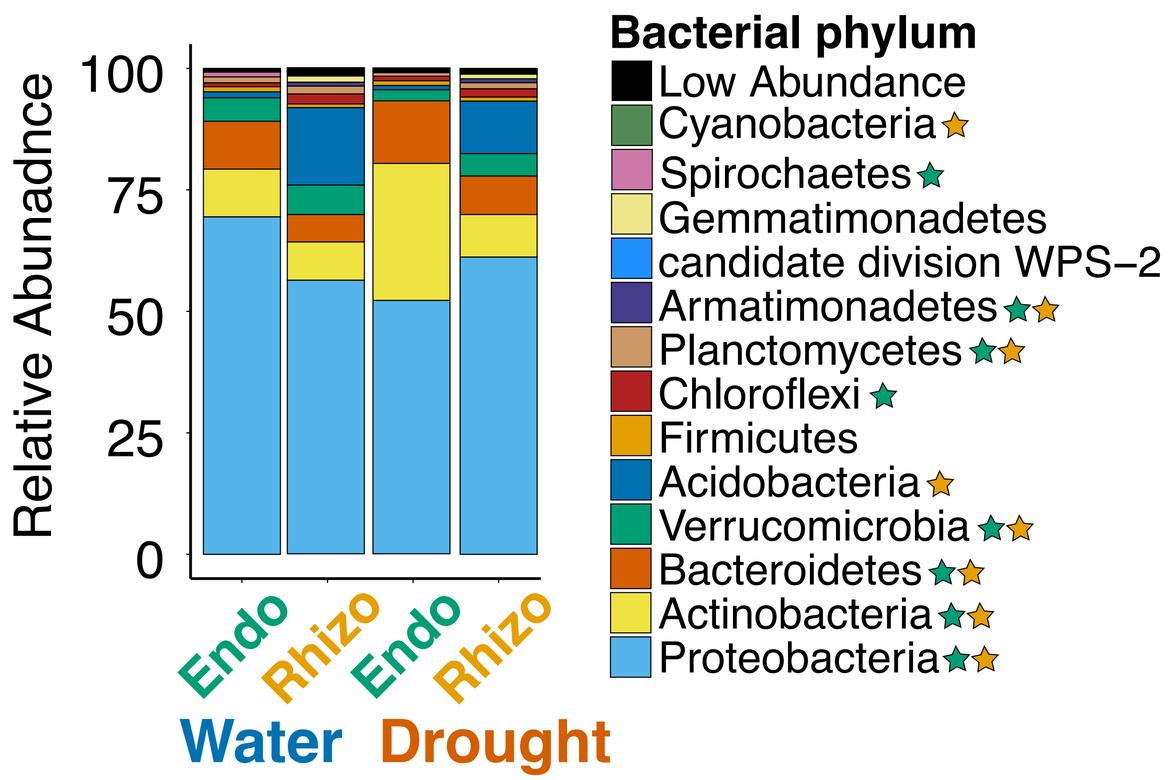
Relative Abunadnce
100
75
50
25
0
Endo
Rhizo
Endo
Rhizo
Water
Drought
Bacterial phylum
Low Abundance
Cyanobacteria
Spirochaetes
Gemmatimonadetes
candidate division WPS–2
Armatimonadetes
Planctomycetes
Chloroflexi
Firmicutes
Acidobacteria
Verrucomicrobia
Bacteroidetes
Actinobacteria
Proteobacteria

C

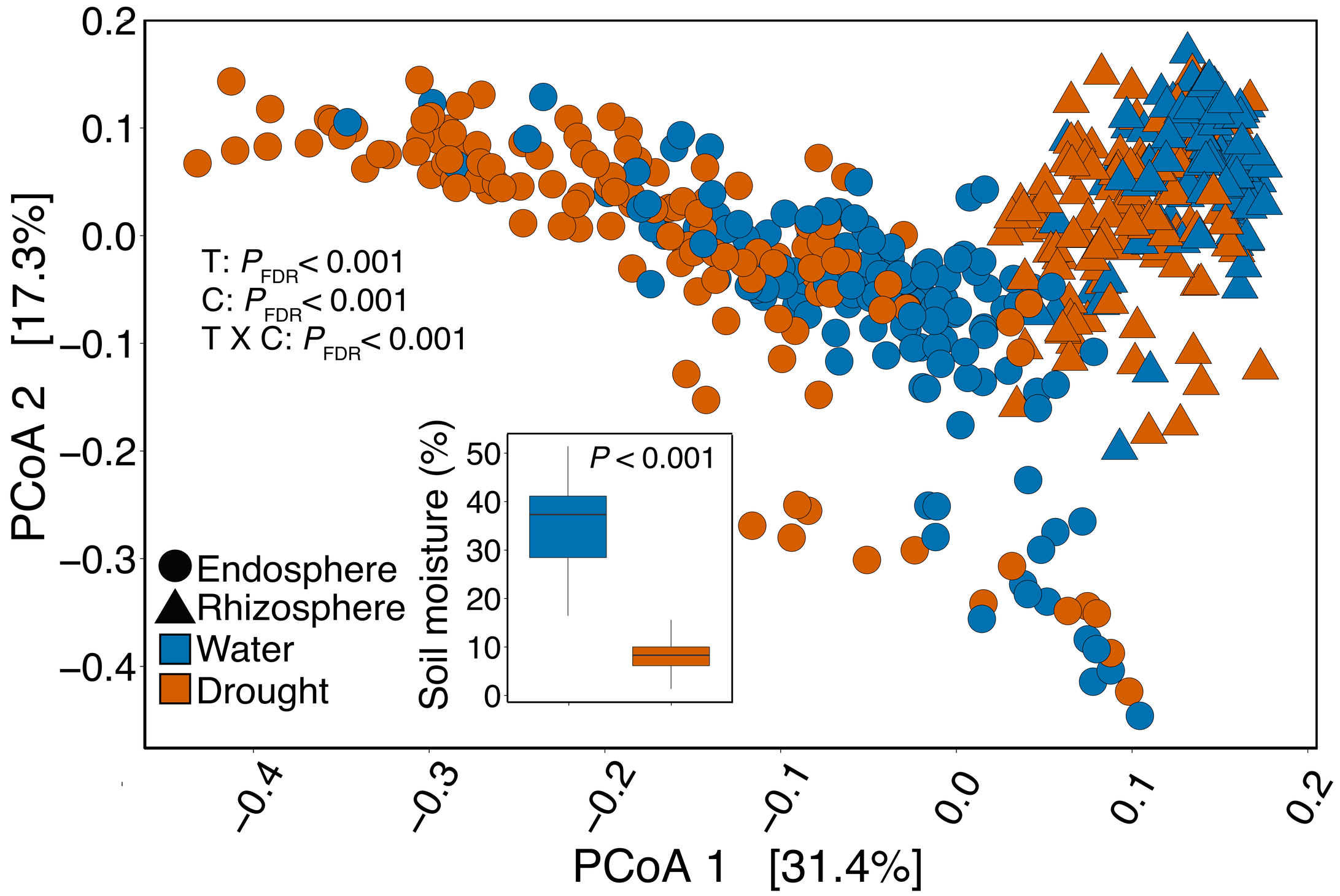
PCoA 2 [17.3%]
0.2
0.1
0.0
–0.1
–0.2
–0.3
–0.4
T: P_{FDR}< 0.001
C: P_{FDR}< 0.001
T X C: P_{FDR}< 0.001
Endosphere
Rhizosphere
Water
Drought
Soil moisture (%)
50
40
30
20
10
0
P < 0.001
–0.4
–0.3
–0.2
–0.1
0.0
0.1
0.2
PCoA 1 [31.4%]

A

Plant biomass (mg)

2500
2000
1500
1000
500
0

T: $P < 0.001$
T X S: $P < 0.001$

Water Drought

B

Streptomycetaceae (relative abundance %)

50
40
30
20
10
0

T: $P < 0.001$
T X S: $P = 0.05$

Water Drought

C

Plant species drought tolerance

1.0
0.5
0.0
−0.5

$r = 0.62$
$P_{FDR} = 0.01$

0.0 2.5 5.0 7.5 10.0

Streptomyces ASV fold change

$\log_2(\text{abundance}_{\text{drought}} / \text{abundance}_{\text{well-watered}})$

SI Appendix

Materials and Methods

Study system

We selected 30 plant species from 19 plant families (Table S1) that co-occur in old field and wetland habitats across north-eastern North America and span approximately 140 million years of angiosperm evolutionary history since their most recent common ancestor. Our selection includes 21 (70%) exotic species and 9 (30%) native species (USDA: https://www.plants.usda.gov/java/); the exotic species invaded regionally following European colonization. Seeds used in our experiment were collected in southern Ontario during the last 15 years from multiple plants within single open-pollinated populations. The seeds were stored frozen prior to germination. All plants co-occur at University of Toronto's 348 hectare Koffler Scientific Reserve (KSR), 50 km North of Toronto, where our soil was collected for experiments.

Plant Phylogeny

We downloaded accessions of 3 genes (2 plastid and 1 nuclear) for each of our plant species from GenBank: ribulose-bisphosphate carboxylase (*rbc*L); maturase K (*mat*K); and internal transcribed spacer (ITS) adjacent to the 5.8S ribosomal RNA gene (see supplementary material for reference (1). We aligned sequences in MEGA v. 6.0 (2) using MUSCLE (3) with default parameters, followed by manually checking alignments. We used BEAST v. 2.1.3 (4) to build a Bayesian phylogenetic tree. For each locus we implemented a standard general time-reversible model (GTR + I + Γ) and an uncorrelated lognormal clock (UCLN) to determine the rate of nucleotide change. We used BEAUTi (4) to constrain the topology and major clade ages of the tree based on a well-resolved plant phylogeny (5). Our Markov chain Monte Carlo simulation ran for 100 million generations sampled every 10,000 generations, which resulted in 9000 post burn-in trees. We examined stationarity and effective sample sizes of parameter estimates (all ESS > 200) using Tracer v1.6 (http://beast.bio.ed.ac.uk/Tracer). We constructed a consensus tree with mean node heights from the posterior distribution using Tree Annotator v1.6 (Fig. 1). We calculated the phylogenetic relatedness (patristic distance) among all pairs of species and used these measures in our statistical analyses. Phylogenetic relatedness between plants ranged from 0 (conspecifics) to 280 million years.

Comparative root microbiome study

We characterized the root microbiome of 30 plant species in a common rooftop environment in the summer of 2014. We surface sterilized seed using the following protocol: we placed seeds for 1 min in 70% ethanol with 0.1% tween, then 12 min in 10% bleach with 0.1% tween, then we rinsed the seeds 3x with sterile water and plated them on 1% agar media plates (Sigma Aldritch A1296) with half-strength MS nutrients (Sigma Aldritch M5119). We staggered our seed treatment so that all species germinated over a one-week period. We transplanted individual seedlings at the cotyledon stage into 1 L pots filled with a combination of sterilized soil and live inoculum collected from KSR. The sterilized soil was a mixture of potting soil and sand (2:3 V/V) to facilitate root harvesting. After double autoclaving, 250 mL of this sterilized mixture was added to each

pot. We then added 750 mL (3/4 pot volume) of homogenized live inoculum to serve as the source of the soil biota. The live soil inoculum was initially collected in equal amounts (80 L/location) from 6 locations across KSR. These locations were representative of the breadth of habitats across the reserve, which includes sand, loam, and clay soil types, low-lying wetland, hardwood forests, meadow, and old-field sites. We sieved the collected soil to 2mm and thoroughly homogenized it to make a single soil inoculum. We kept the plants in a growth chamber for two weeks set to 25°C and 55% humidity, with a 16 h photoperiod (CAN-TROL Environmental Chamber, Markham, Canada) under well-watered conditions to increase seedling survival. After germination, we moved plants to a polyethylene-covered hoop house on a rooftop at the University of Toronto Mississauga.

Rhizosphere and endosphere sampling

After 16 weeks of growth (May-September 2014) we harvested the experiment. We followed, with slight modification, an established protocol that separates a root sample into rhizosphere and endosphere fractions (6, 7). It was impossible to harvest the entire root system from larger plant species so we standardized by mass (500 mg wet weight), and relative position (we took entire lateral roots starting from the third branch below the root crown). Therefore each standard root sample included tertiary roots, root hairs, and root apical meristems. Additionally, we sonicated root samples for 10 min at 60 Hz (Bransonic 521). After this, roots were placed in clean microcentrifuge tubes, flash frozen in liquid nitrogen, freeze-dried, and stored at -80° C until DNA extraction.

DNA extraction

After partitioning root samples into endosphere and rhizosphere fractions we extracted total DNA. We used 96-well plate extraction kits (Power Soil HTP, MoBIO, CA) following the manufacturer's protocol. These kits use both physical and chemical cell lysing to extract DNA. Due to the physical toughness of the endosphere samples we performed a tissue homogenization step prior to DNA extraction. We ground samples at 20 Hz for 30 seconds using a liquid nitrogen cooled tissue homogenizer (CryoMill, Retsch, Germany). We included rhizosphere and endosphere samples on each DNA extraction plate.

PCR amplification

We amplified the V4 region of the 16S rRNA gene, a frequently used locus for prokaryote community characterization by Illumina sequencing. We used a dual-index approach to barcode amplified DNA at the 3' and 5' ends (8). This allowed us to sequence 192 samples simultaneously while identifying the origin of each sequence. To reduce co-amplification of host plant DNA we included peptide nucleic acid (PNA) clamps to each reaction. PNA clamps are sequence specific and block the amplification of unwanted lineages. We included PNA clamps specific to land plant plastids and mitochondria (9). Each PCR included the following reagents and program:

1.5 μL of 10 μM forward indexed primer (515F)
1.5 μL of 10 μM reverse indexed primer (808R)
1 μL of 25 μM mitochondrial PNA

1 µL of 25 µM plastid PNA
6.5 µL PCR grade H_2O
12.5 µL Kappa 2 G Mastermix
1 µL gDNA template

3 min. 95° C
cycle start
15 sec. 95° C - denaturation
15 sec. 78° C - PNA annealing
15 sec. 50° C - primer annealing
15 sec. 72° C - elongation
cycle end
5 min. 72° C

We optimized our PCR cycle number to avoid over-amplification of our template DNA, which can yield chimeric amplicons and PCR artifacts. Based on band intensity on a 1.5% agarose gel we determined that endosphere samples are optimally amplified using 24 cycles and rhizosphere samples using 20 cycles. We performed all reactions in triplicate using an Eppendorf Mastercycler (Eppendorf, Germany). We ran each individual reaction on a 1.5% agarose gel at 100 V for 25 mins to check the success of each reaction. On each 96 well amplification plate we also included reactions with sterile H_2O sample (negative control), DNA isolated from a pure culture of *Pseudomonas aeuruginosa* (positive control), and DNA isolated from a mock community of known bacteria. After pooling triplicate reactions we flourometrically quantified the amplified and pooled product from each individual sample (PicoGreen, Invitrogen). For each sequencing run we then added product from all individual samples to a single tube at equal DNA concentration. Pooled libraries were purified with 0.8X AMPure XP beads (Beckman Coulter Inc.), and quantified using the Qubit HS DNA assay (Thermo Fisher Scientific). Pooled libraries were sequenced on an Illumina MiSeq using 2 X 150 bp paired-end reads.

Bioinformatic pipeline

After trimming primer and index sequences and demultiplexing, we processed sequencing reads using the R package 'DADA2'(10). Due to poor *Q*-scores we trimmed 5 bp from the start and 10 bp from the end of each paired-end sequence. We removed any sequences with ambiguous nucleotide assignment, with any instance of a *Q*-score less than 2, or with greater than 2 expected errors. Unique sequences were dereplicated prior to inferring bacterial taxa. Unique taxa were inferred by DADA2 as **A**mplicon **S**equence **V**ariants (ASVs) instead of **O**perational **T**axonomic **U**nits (OTUs). OTUs represent collections of unique sequences that share a user-defined sequence similarity. Comparisons across experiments are problematic because OTU identity is dependent on the sequences used to perform OTU clustering. By contrast, ASVs represent exact sequence variants inferred from sequence data that are directly comparable across experiments and samples. Based on sequence data supplied by the user, DADA2 generates an error model that evaluates the probability of each unique sequence being a real sequence variant versus a PCR or sequencing artifact. This results in the

simultaneous reduction of false positive taxa and increased resolution of sequence variants that otherwise would be assigned to an OTU clustered at 97% sequence identity (10). We used 50 random samples (each with > 75,000 reads) to parameterize an error model for each sequencing run, which accounts for differences in sequencing performance across runs. After identifying ASVs, we merged forward and reverse sequences and removed chimeras, which resulted in 56,063 ASVs.

We assigned taxonomy to individual ASVs using the RDP naïve Bayesian classifier (implemented in DADA2) and the 'RDP training set 14' (11). After this we used PASTA to align ASV sequences and build a maximum likelihood phylogenetic tree (12). Next, we used the R package 'phyloseq' to further process our samples (13). We removed ASVs that were unassigned to the Bacterial kingdom (1,333 ASVs removed), unassigned to a bacterial phylum or assigned to plastid and mitochondrial lineages (19,129 ASVs removed). This left 24,968,055 sequenced reads distributed across 35,965 ASVs (Fig. S14). Finally, after the above filtering, we removed samples that did not have at least 800 individual sequences (6). Our final dataset consisted of 580 unique microbiome samples (Table S1), each with on average 38,720 high quality sequences (± 1452; SE).

To facilitate the comparison of community composition and differential abundance testing of bacterial taxa we first simplified our dataset to include only the common ASVs. We applied a prevalence and abundance threshold using the full dataset where ASVs had to be found in at least 1% of samples (7 samples) at an abundance of at least 25 sequences per sample (6). Using this prevalence and abundance threshold yielded the expected number of ASVs amongst our control samples. This threshold yielded 2,799 ASVs, which accounted for 94% of the total number of sequences in the dataset (Fig. S14). For downstream composition analyses we performed proportional abundance normalization (relative abundance) on this common set of ASVs, where the sequencing reads for an ASV in a given sample were divided by the total number of sequencing reads in that sample (14). As an additional set of analyses, we also used the traditional approach of rarefaction (to 800 reads) to normalize our dataset, which yielded approximately 13,000 ASVs and accounted for less than 2% of the total read count (Fig. S14). Both methods yielded qualitatively identical results; therefore we focus our interpretation on the non-rarefied data because it retained a much larger portion of our available data.

Plant-soil feedback experiment

To investigate how variation in the root microbiome across plant species contributes to plant-soil feedback, we performed a two-generation experiment (plant-soil feedback data available in reference (1). In the first generation we used our 30 plant species to condition an initially homogenous field soil collected from the University of Toronto's Koffler Scientific Reserve. Pots were filled with 800 mL of sterilized soil (mixture of potting soil and sand [2:3 V/V]) and 200 mL of live inoculum collected from KSR. We grew five individuals from each of our 30 species under well-watered conditions following the same protocol as described above for the rooftop experiment. At the end of generation

one (12 weeks) we harvested and pooled bulk and rhizosphere soil from five individuals for each of our 30 species. Soil was preserved at -20°C until the second generation.

In the second generation we selected five focal species that span the evolutionary and phenotypic breadth of the 30 species from generation one. We grew *Oenothera biennis* (Onagraceae), *Plantago rugelii* (Plantaginaceae), *Phleum pratense* (Poaceae), *Lepidium densiflorum* (Brassicaceae), and *Geum canadense* (Rosaceae), in each of the 30 conditioned soil treatments harvested from generation one. We germinated the focal species in the same manner as described previously and planted seedlings singly into 500 mL pots. We planted each of our five focal species into soil conditioned by each of the 30 species (including soil conditioned by the focal species themselves) from generation one, plus a sterile potting mix treatment, for a total of 155 unique focal plant x soil treatment combinations with 4 replicate pots per combination. Each pot received 400 mL of a sterile potting soil and sand mixture (2:3 V/V) and 100 mL of live soil inoculum, preserved from the first generation. We grew plants in a growth chamber (Conviron CMP6050, Winnipeg, Canada) in a randomized block design. We placed plastic portion cups under plant pots to minimize the transfer of water, soil material, and microorganisms between pots. Plants were unfertilized and watered *ad libitum*. We programmed the chambers to simulate the average daily and weekly temperature fluctuations during the months of May-August in Toronto, ON. After 8 weeks we harvested all above and belowground tissue from each pot and oven-dried tissue at 60 °C for 72 hours and weighed it to the nearest 0.1 mg. We used these biomass measurements to calculate our plant-soil feedback metric.

Our plant-soil feedback metric compares focal plant performance in soil conditioned by a conspecific plant versus soil conditioned by a heterospecific plant. First, we normally standardized our raw biomass data (mean = 0, sd = 1), and removed the effect of spatial blocks in generation two by fitting a linear model with only block included as a predictor variable. We used the residuals from this model as our new response variable. For each focal species x soil conditioning combination, we calculated the feedback metric as: ln ((mean total biomass of focal species$_x$ in soil conditioned by species$_y$)/(mean total biomass of focal species$_x$ in soil conditioned by species$_x$)). Positive values indicate that a focal species performed better in soil conditioned by a heterospecific plant compared to a conspecific plant, whereas negative values indicate the opposite. This feedback metric is symmetrical which means positive and negative values are directly comparable. We chose this particular plant-soil feedback metric because it is best suited for investigating plant-soil feedbacks among multiple plant species (15, 16). We used differences in root microbiome composition and differential abundance of particular bacterial taxa to predict the variation in plant-soil feedback strength and direction across our pairs of interacting plant species.

Water manipulation experiment

In our comparative root microbiome study we characterized the root microbiome of 30 plant species in well-watered and water-limited conditions. We used a drip irrigation system to precisely control the amount of water delivered to individual pots. In a fully randomized block design we grew 5 individuals from each species in well-watered

conditions and 5 individuals in drought conditions. Well-watered pots received approximately 1L of water/day and water-limited pots received approximately 0.25L of water/day. Individual pots were placed in plastic dishes to eliminate the transfer of material between pots. We measured the percent volumetric water content in 40 random pots in each treatment bi-weekly for the course of the experiment (TDR 300, Spectrum Technologies, Aurora, IL, USA). To test whether our treatment significantly altered soil moisture we used a linear mixed model with watering treatment as a fixed effect and time and treatment X time as random effects. We used type III Welch tests and the Kenward-Roger estimator of denominator degrees of freedom from the R package 'car' to test the significance of fixed effects. We used likelihood ratio tests comparing full and reduced models to test the significance of random effects. We achieved a four-fold difference in soil moisture between the two treatments throughout the experiment. To determine how soil microbial communities respond to water limitation in the absence of plants we also included 10 unplanted pots filled with the identical soil mixture in each watering treatment. Alongside plants we also included identically treated, non-living structures (bamboo toothpicks) analogous to plant roots in our root microbiome characterization (7). Comparing the bacterial communities in living roots to non-living root analogues reveals the indirect, host-mediated effects of drought. Our root analogues were treated identically to plant roots during harvesting, DNA extraction, and rhizosphere/endosphere partitioning.

Phenotypic measurements

We measured traits on five well-watered individuals for each of our 30 species during our rooftop water manipulation experiment (Table S2): i) total aboveground biomass, ii) total belowground biomass, iii) length of longest root, iv) rooting angle; v) leaf dry matter content (LDMC); vi) specific leaf area (SLA); vii) root hair density; and viii) specific root length (SRL). We selected these particular traits due to their documented effects on soil ecosystems and their importance in general plant ecology. Biomass traits can have large effects on soil ecosystems and are often correlated with plant fitness. Root morphological traits influence the physical attributes of surrounding soil and can affect the colonization of particular soil microbes (17). Physiological traits of leaves and roots describe soil resource consumption and can influence plant competition (18, 19). In particular, SLA describes the broad resource acquisition strategy of a plant and scales positively with relative growth rate and negatively with interspecific competition (19-21).

We used a standardized protocol to measure phenotypic traits on each individual (22). After 8 weeks we removed a leaf disc of equal area (1.54 cm^2) from each plant and measured wet weight to the nearest 0.1 μg on a microbalance (XP2U, Mettler Toledo, Mississauga, Canada). Then, we dried the leaf discs at 72°C for 3 days and weighed them to calculate LDMC as the dry weight divided by the wet weight. Using the same leaf disc we divided the area of the leaf portion by its dry mass to calculate SLA. After 16 weeks of growth we cut each plant at the base of the stem where it met the soil surface and placed all aboveground tissue in a paper bag and dried it for 3 days at 72° C. After harvesting a standard root sample for microbiome profiling we measured root traits. We used a string to trace the length of the longest root from tip to attachment to the main aboveground stem and measured the length of the string. We measured root angle as the

average angle of the first three lateral roots below the root crown using a protractor, capturing the degree of lateral versus vertical root growth. To measure SRL we removed the distal 5 cm of the first 3 lateral roots below the root crown and photographed them before drying. We measured the total area of these root portions and divided this by their dry weight (72°C for 3 days) to calculate SRL. We also calculated the average root hair density by counting the number of root hairs occurring across these 3 fragments. We washed remaining belowground tissue using a sieve and water to remove all soil particles and dried it for 3 days at 72° C. We weighed all tissue to the nearest 0.1g to determine aboveground, belowground and total dry biomass. To create a metric of phenotypic similarity we normally standardized species' mean trait values and calculated the multi-trait Euclidean distance between species.

Statistical analyses

α-diversity describes the number of taxa within a community, while β-diversity measures compositional differences between communities. For each sample we calculated observed species richness, Shannon's diversity, inverse Simpson's diversity, and evenness (measured as inverse Simpson's diversity/observed richness). We present results using the full dataset but results are qualitatively similar to those obtained when using the simplified or rarefied datasets (Fig. S15). Estimates of alpha diversity using the full dataset are highly correlated with estimates obtained when using the simplified (R^2 = 0.99, $P < 0.001$), or rarefied datasets ($R^2 = 0.97$, $P < 0.001$). Using the simplified dataset we performed a Principle Coordinate Analysis (PCoA) using weighted and unweighted UniFrac, and Bray-Curtis dissimilarity matrices. UniFrac distance provides a measure of the unique fraction of phylogenetic diversity (non-shared) between samples. The weighted version of UniFrac takes into account differences in taxon abundance while the unweighted version does not. The Bray-Curtis dissimilarity provides a measure of differences in taxon abundance between communities. Thus, two samples which exhibit high Bray-Curtis dissimilarity yet relative low weighted UniFrac distance will differ in their abundance of particular taxa but those taxa will be closely related to one another. Analysis of these three distance measures yielded qualitatively similar results, thus we focus our attention on the analysis of the weighted UniFrac distance due to its increased ability to separate microbial community composition (23). We generated these dissimilarity matrices from the proportional-abundance normalized (relative abundance) dataset (14). We repeated the above analysis for endosphere and rhizosphere samples separately. We also repeated all the above analyses using our rarefied dataset to verify that our proportional-abundance normalized and rarefied datasets exhibited similar trends (Fig. S4). Mantel tests between weighted UniFrac distance matrices calculated using either proportional-abundance normalized or rarefied datasets yielded very high correlations (endosphere, $r = 0.99$, $P < 0.001$; rhizosphere, $r = 0.98$, $P < 0.001$). We analyzed sample scores along PCoA axes to determine the effect of compartment (endosphere versus rhizosphere), watering treatment, and host plant species on composition (Table S4).

The effect of compartment, host plant, and watering treatment on α- and β-diversity

We used linear mixed effects models (24) to analyze the effects of compartment, watering treatment, and host plant species on α-diversity and β-diversity of our plant root

microbiomes (Table S3, S4). α-diversity was measured as observed species richness, Shannon's diversity index, inverse Simpson's index, and evenness. We used the natural log of Shannon's diversity and inverse Simpson's index. β-diversity was quantified according to the sample scores along the first three PCoA axes repeated for Bray-Curtis, weighted UniFrac, and unweighted UniFrac PCoA analyses. Initially we fit a model on the full dataset which included:

response variable = compartment + treatment + compartment x treatment + log(useable sequences) + host species + host species x compartment + host species x treatment + host species x compartment x treatment + MiSeq run + experimental block

Usable sequences was the total number of Illumina MiSeq sequence reads retained in each sample; MiSeq run was the sequencing run each sample occurred on; and experimental block was the randomized block in the water manipulation experiment that each sample came from. Compartment, treatment and usable sequences were treated as fixed effects and host species (including interactions), MiSeq run and experimental block were treated as random effects. We used type III ANOVA from the R package 'car' to test the significance of fixed effects (25). We performed likelihood ratio tests comparing full and reduced models to test the significance of random effects using the R package 'lmerTest' (26). Since we found significant interactions between compartment and other experimental factors we also analyzed the endosphere and rhizosphere datasets separately (Table S3, S4). For these analyses using either the endosphere or rhizosphere samples our model included:

response variable = treatment + log(useable sequences) + host species + host species x compartment + host species x treatment + host species x compartment x treatment + MiSeq run + experimental block

We diagnosed the fit of our models by examining the homoscedasticity of residuals versus fitted values, as well as the normality of residuals. We used the false discovery rate to control for multiple hypothesis testing (27). For our analysis of community composition we also performed PERMANOVA using the *adonis* function from the 'vegan' package in R (Table S5). PERMANOVA is a non-parametric method of multivariate analysis of variance, which partitions variation in distance matrices between microbial community samples among experimental factors. Findings from our mixed models and PERMANOVA were very similar (Table S4, S5). We performed all the above analyses with our rarefied dataset and obtained qualitatively and quantitatively very similar results (Fig. S3, S4; Table S3, S4, S5).

The effect of host phylogenetic relatedness on the root microbiome

To understand how macroevolution across our clade of plant species influences the root microbiome we estimated the phylogenetic signal occurring in measures of diversity. We estimated Blomberg's K which measures the distribution of a trait across a phylogeny and compares it to the distribution under a model of constant Brownian motion evolution

across the phylogeny, which is the expectation under genetic drift (28). A K of 1 indicates that the trait distribution across a phylogeny corresponds to a Brownian motion model of evolution, whereas an increase or decrease from 1 indicates evolution has caused close relatives to resemble one another more or less, respectively, than expected due to genetic drift. We used the R package 'phytools' (29) to calculate K* (as per 30), which accounts for within-species variation, for each of our measures of community diversity across our host plant species (Table S6). To test the significance of K* we performed a randomization test whereby tip data are randomized across the phylogeny repeatedly while K is re-calculated each time to give the expected distribution of K if there were no phylogenetic signal. The observed value of K is then compared to this distribution to obtain a P-value. Additionally, we calculated Pagel's λ and found qualitatively similar patterns of phylogenetic signal.

We used the patristic distance and phenotypic distance between host plant species to test whether phylogenetic relatedness or overall phenotypic similarity predicted root microbiome similarity. To produce a distance matrix for host plant species differences in root microbiome composition, we took the Euclidean distance between host species' centroids calculated from our PCoA axes. We performed Mantel tests (matrix correlation) between the patristic distance or phenotypic distance matrix and the Euclidean distance matrix of host plant species PCoA axis scores. For example, a Mantel test between host plant patristic distance and host plant endosphere PCoA scores would yield a measure of the correlation between host plant phylogenetic relatedness and endosphere compositional similarity. We repeated the analysis for each of our PCoAs (Bray-Curtis, weighted UniFrac, unweighted UniFrac), for endosphere and rhizosphere compartments (Table S7).

The effect of plant traits on the root microbiome

We used phylogenetic generalized least squares regression (PGLS) to analyze the effect of individual plant traits on the diversity and composition of the endosphere and rhizosphere microbiome using the R package 'ape'(31). PGLS accounts for the evolutionary non-independence among species by modelling residual error according to a phylogenetic tree and a particular model of evolution. For each multiple regression PGLS model, we determined whether the data fit an error structure corresponding to a Brownian motion, adaptive optimum (Ornstein-Uhlenbeck), or a null (i.e. no phylogenetic signal) model of evolution. We then used the dredge function from the R package MuMIn (32), which uses maximum likelihood to evaluate multiple regression models including all possible combinations of predictors. We used Akaike information criterion scores to identify the best fitting models (ΔAIC 2), and report averaged, standardized trait coefficients weighted by each model's AIC score. We built separate multiple regression models for each of our estimates of diversity and composition. We modelled the effect of individual plant traits on plant species' means for observed species richness, Shannon's and inverse Simpson's diversity, and evenness for endosphere and rhizosphere compartments separately (Table S8). For estimates of community composition, we took the host species' centroids calculated from our PCoA axes using weighted UniFrac distances and modelled the effect of individual plant traits. We repeated the analysis for

endosphere and rhizosphere compartments (Table S8). We used the false discovery rate to correct for multiple hypothesis testing.

Differential abundance testing

The common ASV datasets (i.e. dataset filtered using the prevalence and abundance threshold), were used to test how compartment, watering treatment, and host plant species affect the abundance of bacterial phyla, classes, orders, families, genera, and individual ASVs (33). We used phyloseq to agglomerate our ASV count table into higher taxonomic ranks and produce count tables for bacterial genera up to phyla. We used the R package 'DESeq2', which was originally designed for RNA-seq data but is an effective method to test for differential abundance in deep-amplicon sequencing studies (34). DESeq2 fits negative binomial generalized linear models to count data (number of reads, ASVs etc.) and estimates their $\log_2$-fold change in abundance across one or more interacting experimental factors. Overdispersion (high variance:mean abundance ratio) is modeled by estimating feature-specific dispersion parameters. Recent benchmarking work demonstrated that DESeq2 exhibits high false positive rates and reduced sensitivity when library sizes across factor levels are very uneven (35). Given that our dataset exhibits even library size across each of the levels of our experimental factors, we used DESeq2 to determine which bacterial taxa are influenced, and how strongly, by community fraction, watering treatment, and host plant species.

Initially we fit a model to the full dataset, which included compartment, watering treatment, host species and compartment by host species interaction. We then performed likelihood ratio tests to determine whether the compartment (endosphere versus rhizosphere) and the compartment by host species interaction affected the abundance of individual bacterial taxa. We analyzed the effect of host species and watering treatment on endosphere and rhizosphere compartments separately because our PCoA plots demonstrated that these communities respond very differently to these factors. We fit a model with watering treatment, host species and the watering treatment by host species interaction for endosphere and rhizosphere compartments separately. We then performed a series of likelihood ratio tests on nested models to determine the significance of each factor on the abundance of each individual bacterial taxon. We repeated the above analyses for each bacterial taxonomic level (Fig. S4). Multiple hypothesis testing at each taxonomic level was corrected for by applying the false discovery rate (27).

To estimate $\log_2$ fold changes in abundance for a given taxon we used specific contrasts implemented with a Wald test of significance. For the effect of community fraction we used the full dataset to estimate the $\log_2$-fold change in abundance for each bacterial taxon between endosphere and rhizosphere compartments. For the effect of watering treatment, separate tests were performed on endosphere and rhizosphere taxa to estimate the $\log_2$-fold change in abundance for each bacterial taxon between well-watered and water-limited treatments. For the effect of host plant species, we estimated the $\log_2$-fold change in abundance for each bacterial taxon for every pairwise comparison between host species and the grand mean estimated across all host species. For the interaction between host plant species and watering treatment we estimated the $\log_2$-fold change in abundance for each bacterial taxon between well-watered and drought communities

separately for each host plant species. We repeated all of these analyses at each bacterial taxonomic level (i.e., phylum, class, order, family, genus, ASVs). We used the false discovery rate to isolate only significant estimates of $\log_2$-fold change occurring at each taxonomic level and for each taxon within a level. We repeated the above analysis using our root analogue (toothpick) samples to determine what bacterial taxa were enriched in non-living root samples and drought (Dataset S3).

Plant-soil feedbacks and the root microbiome

We sought to understand how variation in root microbial communities influenced the soil feedbacks between plant species. This analysis required a measure of root microbial community similarity between species to predict variation in our experimentally measured plant-soil feedback. To produce a distance matrix of host plant species root microbiome composition we took the Euclidean distance between host species' centroids calculated from our PCoA axes (weighted and unweighted UniFrac distances). We used simple linear models using pairwise plant-soil feedback measures between plant species as our response variable and their pairwise root microbial community Euclidean distance as our explanatory variable (Fig. S8). We then performed a permutation test to determine the significance of the observed slope from our linear regression. We compared our observed value to a distribution obtained after randomizing the microbial community composition data and performing the same linear regression 10,000 times (Fig. S8). For each randomization, values of endosphere or rhizosphere dissimilarity were permuted among pairs of plant species while their phylogenetic relatedness was left intact.

To understand how individual bacterial taxa might be driving plant-soil feedbacks, we performed a more targeted analysis. First, using the differential abundance results, we created a list of all bacterial taxa at each taxonomic rank in the endosphere and rhizosphere that were significantly affected by host plant species (host-responsive). We then calculated $\log_2$-fold changes occurring for each of these taxa between each unique focal plant species X soil-conditioning plant species pairs using DESeq2. We used the common endosphere or rhizosphere dataset and fit a model with watering treatment and host plant species. Using specific contrasts implemented with a Wald χ^2 test we obtained $\log_2$ fold change estimates for each bacterial taxon between focal plant species X soil-conditioning species pairs. We correlated the pairwise plant-soil feedback measures between plant species with their $\log_2$ fold change estimate for each of our host-responsive bacterial taxa (Dataset S2). We used the false discovery rate to control for multiple hypothesis testing (27). These correlations identify bacterial taxa whose differential abundance between plant host species is significantly related to the strength of plant-soil feedback.

The effect of root microbiome composition on drought tolerance

The effect of drought on the composition of the root microbiome was not uniform across plant species (Fig. S7, Table S4). We sought to test whether differences in root microbial composition across plant species in response to drought was related to drought tolerance of host plants. Drought tolerance of each species was calculated as the proportional reduction in biomass due to drought:

$$\textbf{Drought tolerance} = \frac{\textbf{Biomass}_{\textbf{drought}} - \textbf{Biomass}_{\textbf{watered}}}{\textbf{Biomass}_{\textbf{watered}}}$$

Negative values indicate a loss of biomass in response to drought while positive values indicate a gain in biomass (Fig. S10). Next, average plant species scores along the first two PCoA axes of the weighted UniFrac distance ordination of endosphere and rhizosphere communities in drought conditions were correlated with drought tolerance. This tested whether overall measures of community composition, captured by our ordinations, predicted variation in drought tolerance among plant species. We also tested whether compositional shifts in response to drought, captured by our ordinations, predicted drought tolerance. Our measure of compositional shift was the Euclidean distance between plant species' PCoA (weighted and unweighted UniFrac distance) centroids of endosphere and rhizosphere compartments in drought versus well-watered conditions. Additionally, we tested whether endosphere or rhizosphere diversity under drought conditions was correlated with drought tolerance across host plant species.

Next, we asked how individual bacterial taxa in roots might be related to plant drought tolerance. First, using our differential abundance results, we created a list of all bacterial taxa found in endosphere and rhizosphere compartments at each taxonomic rank that were significantly affected by the drought treatment (e.g. Fig. S9 and S11). We estimated the $\log_2$-fold change in abundance for each bacterial taxon between well-watered and drought conditions separately for each host plant species. We used the common endosphere or rhizosphere dataset and fit a model with watering treatment and host plant species and obtained specific contrasts implemented with a Wald χ^2 test . We correlated the $\log_2$-fold change between watering treatments for each drought-sensitive bacterial taxon with host plant species' drought tolerance (Dataset S4). We used the false discovery rate to control for multiple hypothesis testing. These correlations identify bacterial taxa whose host-specific change in abundance between watering treatments is significantly related to host drought tolerance.

SI References

1. Fitzpatrick CR, Gehant L, Kotanen PM, Johnson MTJ (2017) Phylogenetic relatedness, phenotypic similarity and plant–soil feedbacks. *J Ecol* 105(3):786–800.

2. Tamura K, Stecher G, Peterson D, Filipski A, Kumar S (2013) MEGA6: Molecular evolutionary genetics analysis version 6.0. *Mol Biol Evol* 30(12):2725–2729.

3. Edgar RC (2004) MUSCLE: multiple sequence alignment with high accuracy and high throughput. *Nucleic Acids Res* 32(5):1792–1797.

4. Drummond AJ, Suchard MA, Xie D, Rambaut A (2012) Bayesian phylogenetics with BEAUti and the BEAST 1.7. *Mol Biol Evol* 29(8):1969–1973.

5. Bell CD, Soltis DE, Soltis PS (2010) The age and diversification of the angiosperms re-revisited. *Am J Bot* 97(8):1296–1303.

6. Lundberg DS, et al. (2012) Defining the core *Arabidopsis thaliana* root microbiome. *Nature* 488(7409):86–90.

7. Bulgarelli D, et al. (2012) Revealing structure and assembly cues for *Arabidopsis* root-inhabiting bacterial microbiota. *Nature* 488(7409):91–95.

8. Kozich JJ, Westcott SL, Baxter NT, Highlander SK, Schloss PD (2013) Development of a dual-index sequencing strategy and curation pipeline for analyzing amplicon sequence data on the MiSeq Illumina sequencing platform. *Appl Environ Microbiol* 79(17):5112–5120.

9. Lundberg DS, Yourstone S, Mieczkowski P, Jones CD, Dangl JL (2013) Practical innovations for high-throughput amplicon sequencing. *Nat Meth* 10(10):999–1002.

10. Callahan BJ, et al. (2016) DADA2: High-resolution sample inference from Illumina amplicon data. *Nat Meth* 13(7):581–583.

11. Wang Q, Garrity GM, Tiedje JM, Cole JR (2007) Naive Bayesian classifier for rapid assignment of rRNA sequences into the new bacterial taxonomy. *Appl Environ Microbiol* 73(16):5261–5267.

12. Mirarab S, et al. (2015) PASTA: ultra-large multiple sequence alignment for nucleotide and amino-acid sequences. *J Comput Biol* 22(5):377–386.

13. McMurdie PJ, Holmes S (2013) phyloseq: an R package for reproducible interactive analysis and graphics of microbiome census data. *PLoS ONE* 8(4):e61217–11.

14. McMurdie PJ, Holmes S (2014) Waste not, want not: why rarefying microbiome data is inadmissible. *PLoS Comput Biol* 10(4):e1003531–12.

15. Pernilla Brinkman E, van der Putten WH, Bakker E-J, Verhoeven KJF (2010) Plant-soil feedback: experimental approaches, statistical analyses and ecological interpretations. *J Ecol* 98(5):1063–1073.

16. Klironomos JN (2002) Feedback with soil biota contributes to plant rarity and invasiveness in communities. *Nature* 417(6884):67–70.

17. Bardgett RD, Mommer L, de Vries FT (2014) Going underground: root traits as drivers of ecosystem processes. *Trends Ecol Evol* 29(12):692–699.

18. Orwin KH, et al. (2010) Linkages of plant traits to soil properties and the functioning of temperate grassland. *J Ecol* 98(5):1074–1083.

19. Kraft NJB, Godoy O, Levine JM (2015) Plant functional traits and the multidimensional nature of species coexistence. *Proc. Natl. Acad. Sci. U.S.A* 112(3):797–802.

20. Westoby M (1998) A leaf-height-seed (LHS) plant ecology strategy scheme. *Plant Soil* 199(2):213–227.

21. Kunstler G, et al. (2016) Plant functional traits have globally consistent effects on competition. *Nature* 529(7585):204–207.

22. Cornelissen JHC, et al. (2003) A handbook of protocols for standardised and easy measurement of plant functional traits worldwide. *Aust J Bot* 51(4):335-380.

23. Thorsen J, et al. (2016) Large-scale benchmarking reveals false discoveries and count transformation sensitivity in 16S rRNA gene amplicon data analysis methods used in microbiome studies. *Microbiome* 4(1):62. doi:10.1186/s40168-016-0208-8.

24. Bates D, Maechler M, Bolker B, Walker S (2015) Fitting linear mixed-effects models using lme4. *J Stat Softw* 67(1):1-48.

25. Fox J, Weisberg S (2011) *An {R} companion to applied regression*. Thousand Oaks, CA.

26. Kuznetsova A, Brockhoff PB, Christensen R (2017) lmerTest package: tests in linear mixed effects models. *J Stat Softw* 82(13):1–26.

27. Benjamini Y, Hochberg Y (1995) Controlling the false discovery rate: a practical and powerful approach to multiple testing. *J R Stat Soc Series B Stat Methodol* 57(1):289–300.

28. Blomberg SP, Garland T, Ives AR (2003) Testing for phylogenetic signal in comparative data: behavioral traits are more labile. *Evolution* 57(4):717–745.

29. Revell LJ (2011) phytools: an R package for phylogenetic comparative biology (and other things). *Methods Ecol Evol* 3(2):217–223.

30. Ives AR, Midford PE, Garland T JR. (2007) Within-species variation and measurement error in phylogenetic comparative methods. *Systematic Biol* 56(2):252–270.

31. Paradis E, Claude J, Strimmer K (2004) APE: analyses of phylogenetics and evolution in R language. *Bioinformatics* 20(2):289–290.

32. Barton K (2015) MuMIn: multi-model inference. Version 1.40.0 http://mumin.r-forge.r-project.org/MuMIn-manual.pdf

33. Wagner MR, Lundberg DS, Del Rio TG, Tringe SG, Dangl JL, Mitchell-Olds T (2016) Host genotype and age shape the leaf and root microbiomes of a wild perennial plant. *Nat Commun* 7:12151.

34. Love MI, Huber W, Anders S (2014) Moderated estimation of fold change and dispersion for RNA-seq data with DESeq2. *Genome Biology* 15(12):31–21.

35. Weiss S, et al. (2017) Normalization and microbial differential abundance strategies depend upon data characteristics. *Microbiome* 5(1):27. doi:10.1186/s40168-017-0237-y.

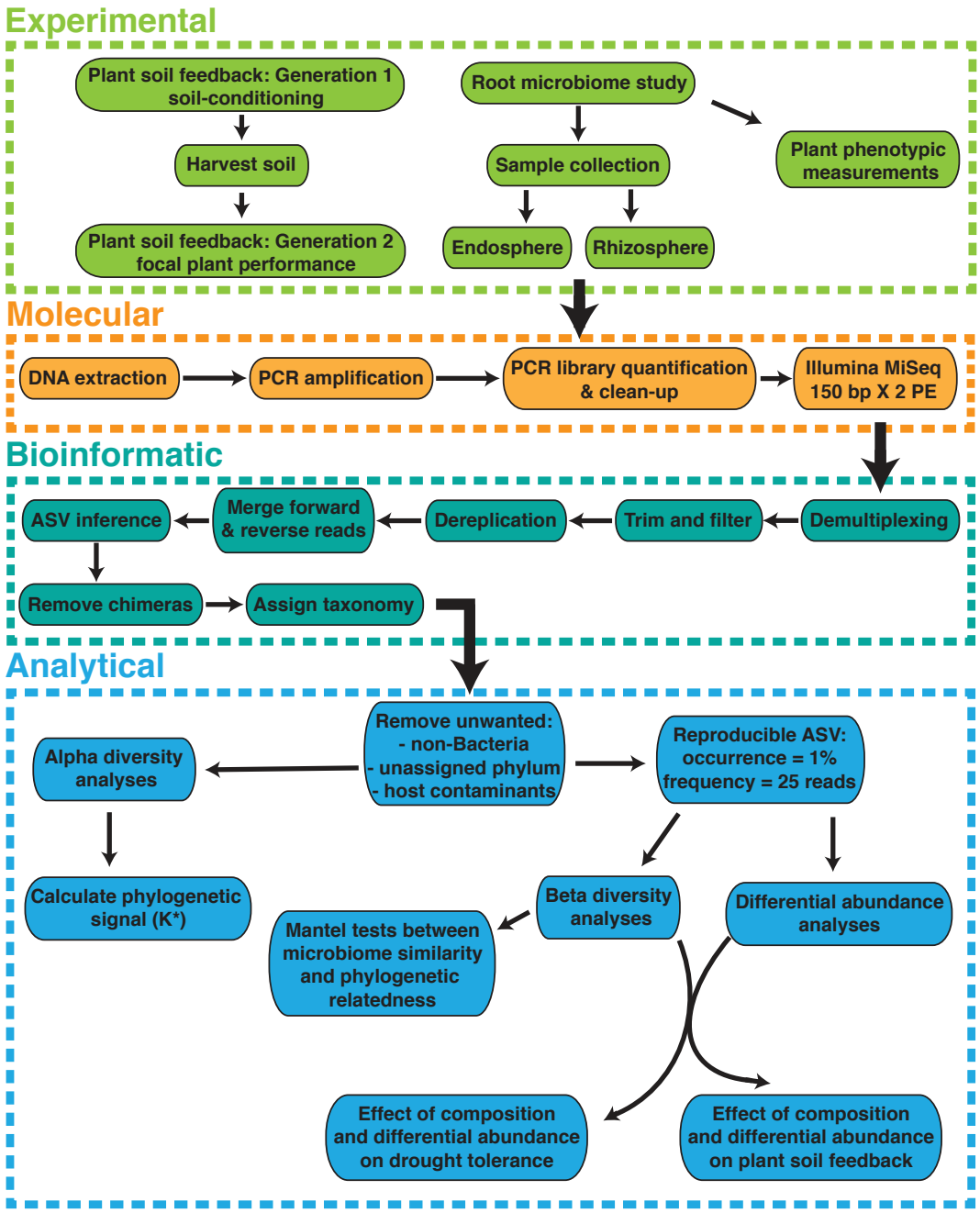

Fig. S1 | Flow chart of the experimental, molecular, bioinformatic and analytical components of the project.

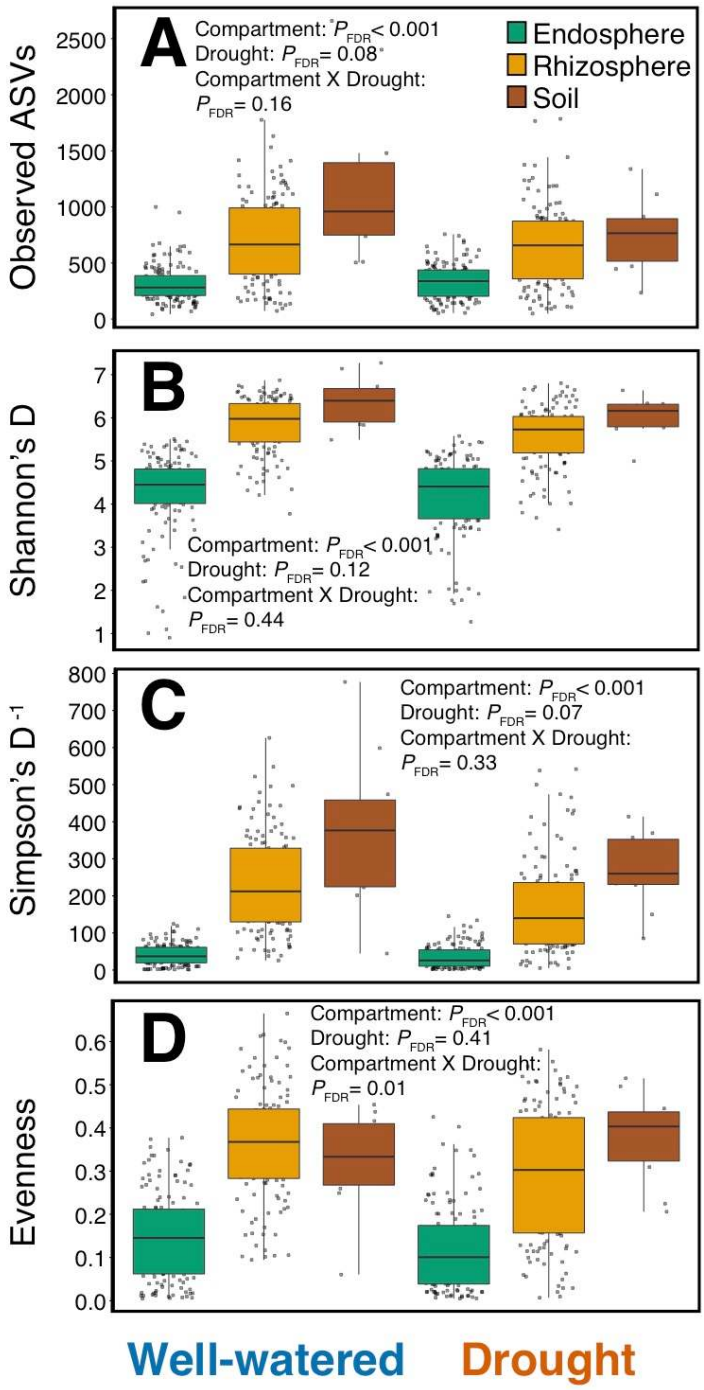

Fig. S2 | Alpha diversity varies across bacterial compartment and watering treatment. (*A*) Compartment has strong effects on species richness (*B*), Shannon's diversity (*C*), Simpson's diversity^{-1} and (*D*), evenness. Drought only directly influences Simpson's diversity^{1} and interacts with compartment to influence evenness. All *P*-values adjusted using the false discovery rate.

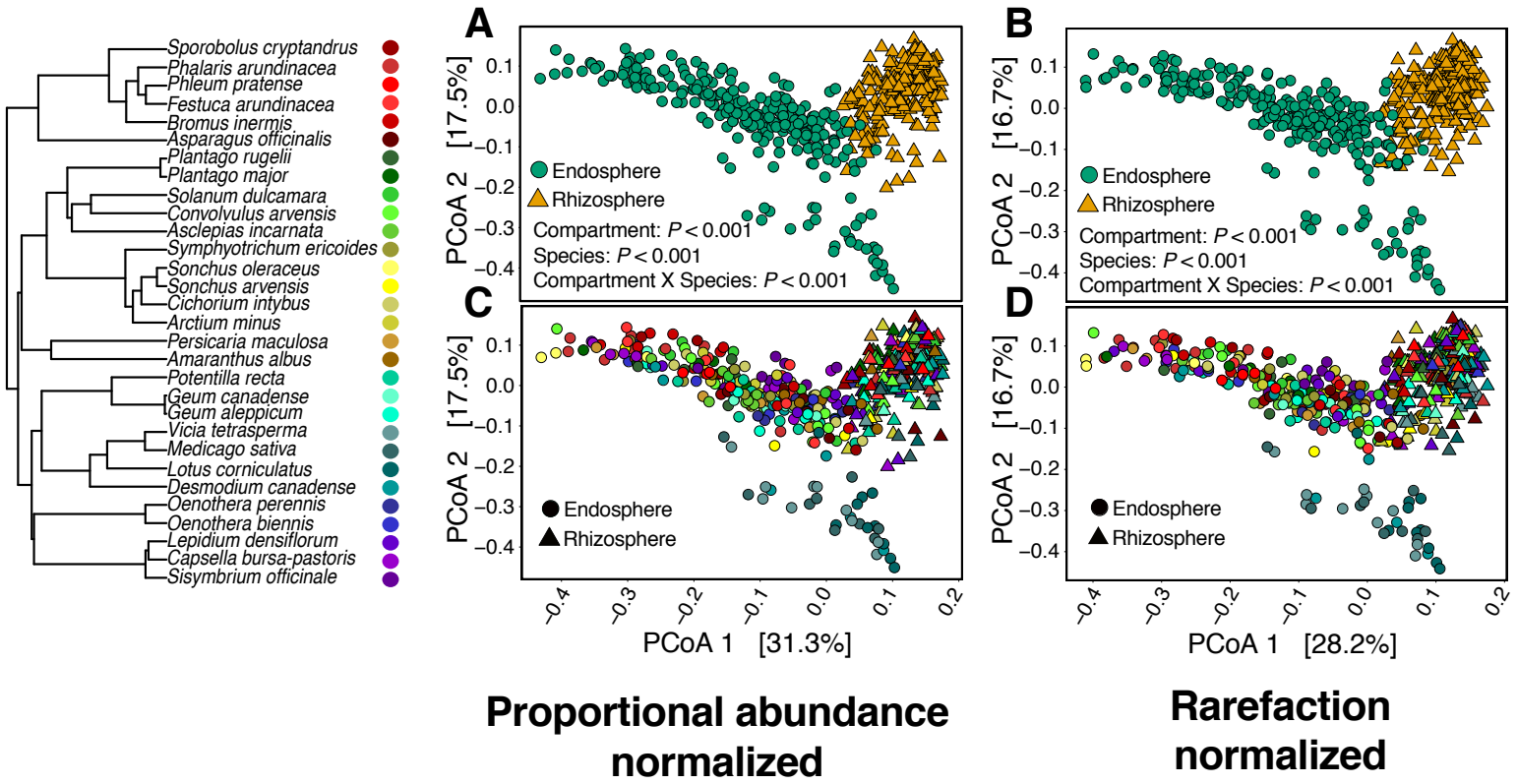

Fig. S3 | Principal coordinate analysis grouped by compartment and host plant species across ASV processing method. (*A* and *C*) PCoA using weighted pairwise UniFrac distances and proportional abundance normalized or (*B* and *D*)**,** rarefaction normalized datasets. The proportional abundance normalized dataset also includes a 1% sample occurrence X number of read ≥ 25 threshold i.e. an ASV must be found in 7 samples at a frequency of at least 25 reads. (*A* and *B*)**,** Using either ASV processing method yields nearly identical patterns of ordination across compartment or (*C* and *D*)**,** host plant species. Host plant species are colored to represent evolutionary relationships. We report *P* values from our PERMANOVA results.

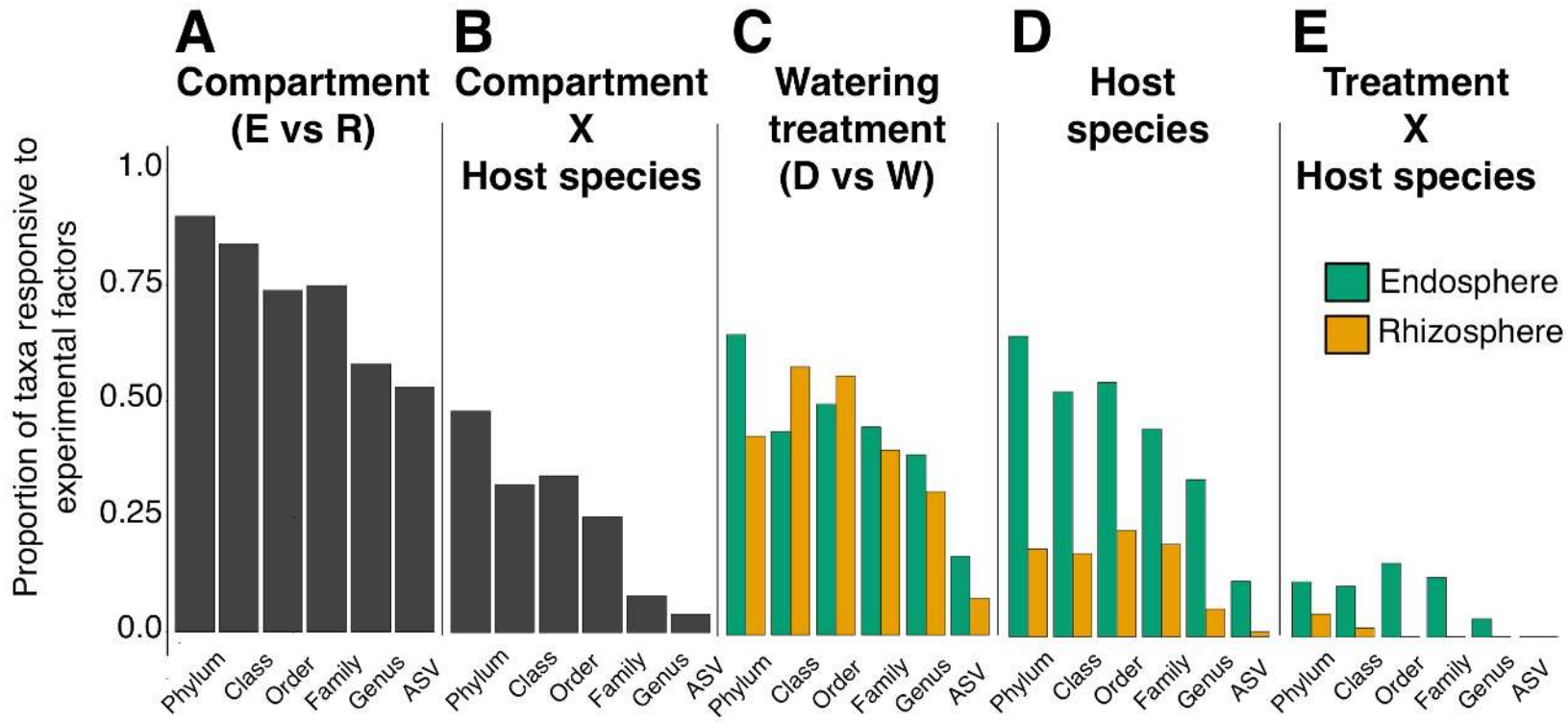

Fig. S4 | The proportion of bacterial taxa exhibiting differential abundance across experimental factors at different taxonomic levels. We grouped individual ASVs according to taxonomic level (phylum, class, order, family, and genus). Then, negative binomial models were implemented in the R package 'DESeq2' to test whether individual taxa at each taxonomic level exhibit differential abundance across experimental factors: (*A*) compartment; (*B*) compartment X host plant species; (*C*) watering treatment; (*D*) host plant species; (*E*) watering treatment X host plant species. We tested for significance using negative binomial generalized linear models and corrected *P*-values using the false-discovery rate.

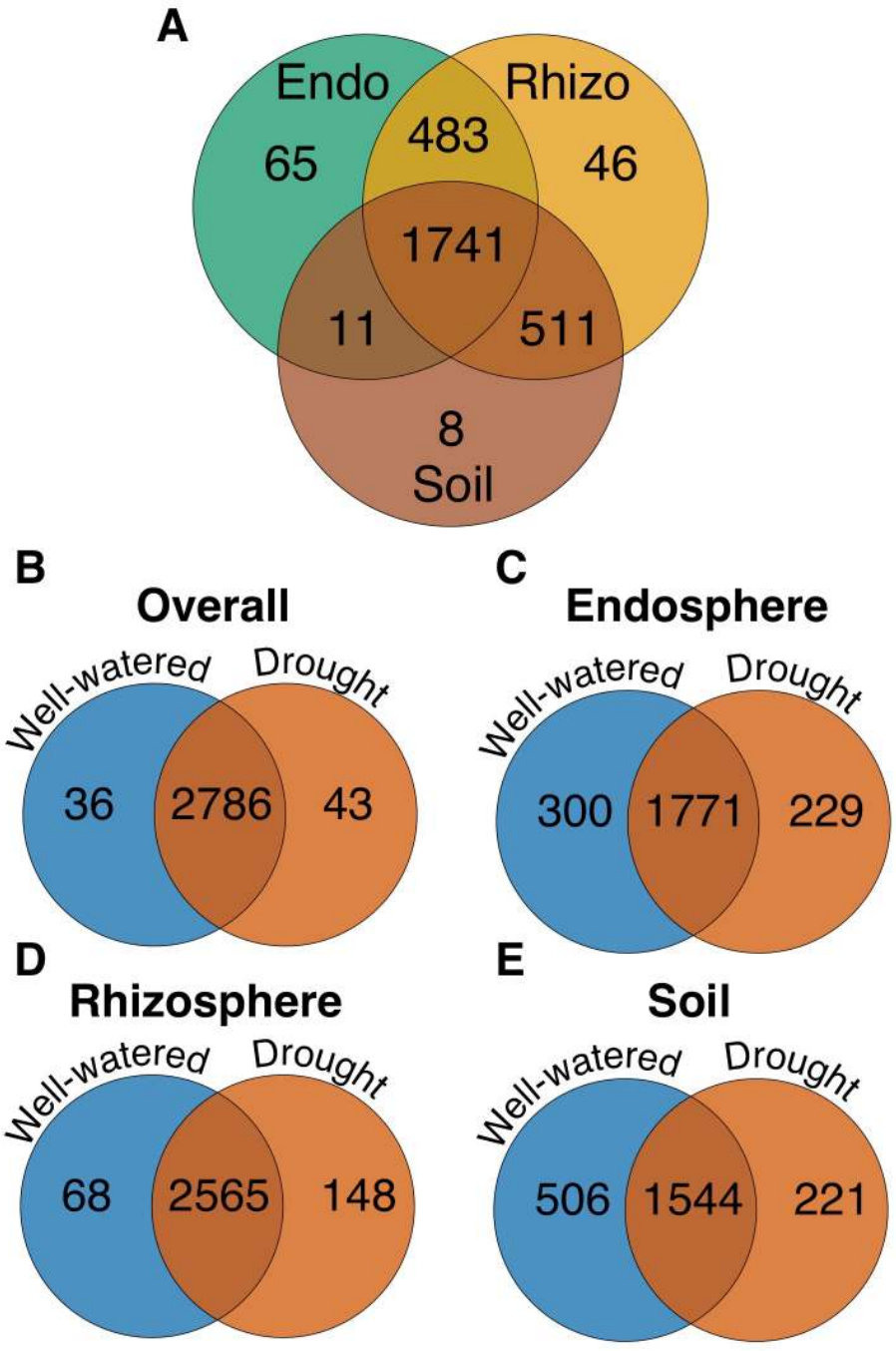

Fig. S5 | The number of bacterial ASVs found exclusively in particular root compartments or watering treaments. Venn diagrams illustrating bacterial ASVs shared among (*A*) compartments, (*B*) well-watered and drought compartments, and between watering treatments in each of (*C*) endosphere, (*D*) rhizosphere, and (*E*) soil compartments.

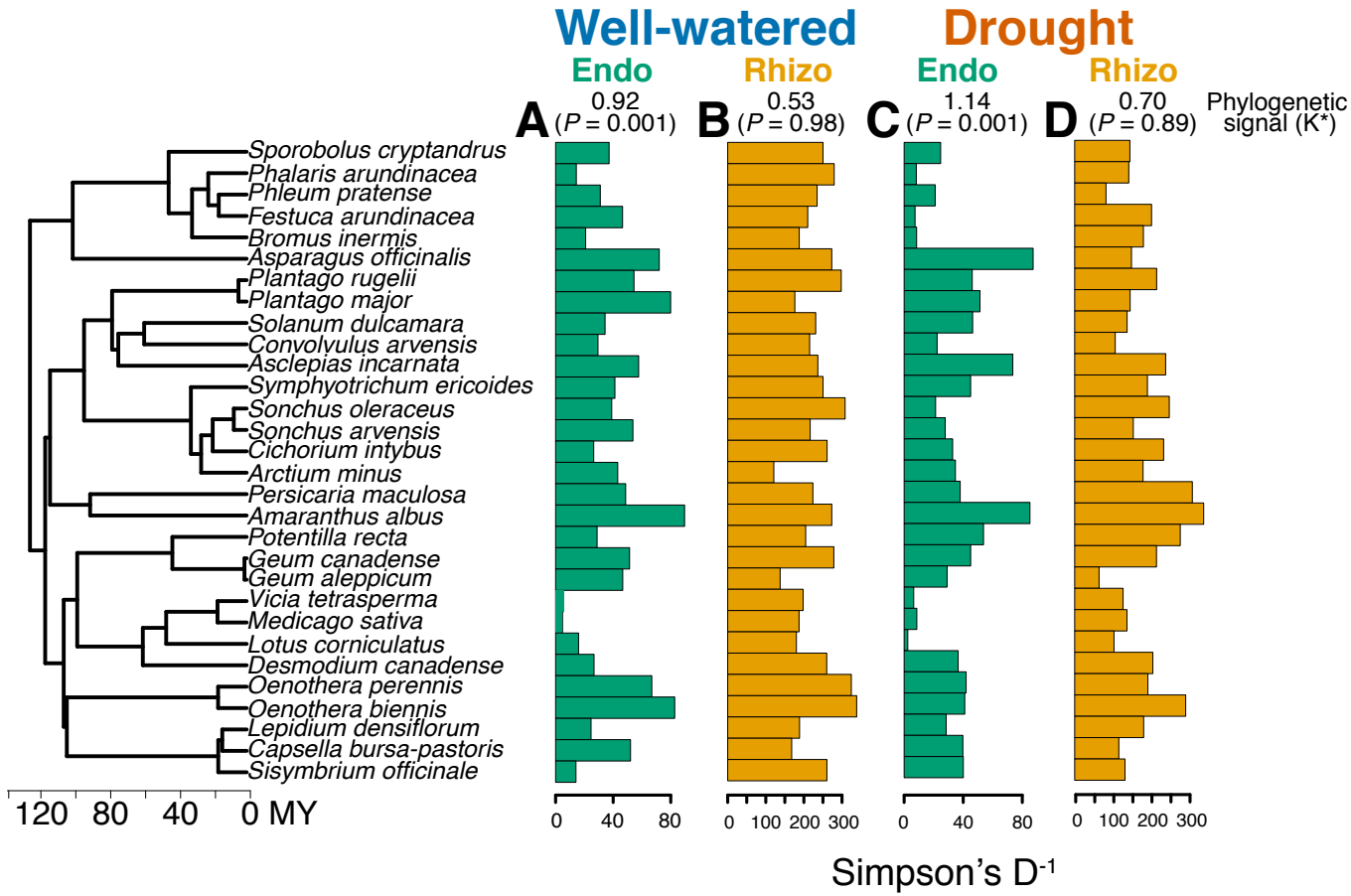

Fig. S6 | The effect of host plant species and watering treatment on endosphere and rhizosphere diversity. Simpson's diversity^{-1} in (*A* and *C*) endosphere and (*B* and *D*) rhizosphere compartments across (*A* and *B*) well-watered and (*C* and *D*) drought treatments**.** Regardless of watering treatment endosphere diversity exhibited significant phylogenetic signal while rhizosphere diversity did not.

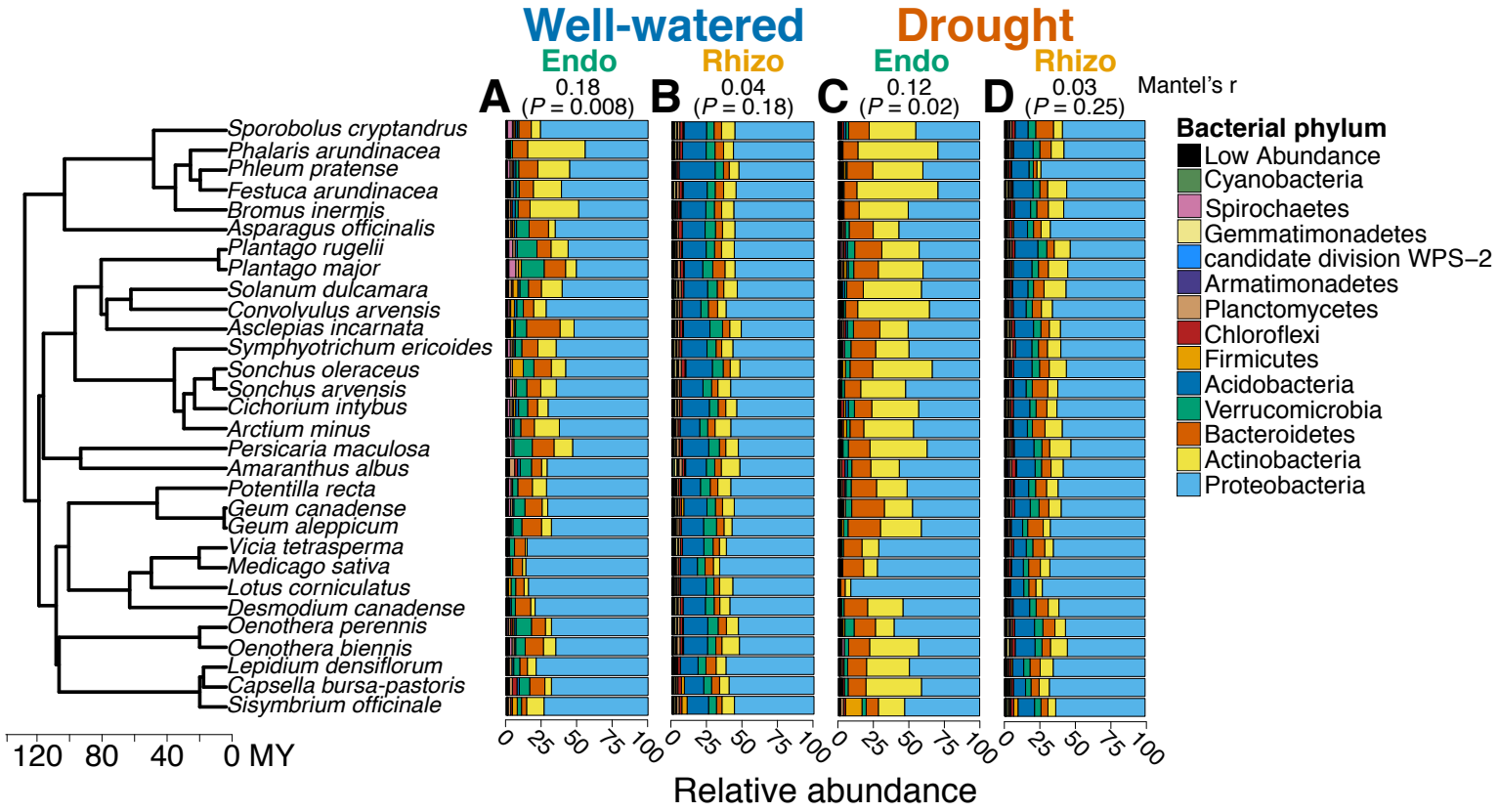

Fig. S7 | The relative abundance of bacterial phyla in the endosphere and rhizosphere of different host plant species under drought and well-watered conditions. We found evidence of a significant interaction between compartment, watering treatment, and host plant species on the composition of root microbial communities (see Table S6). Host plant species differ in the composition of their endosphere under (*A*) well-watered versus (*C*) drought, whereas host plant species do not differ in the composition of their rhizosphere under (*B*) well-watered or (*D*) drought conditions. Using Mantel tests, we also found a significant correlation between endosphere similarity and phylogenetic relatedness among host plants, whereas rhizosphere similarity was uncorrelated with host plant phylogenetic relatedness.

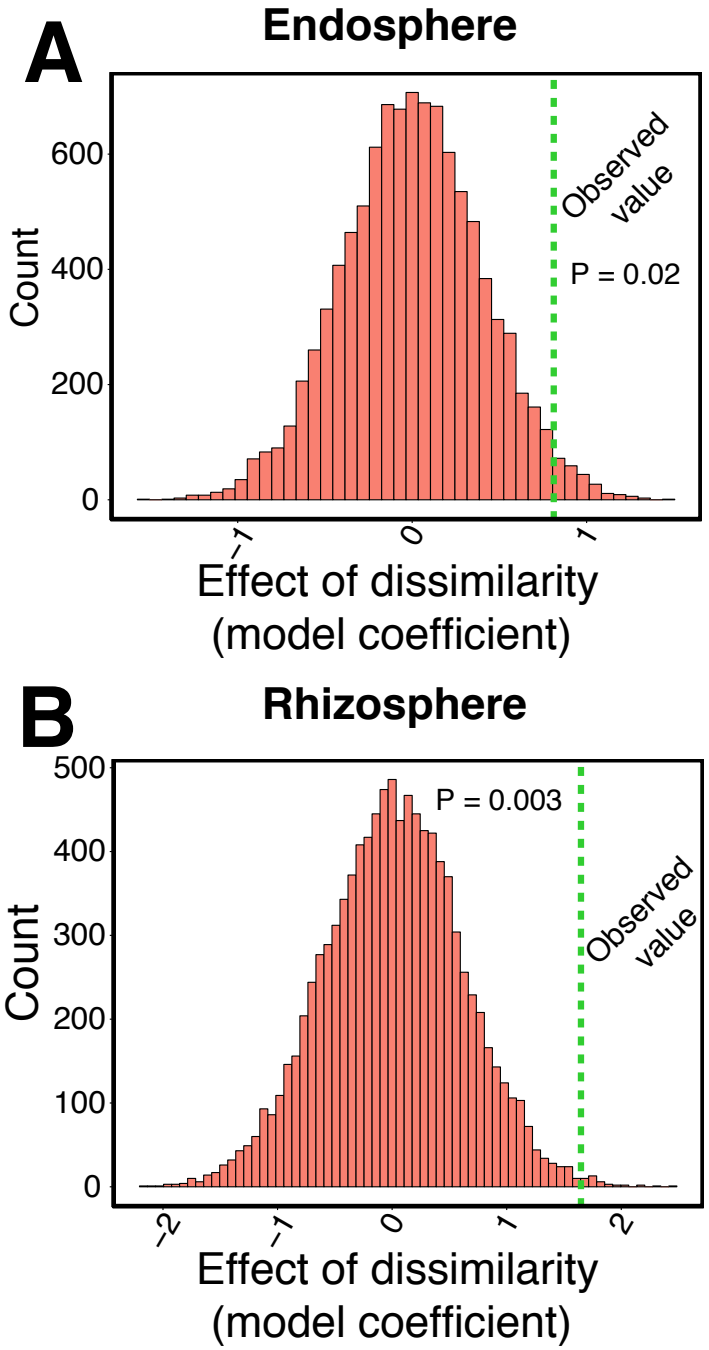

Fig. S8 | The effect of community composition on plant-soil feedback. We tested whether (*A*) endosphere or (*B*) rhizosphere similarity between pairs of species is related to their experimentally measured plant-soil feedback. We then performed a permutation test to determine the significance of the observed slope (model coefficient) from our linear regression relative to a null distribution. We compared our observed value to a distribution obtained after randomizing the microbial similarity data and performing the same linear regression 10000 times.

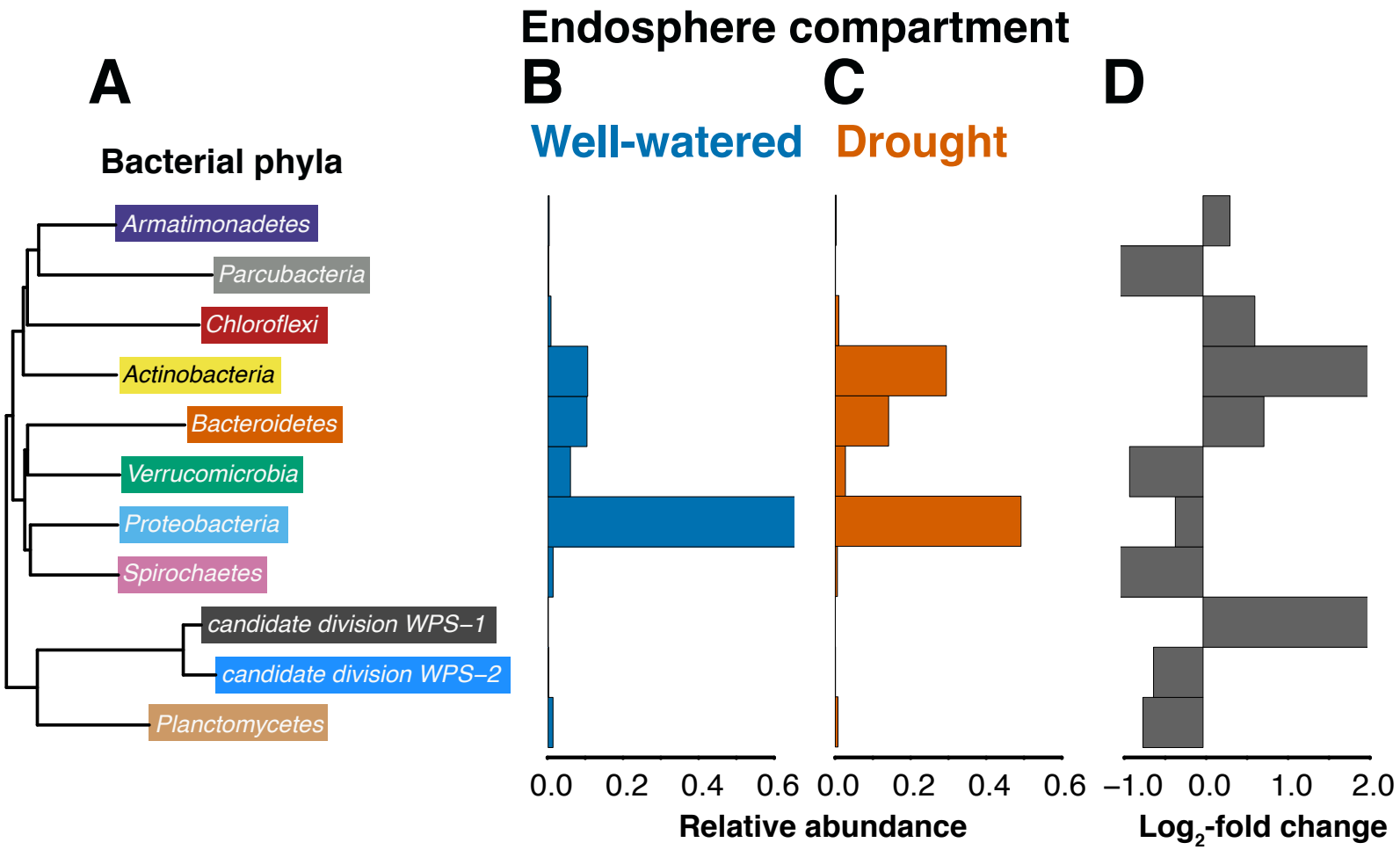

Fig. S9 | Bacterial phyla enriched in the endosphere under drought. (*A*) Bacterial phyla that exhibit significant differential relative abundance between (*B*) well-watered and (*C*) drought conditions. Significance testing and (*D*) estimates of log-fold changes were obtained from the R package 'DESeq2'. Bars represent relative abundance of taxa averaged across all host plants in each watering treatment calculated from our 1% sample occurrence X number of read ≥ 25 threshold dataset.

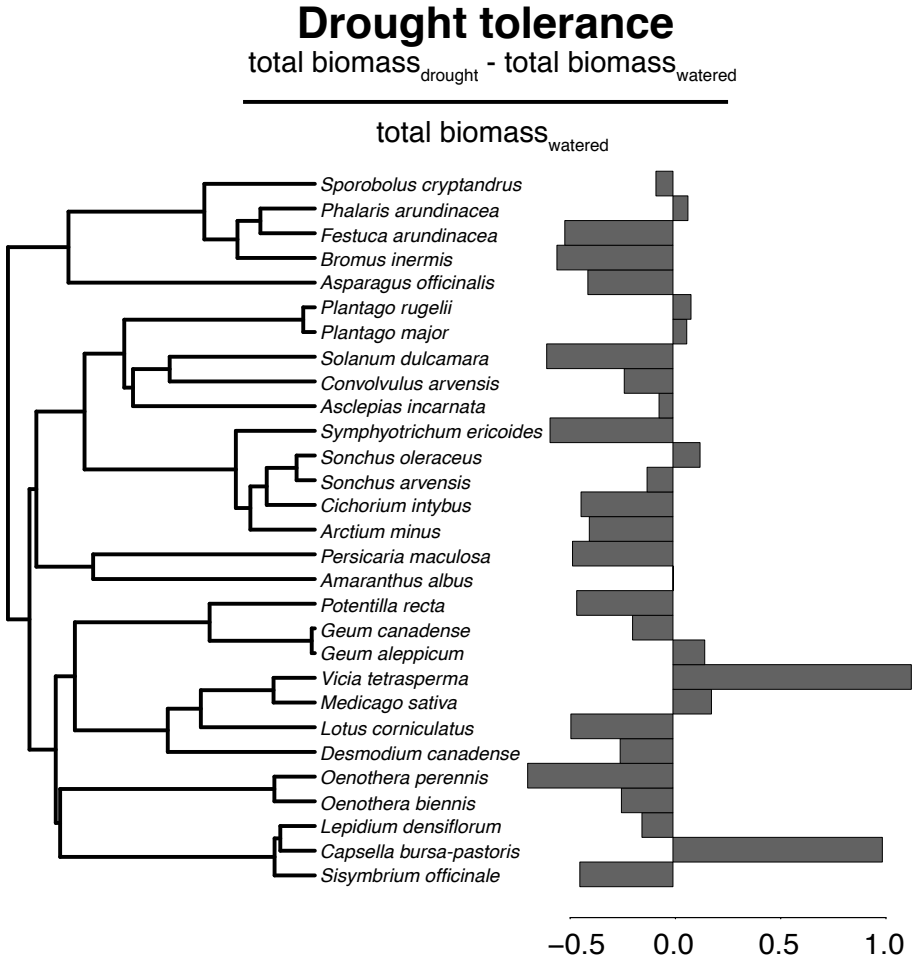

Fig. S10 | Plant species vary in drought tolerance. We measured drought tolerance in each plant species by the proportional mass loss calculated from 5 individuals growing in well-watered and 5 individuals growing in drought conditions. Drought tolerance did not exhibit significant phylogenetic signal across plant species.

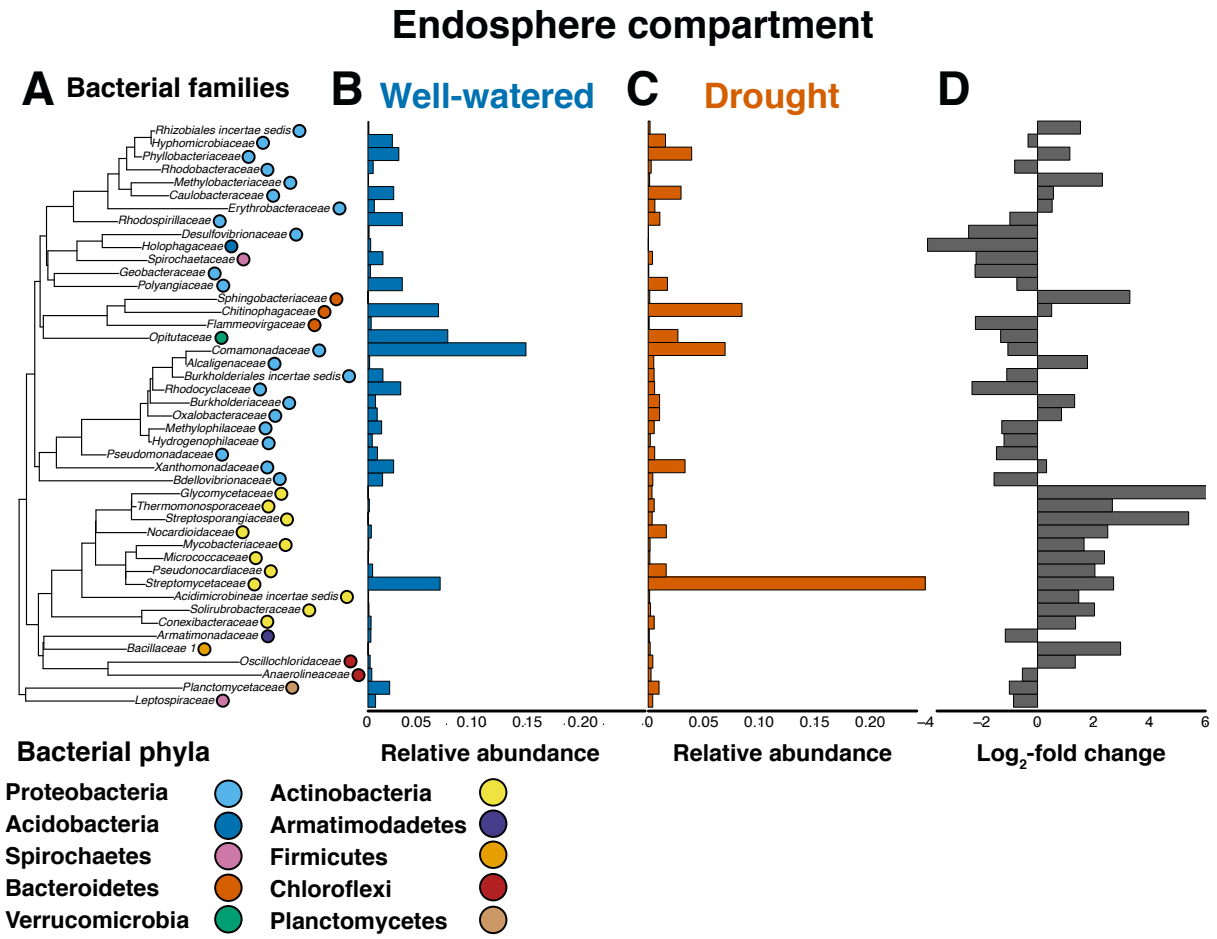

Fig. S11 | Bacterial families enriched in the endosphere under drought. (*A*) Bacterial families that exhibit significant differential relative abundance between (*B*) well-watered and (*C*) drought conditions. Significance testing and (*D*) estimates of log-fold changes were obtained from the R package 'DESeq2'. Bars represent relative abundance of taxa averaged across all host plants in each watering treatment calculated from our 1% sample occurrence X number of read ≥ 25 threshold dataset.

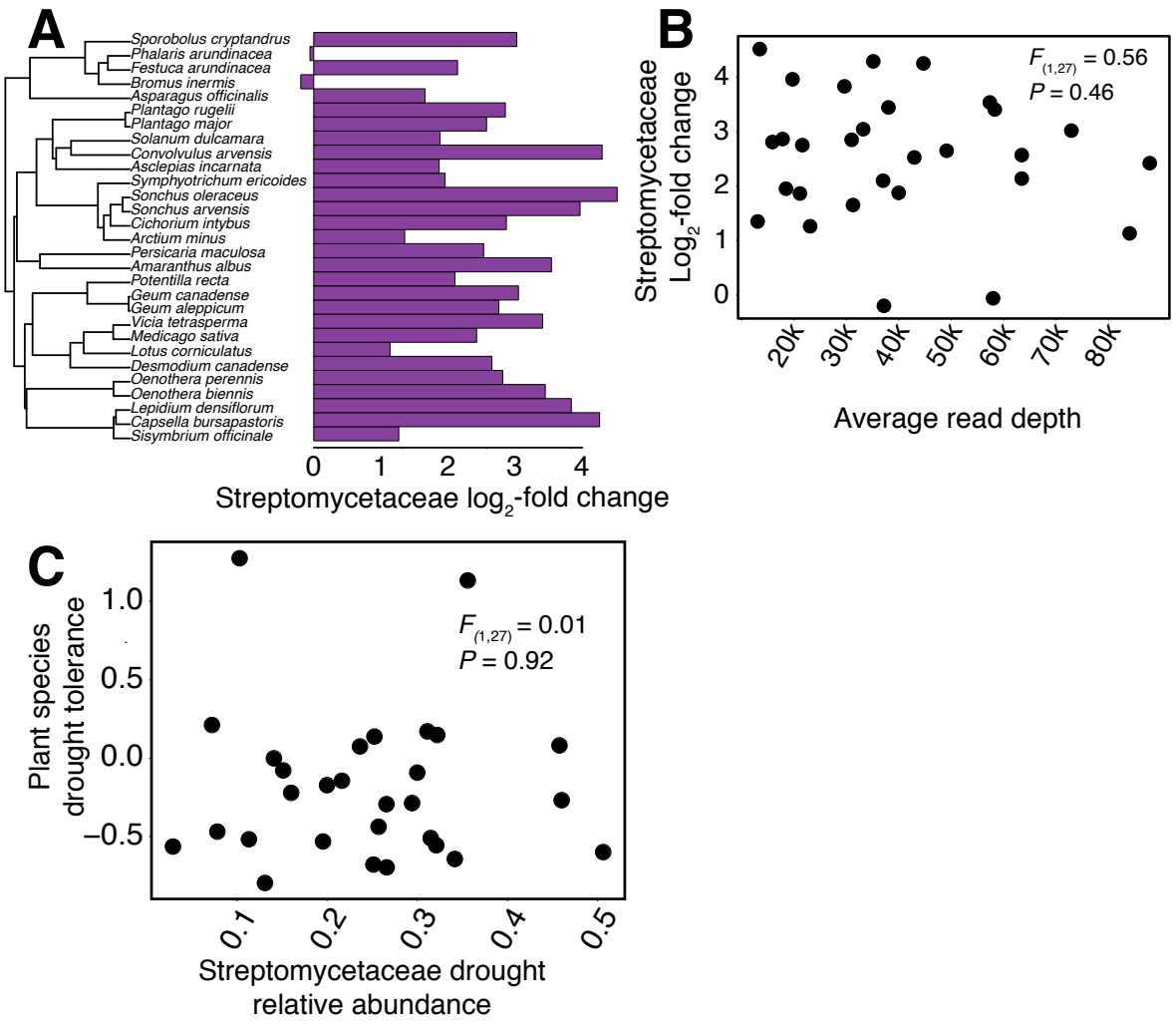

Fig. S12 | Variation in the relative enrichment of endosphere Streptomycetaceae is unrelated to read depth or relative abundance under drought conditions. (*A*) Host plant species varied in their relative enrichment of Streptomycetaceae under drought. (*B*) Relative enrichment of Streptomycetaceae is unrelated to read depth across plant species, which demonstrates that variation in Streptomyceatace enrichment is not simply an artifact of sequencing depth. (*C*) The relative abundance of Streptomycetaceae under drought conditions is uncorrelated with relative enrichment of Streptomycetaceae. This result indicates that the benefit of endosphere Streptomycetaceae under drought conditions is not reflected in relative abundance but instead relative enrichment (main text Fig. 4*C*) and that plant species exhibiting high relative enrichment do not necessarily exhibit high relative abundance.

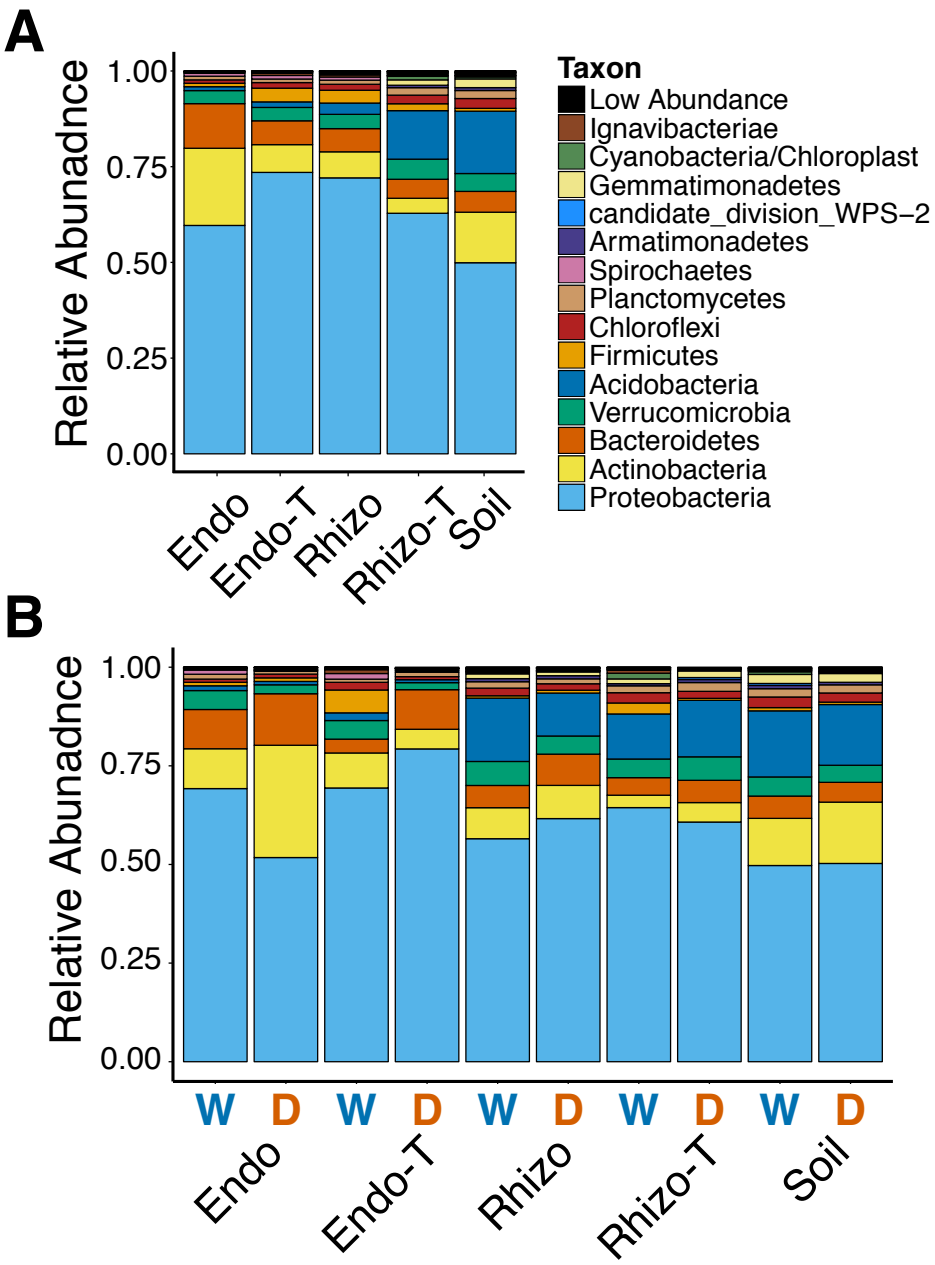

Fig. S13 | Comparing the plant root microbiome to an artificial root analog microbiome. We used autoclaved bamboo toothpicks (T) to serve as structural analogs to living roots (Rhizo-T = root analog rhizosphere; Endo-T = root analog endosphere). (*A*) Comparing the community composition of living plant roots to root analogs distinguish between bacterial taxa that might be responsive to features of live roots versus taxa inhabiting any structure composed of plant cells. (*B*) Furthermore, we did not observe congruent compositional shifts between the microbiota of living plant roots and root analogues, which indicates that our observed effects of drought on root microbiota are largely driven by living, host plant responses.

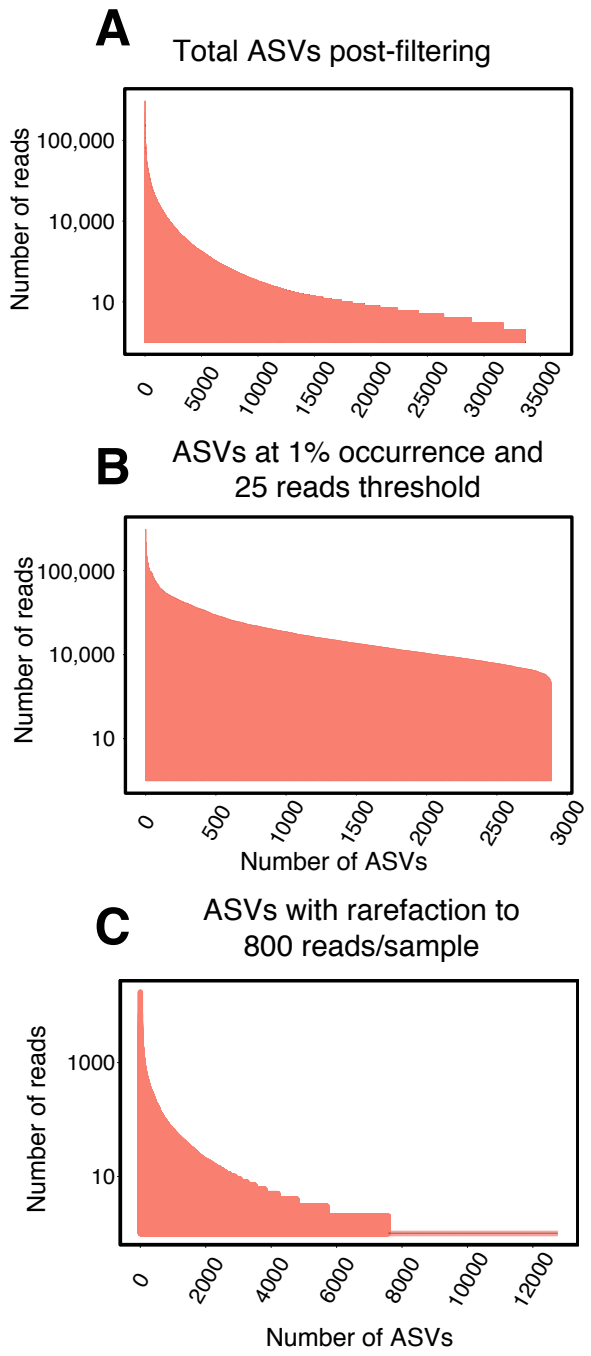

Fig. S14 | The effect of ASV processing method on read distribution across bacterial ASVs. The number of sequencing reads associated with individual bacterial ASVs in the entire dataset when applying: (*A*) no normalization, (*B*) a 1% relative abundance sample occurrence and a read depth of ≥ 25 per ASV, or (*C*) rarefaction to 800 reads per sample. A 1% sample occurrence and ≥ 25 read depth threshold captures 94% of all sequenced reads from (*A*), whereas rarefaction captures < 2%.

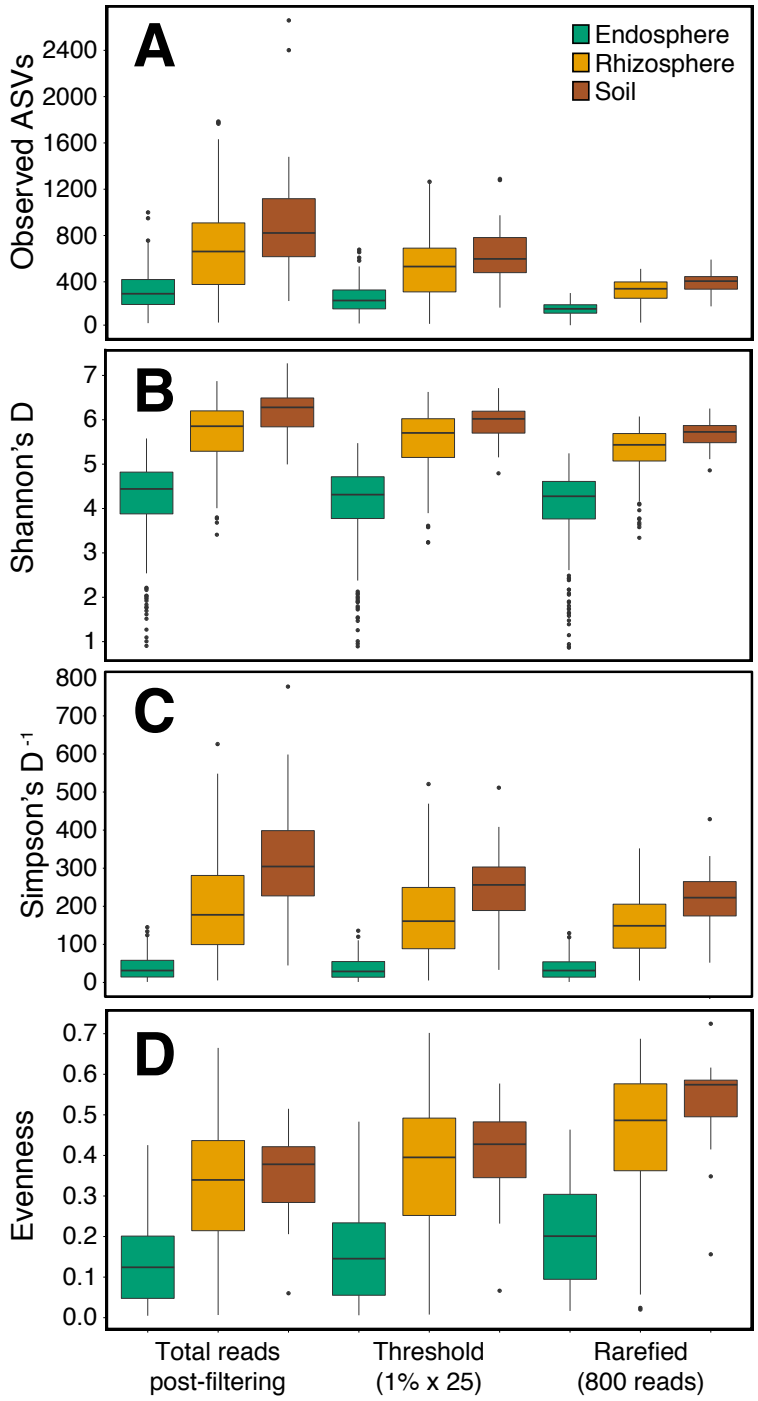

Fig. S15 | The effect of ASV processing method on alpha diversity. Shown is the average microbial diversity per plant according to (*A*) species richness, (*B*) Shannon's diversity, (*C*) Simpson's diversity, or (*D*) evenness. Using total reads post-filtering, a 1% relative abundance sample occurrence and a read depth of ≥ 25 per ASV or rarefaction to 800 reads per sample changes the estimates of alpha diversity across bacterial compartments. ASV processing method has no effect on the qualitative differences in diversity between endosphere, rhizosphere and soil.

Table S1 | The total number of endosphere and rhizosphere samples for each host plant species in each watering treatment. Additionally, the number of bulk soil and toothpick samples collected from each watering treatment. Note, we collected endosphere and rhizosphere samples for toothpicks as described in the supplemental materials and methods.

Host Plant Species			Endosphere		Rhizosphere	
Species	**Family**	**Native/Exotic**	**Well-watered**	**Drought**	**Well-watered**	**Drought**
Amaranthus albus	Amaranthaceae	Exotic	5	5	4	5
Asclepias incarnata	Apocynaceae	Native	5	5	4	4
Asparagus officinalis	Asparagaceae	Exotic	4	5	5	4
Arctium minus	Asteraceae	Exotic	2	5	4	4
Symphyotrichum ericoides	Asteraceae	Native	4	5	2	4
Sonchus oleraceus	Asteraceae	Exotic	5	4	4	4
Sonchus arvensis	Asteraceae	Exotic	4	6	4	5
Capsella bursa-pastoris	Brassicaceae	Exotic	6	3	4	3
Lepidium densiflorum	Brassicaceae	Native	4	4	5	5
Sisymbrium officinale	Brassicaceae	Exotic	6	3	4	3
Convolvulus arvensis	Convolvulaceae	Exotic	5	5	4	3
Desmodium canadense	Fabaceae	Native	5	5	4	5
Lotus corniculatus	Fabaceae	Exotic	5	5	5	5
Medicago sativa	Fabaceae	Exotic	4	5	5	5
Vicia tetrasperma	Fabaceae	Exotic	5	5	5	5
Oenothera biennis	Onagraceae	Native	5	5	2	4
Oenothera perennis	Onagraceae	Native	4	4	4	5
Plantago major	Plantaginaceae	Exotic	6	2	7	2
Plantago rugelii	Plantaginaceae	Status disputed	4	5	5	5
Bromus inermis	Poaceae	Exotic	5	5	5	5
Festuca arundinacea	Poaceae	Exotic	3	6	4	6
Phalaris arundinacea	Poaceae	Exotic	6	4	6	4
Phleum pratense	Poaceae	Exotic	3	3	2	3
Sporobolus cryptandrus	Poaceae	Native	4	4	4	4
Persicaria maculosa	Polygonaceae	Exotic	4	5	4	3
Geum aleppicum	Rosaceae	Native	3	5	2	4
Geum canadense	Rosaceae	Native	5	5	5	5
Potentilla recta	Rosaceae	Exotic	5	5	5	5
Solanum dulcamara	Solanaceae	Exotic	3	5	3	6
Cichorium intybus	Asteraceae	Exotic	3	6	4	5
Bulk soil samples			NA	NA	10	10
Toothpick samples			10	10	9	9
		Total	142	149	144	149

Table S2 | Host plant species phenotypic traits. Mean, standard error, and phylogenetic signal for each of the eight phenotypic plant traits measured. These data represent a subset of the trait data from Fitzpatrick et al. (1). We re-calculated phylogenetic signal (Blomberg's K and Pagel's λ) for these traits according to the species used in the current study.

	Mean	SE	Mean	SE	Mean	SE	Mean	SE	Mean	SE	Mean	SE	Mean	SE	Mean	SE
Plant Species	**Aboveground biomass (mg)**		**Belowground biomass (mg)**		**Root length (cm)**		**Root angle (°)**		**Water content (%)**		**Specific leaf area (cm^2/mg)**		**Root hair density (#/mm)**		**Specific root length (cm^2/mg)**	
Amaranthus albus	988.66	157.47	37.07	13.75	16.03	1.29	51.67	15.62	75.47	2.20	49.25	3.63	3.15	0.83	0.76	0.23
Arctium minus	389.82	33.07	439.51	75.39	30.11	2.42	62.15	6.76	77.73	2.17	57.54	4.02	1.74	0.29	0.51	0.34
Asclepias incarnata	517.33	76.89	261.09	45.83	23.44	2.58	52.56	8.69	75.16	5.09	70.76	7.40	0.90	0.38	0.44	0.09
Asparagus officinalis	238.42	43.60	323.32	76.31	22.20	1.76	56.91	6.43	NA	NA	NA	NA	3.83	1.27	0.45	0.09
Bromus inermis	1276.89	830.57	442.25	60.00	28.50	3.50	53.67	5.72	66.61	4.16	46.08	8.02	2.93	0.92	0.23	0.10
Capsella bursa-pastoris	173.98	15.19	21.37	7.07	20.00	6.78	48.89	16.73	83.44	1.74	86.00	14.81	5.12	0.50	0.68	0.32
Cichorium intybus	765.03	288.26	910.16	144.60	44.65	6.11	54.07	10.13	79.56	2.34	71.86	5.62	1.23	0.12	0.34	0.09
Convolvulus arvensis	192.64	41.50	110.37	39.53	32.90	5.93	46.05	12.32	77.75	2.26	47.85	2.49	1.60	0.29	0.27	0.05
Desmodium canadense	995.14	220.72	457.89	158.79	32.10	1.33	44.37	5.66	74.29	1.35	103.84	8.46	2.80	0.65	0.33	0.09
Festuca arundinacea	1062.25	262.77	547.02	66.19	26.10	1.44	57.87	8.82	76.83	1.94	46.79	4.55	3.04	0.98	NA	NA
Geum aleppicum	320.02	49.90	88.17	26.44	26.14	1.86	70.00	5.41	70.08	2.04	47.27	9.53	1.48	0.45	0.52	0.07
Geum canadense	344.24	98.93	75.53	41.66	21.00	2.71	58.29	6.97	64.29	4.47	56.09	4.81	2.26	0.50	0.48	0.09
Lepidium densiflorum	357.01	88.37	100.61	40.79	18.05	3.56	48.97	8.33	74.95	1.14	38.65	3.12	2.63	1.33	0.26	0.10
Lotus corniculatus	613.82	142.89	220.99	39.95	33.10	3.90	55.27	6.68	74.93	2.81	51.47	7.63	0.64	0.09	0.31	0.08
Medicago sativa	624.84	360.48	315.95	193.63	29.85	2.43	53.16	8.69	69.95	4.12	49.50	3.94	1.64	0.43	0.31	0.19
Oenothera biennis	1188.35	180.69	108.67	28.81	14.60	2.44	51.80	8.10	70.15	2.52	38.58	2.26	1.51	0.34	0.44	0.15
Persicaria maculosa	1131.62	203.98	278.37	68.48	28.33	3.01	46.04	7.62	75.10	2.77	53.35	1.97	3.72	0.77	0.55	0.11
Phalaris arundinacea	745.08	107.86	452.91	74.11	22.10	3.12	65.00	6.00	72.25	1.36	81.31	18.80	2.84	0.49	2.40	1.78
Phleum pratense	1150.92	337.47	505.04	55.93	25.67	2.52	63.30	7.78	77.46	2.20	79.39	3.97	2.81	0.29	0.46	0.37
Plantago major	633.74	164.70	305.38	75.27	29.80	7.69	68.90	8.83	73.96	5.07	41.47	18.89	1.77	0.10	0.33	0.07
Plantago rugelii	839.95	165.29	261.92	38.34	25.10	2.39	65.40	6.26	83.04	1.69	46.54	2.93	2.04	0.21	0.73	0.30
Potentilla recta	514.15	155.02	162.44	77.86	27.56	2.73	54.93	7.52	69.31	4.97	65.83	12.48	1.69	0.10	0.38	0.19
Sisymbrium officinale	219.38	105.87	63.45	89.86	6.63	2.25	49.58	15.65	76.93	1.81	66.71	0.82	NA	NA	0.15	0.12
Solanum dulcamara	406.59	57.02	124.69	17.68	32.56	2.16	45.26	5.98	75.71	4.18	58.36	8.80	1.15	0.30	0.51	0.23
Sonchus arvensis	415.89	82.82	488.72	152.45	39.78	6.75	48.59	4.47	78.60	2.84	71.56	5.98	2.27	0.65	0.40	0.05
Sonchus oleraceus	544.88	158.25	126.86	61.28	20.33	0.37	53.52	8.68	81.07	3.22	91.85	12.18	1.48	0.92	0.37	0.17
Sporobolus cryptandrus	636.84	220.48	70.89	12.23	25.88	3.25	64.14	7.81	71.30	2.01	45.28	2.39	5.21	1.15	0.31	0.12
Symphyotrichum ericoides	331.87	101.22	157.90	86.13	22.79	2.06	54.86	6.64	76.83	3.60	44.65	5.26	1.65	0.26	0.29	0.09
Vicia tetrasperma	164.36	22.37	56.32	8.69	18.48	2.74	52.85	5.61	64.34	6.83	23.56	3.34	0.96	0.09	0.48	0.06
Oenothera perennis	271.56	105.54	30.40	12.05	14.31	1.40	58.67	9.37	82.78	2.51	61.04	16.21	1.10	0.53	0.52	0.08
Blomberg's K* (*P* value)	**0.72 (0.05)**		**0.83 (0.01)**		**0.65 (0.05)**		0.68 (0.14)		0.74 (0.26)		0.42 (0.39)		**1.07 (<0.01)**		1.48 (0.13)	
Pagel's λ (*P* value)	0.65 (0.20)		**0.59 (0.03)**		0.45 (0.16)		0.87 (0.59)		0.43 (0.17)		0.00 (1.00)		**1.00 (<0.01)**		0.00 (1.00)	

Table S3 | Linear mixed model results for the analysis of alpha diversity. We estimated alpha diversity for every individual sample with the total number of observed species, Simpson's diversity^{-1} index, and evenness. We include results for the entire dataset and results for the endosphere and rhizosphere compartments analyzed separately. Compartment, treatment, and useable reads were treated as fixed effects, while species (including interaction terms with species), sequencing run and experimental block were treated as random effects. Significance of fixed effects was determined using type III ANOVA with Kenward-Roger estimates of denominator degrees-of-freedom. We used likelihood ratio tests with full and reduced models to determine the significance of random effects. We include the results using the non-normalized dataset (full dataset), and the results using the rarefied dataset.

Full dataset

	Endosphere and rhizosphere combined					
	log(Observed species richness)		log(Simpson's diversity $^{-1}$)		Evenness	
	F/X^2	*P* (FDR)	F/X^2	*P* (FDR)	F/X^2	*P* (FDR)
Compartment (C)	124.79	**<0.001**	64.62	**<0.001**	73.89	**<0.001**
Treatment (T)	3.85	0.08	5.56	0.06	1.58	0.20
T X C	2.60	0.14	1.87	0.17	7.03	**0.006**
log(usable reads)	3024.78	**<0.001**	35.82	**<0.001**	218.28	**<0.001**
Species (S)	1.14	0.29	3.28	0.09	7.5	**0.01**
S X C	25.70	**<0.001**	17.72	**<0.001**	2.69	0.10
S X T	0.05	1.00	3.60	0.18	0.00	1.00
S X C X T	0.00	1.00	0.15	1.00	0.00	1.00
Sequencing run	0.00	1.00	2.08	0.26	2.19	0.24
Experimental block	0.23	1.00	0.00	1.00	0.00	1.00

	Endosphere only					
	log(Observed species richness)		log(Simpson's diversity $^{-1}$)		Evenness	
	F/X^2	*P* (FDR)	F/X^2	*P* (FDR)	F/X^2	*P* (FDR)
Treatment (T)	1.14	0.30	3.36	0.12	3.31	0.12
log(usable reads)	703.96	**<0.001**	0.12	0.73	176.96	**<0.001**
Species (S)	18.36	**<0.001**	23.91	**<0.001**	14.75	**<0.001**
S X T	0.67	0.41	2.08	0.11	2.97	0.11
Sequencing run	0.04	0.93	0.32	0.85	4.51	0.09
Experimental block	0.00	1.00	0.00	1.00	0.00	1.00

	Rhizosphere only					
	log(Observed species richness)		log(Simpson's diversity $^{-1}$)		Evenness	
	F/X^2	*P* (FDR)	F/X^2	*P* (FDR)	F/X^2	*P* (FDR)
Treatment (T)	63.31	**<0.001**	27.01	**<0.001**	22.33	**<0.001**
log(usable reads)	4037.77	**<0.001**	76.21	**<0.001**	82.72	**<0.001**
Species (S)	3.05	0.08	11.94	**<0.001**	6.44	**0.02**
S X T	0.00	1.00	1.85	0.51	0.00	1.00
Sequencing run	0.00	1.00	0.06	1.00	0.93	0.99
Experimental block	3.01	0.24	0.00	1.00	0.00	1.00

Table S3 Continued

Rarefied dataset (800 reads)

	Endosphere and rhizosphere combined					
	log(Observed species richness)		log(Simpson's diversity $^{-1}$)		Evenness	
	F/X^2	*P* (FDR)	F/X^2	*P* (FDR)	F/X^2	*P* (FDR)
Compartment (C)	56.82	**<0.001**	58.19	**<0.001**	73.93	**<0.001**
Treatment (T)	0.16	0.69	3.92	0.08	5.44	0.06
T X C	2.36	0.18	1.45	0.26	3.81	0.12
log(usable reads)	NA	NA	NA	NA	NA	NA
Species (S)	0.37	0.56	1.83	0.27	7.94	**0.02**
S X C	9.05	0.01	20.05	**<0.001**	6.03	**0.04**
S X T	0.00	1.00	0.93	0.56	0.15	1.00
S X C X T	0.00	1.00	0.01	1.00	0.00	1.00
Sequencing run	8.96	**0.01**	5.32	**0.05**	1.36	0.24
Experimental block	6.52	0.09	0.12	1.00	0.00	1.00

	Endosphere					
	log(Observed species richness)		log(Simpson's diversity $^{-1}$)		Evenness	
	F/X^2	*P* (FDR)	F/X^2	*P* (FDR)	F/X^2	*P* (FDR)
Treatment (T)	0.14	0.71	3.07	0.14	6.31	0.06
log(usable reads)	NA	NA	NA	NA	NA	NA
Species (S)	11.26	**<0.001**	24.31	**<0.001**	20.39	**<0.001**
S X T	0.12	0.73	2.90	0.14	3.01	0.16
Sequencing run	1.86	0.17	0.38	0.54	0.39	0.53
Experimental block	0.27	0.60	0.00	1.00	0.00	1.00

	Rhizosphere					
	log(Observed species richness)		log(Simpson's diversity $^{-1}$)		Evenness	
	F/X^2	*P* (FDR)	F/X^2	*P* (FDR)	F/X^2	*P* (FDR)
Treatment (T)	3.96	0.09	22.48	**<0.001**	26.02	**<0.001**
log(usable reads)	NA	NA	NA	NA	NA	NA
Species (S)	2.71	0.10	7.81	**0.02**	8.66	**<0.001**
S X T	0.00	1.00	0.00	1.00	0.00	1.00
Sequencing run	2.15	0.21	4.01	0.15	0.10	0.82
Experimental block	16.29	**<0.001**	3.09	0.12	0.00	1.00

Table S4 | Linear mixed model results for the analysis of beta diversity. We estimated beta diversity for every individual sample by obtaining the scores along the first three principle coordinate axes, using three distance measures: the weighted UniFrac, unweighted UniFrac, or Bray-Curtis. Results were qualitatively similar for each distance measure therefore we present only the weighted UniFrac results. We include results for the entire dataset and results for the endosphere and rhizosphere compartments analyzed separately. Compartment, treatment, and useable reads were treated as fixed effects, while species (including interaction terms with species), sequencing run and experimental block were treated as random effects. Significance of fixed effects was determined using type III ANOVA with Kenward-Roger estimates of denominator degrees-of-freedom. We used likelihood ratio tests with full and reduced models to determine the significance of random effects. We include the results using the non-normalized dataset (full dataset), and the results using the rarefied dataset. All *P* values adjusted for multiple comparisons using the false discovery rate.

Proportional-abundance normalization

Endosphere and rhizosphere combined

	PCoA1		PCoA2		PCoA3	
	F/X^2	*P* (FDR)	F/X^2	*P* (FDR)	F/X^2	*P* (FDR)
Compartment (C)	413.09	**<0.001**	2.77	0.12	1.37	0.25
Treatment (T)	215.67	**<0.001**	50.05	**<0.001**	153.92	**<0.001**
T X C	53.84	**<0.001**	98.64	**<0.001**	71.88	**<0.001**
log(usable reads)	0.88	0.40	3.09	0.12	0.13	0.89
Species (S)	0.09	0.94	2.53	0.34	0.00	1.00
S X C	20.06	**<0.001**	44.69	**<0.001**	21.58	**<0.001**
S X T	0.00	1.00	1.26	1.00	0.00	1.00
S X C X T	7.42	**0.05**	0.00	1.00	2.49	0.53
Sequencing run	0.00	1.00	1.57	0.71	0.38	0.96
Experimental block	1.94	0.25	0.00	1.00	5.96	**0.03**

Endosphere

	PCoA1		PCoA2		PCoA3	
	F/X^2	*P* (FDR)	F/X^2	*P* (FDR)	F/X^2	*P* (FDR)
Treatment (T)	101.86	**<0.001**	94.21	**<0.001**	15.47	**<0.001**
log(usable reads)	0.84	0.60	3.38	0.30	0.06	0.82
Species (S)	22.89	**<0.001**	30.98	**<0.001**	11.40	**<0.001**
S X T	7.15	**0.03**	0.00	1.00	1.95	0.48
Sequencing run	0.00	1.00	0.56	1.00	0.01	1.00
Experimental block	0.66	0.62	1.94	0.43	0.00	1.00

Rhizosphere

	PCoA1		PCoA2		PCoA3	
	F/X^2	*P* (FDR)	F/X^2	*P* (FDR)	F/X^2	*P* (FDR)
Treatment (T)	75.53	**<0.001**	3.82	0.07	5.42	**0.04**
log(usable reads)	2.86	0.14	2.47	0.15	121.69	**<0.001**
Species (S)	6.03	**0.05**	1.03	0.81	0.00	1.00
S X T	0.00	1.00	8.08	**0.04**	0.69	1.00
Sequencing run	0.22	1.00	0.00	1.00	0.00	1.00
Experimental block	0.27	0.75	1.35	0.17	0.33	0.76

Table S4 Continued.

Rarefaction normalized

	Endosphere and rhizosphere combined					
	PCoA1		PCoA2		PCoA3	
	F/X^2	*P* (FDR)	F/X^2	*P* (FDR)	F/X^2	*P* (FDR)
Compartment (C)	220.85	**<0.001**	3.63	0.09	0.90	0.39
Treatment (T)	373.59	**<0.001**	42.78	**<0.001**	144.02	**<0.001**
T X C	58.75	**<0.001**	97.07	**<0.001**	67.62	**<0.001**
log(usable reads)	NA	NA	NA	NA	NA	NA
Species (S)	0.16	0.88	2.88	0.32	0.00	1.00
S X C	21.60	**<0.001**	45.7	**<0.001**	19.28	**<0.001**
S X T	0.00	1.00	1.99	1.00	0.00	1.00
S X C X T	4.99	0.08	0.00	1.00	3.81	0.21
Sequencing run	0.00	1.00	1.13	1.00	0.40	1.00
Experimental block	1.65	0.31	0.00	1.00	7.53	**0.02**

	Endosphere					
	PCoA1		PCoA2		PCoA3	
	F/X^2	*P* (FDR)	F/X^2	*P* (FDR)	F/X^2	*P* (FDR)
Treatment (T)	97.06	**<0.001**	89.73	**<0.001**	18.26	**<0.001**
log(usable reads)	NA	NA	NA	NA	NA	NA
Species (S)	24.25	**<0.001**	28.47	**<0.001**	11.60	**<0.001**
S X T	6.91	**0.05**	0.45	0.58	1.42	0.41
Sequencing run	0.00	1.00	0.12	0.94	0.16	0.94
Experimental block	1.11	0.44	1.66	0.44	0.00	1.00

	Rhizosphere					
	PCoA1		PCoA2		PCoA3	
	F/X^2	*P* (FDR)	F/X^2	*P* (FDR)	F/X^2	*P* (FDR)
Treatment (T)	76.74	**<0.001**	2.78	0.11	2.74	0.11
log(usable reads)	NA	NA	NA	NA	NA	NA
Species (S)	5.25	**0.05**	1.65	1.00	0.00	1.00
S X T	0.00	1.00	5.40	0.12	0.00	1.00
Sequencing run	0.75	0.41	0.00	1.00	0.03	1.00
Experimental block	0.70	0.52	1.46	0.46	3.40	0.08

Table S5 | PERMANOVA results for the analysis of beta diversity using a matrix produced with the weighted UniFrac distance measure. We include results for the entire dataset and results for the endosphere and rhizosphere compartments analyzed separately. Significance was determined using F-tests based on permutations of the distance matrix across experimental factors. We include the results using the non-normalized dataset (full dataset), and the results using the rarefied dataset.

	Full dataset				**Rarefied dataset (800 reads)**			
	Endosphere and rhizosphere combined				**Endosphere and rhizosphere combined**			
	df	*Psuedo-F*	R^2	*P*	*df*	*Psuedo-F*	R^2	*P*
Compartment (C)	1	279.13	0.23	**<0.001**	1	222.10	0.21	**<0.001**
Treatment (T)	1	59.60	0.05	**<0.001**	1	49.98	0.05	**<0.001**
Species (S)	29	6.40	0.16	**<0.001**	29	5.64	0.15	**<0.001**
log(usable reads)	1	11.42	0.01	**<0.001**	NA	NA	NA	NA
Sequencing run	1	2.76	0.00	**0.02**	1	2.37	0.00	**0.02**
Experimental block	1	3.32	0.00	**0.01**	1	3.00	0.00	**0.01**
C X T	1	39.82	0.03	**<0.001**	1	33.54	0.03	**<0.001**
C X S	29	4.13	0.10	**<0.001**	29	3.67	0.10	**<0.001**
S X T	29	1.42	0.04	**<0.001**	29	1.46	0.04	**<0.001**
S X C X T	29	1.03	0.03	0.42	29	1.02	0.03	0.43
Error	400		0.33		400		0.38	
Total	522		1.00		522		1.00	

	Endosphere				**Endosphere**			
	DF	*Psuedo-F*	R^2	*P*	*DF*	*Psuedo-F*	R^2	*P*
Treatment (T)	1	67.10	0.12	**<0.001**	1	59.54	0.12	**<0.001**
Species (S)	29	7.57	0.40	**<0.001**	29	6.97	0.39	**<0.001**
log(usable reads)	1	3.12	0.01	**0.01**	NA	NA	NA	NA
Sequencing run	1	1.72	0.00	0.12	1	1.65	0.00	0.13
Experimental block	1	3.24	0.01	**0.01**	1	2.82	0.01	**0.01**
T X S	29	1.47	0.08	**<0.001**	29	1.42	0.08	**0.02**
Error	207		0.38		207		0.40	
Total	269		1.00		269		1.00	

	Rhizosphere				**Rhizosphere**			
	DF	*Psuedo-F*	R^2	*P*	*DF*	*Psuedo-F*	R^2	*P*
Treatment (T)	1	24.43	0.08	**<0.001**	1	18.95	0.06	**<0.001**
Species (S)	29	1.90	0.17	**<0.001**	29	1.70	0.16	**<0.001**
log(usable reads)	1	16.84	0.05	**<0.001**	NA	NA	NA	NA
Sequencing run	1	1.47	0.00	0.12	1	1.78	0.01	**0.05**
Experimental block	1	2.43	0.01	**0.02**	1	2.16	0.01	**0.02**
T X S	29	1.04	0.09	0.34	29	1.00	0.10	0.50
Error	190		0.59		190		0.63	
Total	252		1.00		252		1.00	

Table S6 | Estimates of phylogenetic signal. We estimated phylogenetic signal (Blomberg's K* and Pagel's λ) for each of our measures of alpha diversity while accounting for variation occurring among individuals within a host plant species (as per 30).

	Proportional abundance normalization		Rarefied	
	Endosphere			
	*K**	*P*	*K**	*P*
Observed species richness	1.00	**0.01**	0.89	**0.003**
Simpson's diversity $^{-1}$	1.09	**0.001**	1.14	**0.001**
Evenness	1.28	**0.01**	1.18	**0.001**
	Rhizosphere			
	*K**	*P*	*K**	*P*
Observed species richness	0.84	0.70	0.76	0.56
Simpson's diversity $^{-1}$	0.67	0.94	0.71	0.60
Evenness	0.92	**0.01**	0.79	**0.05**

	Proportional abundance normalization		Rarefied	
	Endosphere			
	λ	*P*	λ	*P*
Observed species richness	0.80	**0.03**	0.76	**0.04**
Simpson's diversity $^{-1}$	1.00	**0.01**	0.98	**0.01**
Evenness	0.67	**0.01**	0.95	**0.01**
	Rhizosphere			
	λ	*P*	λ	*P*
Observed species richness	0.00	0.99	0.05	0.96
Simpson's diversity $^{-1}$	0.00	1.00	0.00	1.00
Evenness	0.25	0.27	0.29	0.82

Table S7 | Mantel test results presenting the relationship between host phylogenetic or phenotypic distance on root microbial community dissimilarity. Overall dissimilarity uses plant species' centroids calculated from both well-watered and dry treatments combined. We also present the correlation between endosphere and rhizosphere compartments and the correlation between distance matrices produced from either the proportional-abundance normalized dataset or the rarefied dataset.

Mantel tests		Proportional abundance normalization		Rarefied	
Matrix 1	**Matrix 2**	r_{Mantel}	*P*	r_{Mantel}	*P*
Patristic distance	Overall endosphere dissimilarity	0.15	**0.004**	0.14	**0.01**
Patristic distance	Overall rhizosphere dissimilarity	0.05	0.15	0.05	0.17
Phenotypic distance	Overall endosphere dissimilarity	0.22	0.09	0.22	0.10
Phenotypic distance	Overall rhizosphere dissimilarity	0.00	0.78	0.00	0.83
Patristic distance	Wet endosphere dissimilarity	0.18	**0.001**	0.18	**0.001**
Patristic distance	Dry endosphere dissimilarity	0.10	**0.02**	0.10	**0.02**
Patristic distance	Wet rhizosphere dissimilarity	0.04	0.20	0.04	0.16
Patristic distance	Dry rhizosphere dissimilarity	0.03	0.27	0.03	0.25
Phenotypic distance	Wet endosphere dissimilarity	0.27	**0.04**	0.26	0.06
Phenotypic distance	Dry endosphere dissimilarity	0.07	0.22	0.07	0.25
Phenotypic distance	Wet rhizosphere dissimilarity	0.09	0.23	0.00	0.58
Phenotypic distance	Dry rhizosphere dissimilarity	0.00	0.94	0.00	0.74
Endosphere dissimilarity	Rhizosphere dissimilarity	0.26	**0.04**	0.26	**0.04**
Endosphere dissimilarity (prop.abund.norm)	Endosphere dissimilarity (rarefied)	0.99	**<0.001**		
Rhizosphere dissimilarity (prop.abund.norm)	Rhizosphere dissimilarity (rarefied)	0.98	**<0.001**		

Table S8 | Results from phylogenetic generalized least squares regression to determine the relationship between plant traits and the diversity and composition of root microbial communities. Our measure of composition was the host plant species' centroid of our PCoA using weighted UniFrac distances. First, we determined whether the data fit an error model represented by a Brownian motion, Ornstein-Uhlenbeck, or a non-phylogenetic model of evolution, which assumes a star phylogeny and is equivalent to an ordinary least-squares regression with uncorrelated residuals among species. We present the coefficients associated with each standardized trait and associated *P* values (adjusted for multiple comparisons using the false discovery rate).

	Endosphere				**Rhizosphere**			
	PCoA 1		PCoA 2		PCoA 1		PCoA 2	
Error model	Brownian motion		Brownian motion		Star-phylogeny		Brownian motion	
	Coefficient	*P*	Coefficient	*P*	Coefficient	*P*	Coefficient	*P*
Aboveground biomass	-0.0141	0.77	0.0045	0.92	-0.0309	**<0.01**	-0.0002	1.00
Belowground biomass	0.0175	0.56	-0.0321	0.23	0.0120	0.36	-0.0011	0.98
Root angle	-0.0422	**<0.01**	0.0017	0.96	-0.0007	0.96	0.0025	0.96
Root hair density	-0.0004	0.98	-0.0269	0.09	0.0052	0.89	0.0017	0.98
Root length	0.0028	0.93	0.0344	**0.03**	0.0007	0.93	0.0016	0.93
Specific leaf area	-0.0420	**0.02**	0.0003	0.98	-0.0002	0.98	0.0023	0.98
Specific root length	-0.0016	0.98	0.0273	**0.01**	-0.0002	0.98	0.0167	**0.01**
log(usable reads)	0.0042	0.82	0.0491	**0.02**	0.0193	0.18	-0.0017	0.82
% Water content	0.0341	**0.04**	0.0000	1.00	-0.0104	0.31	-0.0247	**<0.01**

	Obs. species richness		Shannon's diversity		Obs. species richness		Shannon's diversity	
Error model	Brownian motion		Brownian motion		Star-phylogeny		Brownian motion	
	Coefficient	*P*	Coefficient	*P*	Coefficient	*P*	Coefficient	*P*
Aboveground biomass	2.2507	0.94	-0.0136	0.94	32.1234	**0.01**	0.0247	0.88
Belowground biomass	2.8930	0.98	0.1182	0.69	0.9547	0.98	0.0824	0.42
Root angle	30.1515	**<0.01**	-0.0056	0.96	1.3691	0.96	-0.0933	0.07
Root hair density	23.8490	0.16	0.2696	**0.05**	-18.3135	0.21	0.0013	0.98
Root length	-1.4885	0.93	-0.1263	0.68	-24.0445	0.12	-0.1422	**0.03**
Specific leaf area	5.0408	0.98	0.0082	0.98	32.6105	**0.02**	-0.0050	0.98
Specific root length	-14.8195	0.13	-0.1167	0.26	-0.3299	0.98	0.0141	0.98
log(usable reads)	122.3806	**<0.01**	0.0455	0.82	297.9989	**<0.01**	0.5066	**<0.01**
% Water content	-21.5013	0.08	-0.0219	0.87	0.0700	1.00	0.0134	0.87

	Simpson's diversity $^{-1}$		Evenness		Simpson's diversity $^{-1}$		Evenness	
Error model	Brownian motion		Star-phylogeny		Brownian motion		Brownian motion	
	Coefficient	*P*	Coefficient	*P*	Coefficient	*P*	Coefficient	*P*
Aboveground biomass	0.0003	1.00	0.0129	0.65	25.4363	**0.01**	0.0410	**<0.01**
Belowground biomass	0.0101	0.99	-0.0200	0.36	32.1203	0.12	0.0015	0.98
Root angle	-0.0366	0.96	0.0003	0.96	-22.5845	0.06	-0.0209	0.12
Root hair density	7.6386	**0.05**	0.0003	0.98	-0.1175	0.98	-0.0012	0.98
Root length	0.0061	0.99	-0.0019	0.93	-53.1478	**<0.01**	-0.0235	**0.03**
Specific leaf area	0.0165	0.98	0.0003	0.98	-4.1414	0.98	-0.0071	0.98
Specific root length	-0.5562	0.98	0.0001	0.98	0.4056	0.98	0.0171	**0.04**
log(usable reads)	0.8821	0.82	-0.0995	**<0.01**	69.2019	**<0.01**	-0.0540	**0.02**
% Water content	-1.2284	0.85	0.0009	0.98	18.3917	**0.03**	0.0051	0.85

Table S9 | Common bacterial families across compartment and treatment

The 30 most common bacterial families in each compartment and treatment combination. Toothpick communities are denoted by T.

Soil (well-watered)		Soil (drought)	
Taxon	Relative abundance	Taxon	Relative abundance
Sphingomonadaceae	0.059	Comamonadaceae	0.078
Gaiellaceae	0.054	Gaiellaceae	0.066
Hyphomicrobiaceae	0.050	Xanthomonadaceae	0.050
Gemmatimonadaceae	0.046	Hyphomicrobiaceae	0.050
Planctomycetaceae	0.041	Sphingomonadaceae	0.042
Chitinophagaceae	0.037	Gemmatimonadaceae	0.042
Comamonadaceae	0.037	Planctomycetaceae	0.038
Polyangiaceae	0.035	Erythrobacteraceae	0.032
Bradyrhizobiaceae	0.034	Rhodospirillaceae	0.031
Xanthomonadaceae	0.032	Chitinophagaceae	0.031
Rhodocyclaceae	0.032	Caulobacteraceae	0.029
Sinobacteraceae	0.031	Bradyrhizobiaceae	0.027
Geobacteraceae	0.030	Solirubrobacteraceae	0.027
Rhodospirillaceae	0.030	Rhodocyclaceae	0.027
Erythrobacteraceae	0.026	Sinobacteraceae	0.024
Anaerolineaceae	0.025	Acidimicrobiaceae	0.024
Caulobacteraceae	0.023	Polyangiaceae	0.023
Rhodobacteraceae	0.022	Micromonosporaceae	0.017
Acidimicrobiaceae	0.017	Rhodobacteraceae	0.017
Conexibacteraceae	0.016	Burkholderiaceae	0.015
Opitutaceae	0.016	Mycobacteriaceae	0.014
Solirubrobacteraceae	0.015	Anaerolineaceae	0.014
Xanthobacteraceae	0.013	Opitutaceae	0.014
Mycobacteriaceae	0.013	Rhizobiaceae	0.013
Micromonosporaceae	0.013	Conexibacteraceae	0.013
Cystobacteraceae	0.012	Xanthobacteraceae	0.012
Thermomonosporaceae	0.010	Geobacteraceae	0.012
Burkholderiaceae	0.009	Oxalobacteraceae	0.011
Pseudomonadaceae	0.009	Cytophagaceae	0.011
Rhizomicrobium	0.009	Geodermatophilaceae	0.010

Table S9 Continued.

Rhizosphere (well-watered)		Rhizosphere (drought)		Rhizosphere T (well-watered)		Rhizosphere T (drought)	
Taxon	Relative abundance	Taxon	Relative abundance	Taxon	Relative abundance	Taxon	Relative abundance
Comamonadaceae	0.095	Xanthomonadaceae	0.089	Sphingomonadaceae	0.082	Sphingomonadaceae	0.099
Sphingomonadaceae	0.058	Comamonadaceae	0.084	Rhodospirillaceae	0.079	Erythrobacteraceae	0.075
Rhodocyclaceae	0.045	Sphingomonadaceae	0.069	Erythrobacteraceae	0.070	Sinobacteraceae	0.061
Xanthomonadaceae	0.042	Chitinophagaceae	0.050	Comamonadaceae	0.060	Comamonadaceae	0.052
Hyphomicrobiaceae	0.041	Caulobacteraceae	0.048	Rhodocyclaceae	0.052	Chitinophagaceae	0.052
Rhodospirillaceae	0.041	Hyphomicrobiaceae	0.033	Sinobacteraceae	0.040	Xanthomonadaceae	0.048
Chitinophagaceae	0.038	Burkholderiaceae	0.032	Desulfobulbaceae	0.036	Rhodospirillaceae	0.047
Polyangiaceae	0.034	Rhodospirillaceae	0.032	Ruminococcaceae	0.028	Polyangiaceae	0.043
Caulobacteraceae	0.033	Polyangiaceae	0.028	Polyangiaceae	0.028	Hyphomicrobiaceae	0.042
Planctomycetaceae	0.030	Rhizobiaceae	0.028	Geobacteraceae	0.028	Planctomycetaceae	0.040
Opitutaceae	0.029	Cytophagaceae	0.027	Hyphomicrobiaceae	0.027	Gemmatimonadaceae	0.031
Gaiellaceae	0.028	Bradyrhizobiaceae	0.022	Planctomycetaceae	0.027	Caulobacteraceae	0.030
Geobacteraceae	0.027	Sinobacteraceae	0.020	Caulobacteraceae	0.026	Rhodocyclaceae	0.029
Sinobacteraceae	0.026	Planctomycetaceae	0.020	Anaerolineaceae	0.025	Bradyrhizobiaceae	0.028
Bradyrhizobiaceae	0.026	Oxalobacteraceae	0.020	Chitinophagaceae	0.023	Pseudomonadaceae	0.020
Gemmatimonadaceae	0.023	Rhodocyclaceae	0.020	Xanthomonadaceae	0.022	Rhizobiales incertae sedis	0.012
Rhizobiaceae	0.018	Opitutaceae	0.019	Bradyrhizobiaceae	0.021	Xanthobacteraceae	0.012
Rhodobacteraceae	0.016	Erythrobacteraceae	0.018	Rhodobacteraceae	0.020	Phyllobacteriaceae	0.012
Burkholderiaceae	0.016	Gaiellaceae	0.017	Gemmatimonadaceae	0.019	Gaiellaceae	0.012
Erythrobacteraceae	0.014	Enterobacteriaceae	0.016	GpI	0.018	Opitutaceae	0.012
Anaerolineaceae	0.013	Gemmatimonadaceae	0.016	Pseudomonadaceae	0.016	Rhizobiaceae	0.011
Bdellovibrionaceae	0.013	Pseudomonadaceae	0.015	Opitutaceae	0.015	Burkholderiales incertae sedis	0.010
Cytophagaceae	0.012	Streptomycetaceae	0.013	Cystobacteraceae	0.015	Burkholderiaceae	0.010
Solirubrobacteraceae	0.012	Bdellovibrionaceae	0.012	Ignavibacteriaceae	0.012	Haliangiaceae	0.010
Pseudomonadaceae	0.011	Rhodobacteraceae	0.011	Desulfovibrionaceae	0.011	Acetobacteraceae	0.009
Mycobacteriaceae	0.010	Nocardioidaceae	0.011	Neisseriaceae	0.010	Mycobacteriaceae	0.008
Acidimicrobiaceae	0.010	Geobacteraceae	0.011	Rhizobiaceae	0.010	Methylophilaceae	0.007
Conexibacteraceae	0.010	Burkholderiales incertae sedis	0.010	Acetobacteraceae	0.009	Alteromonadaceae	0.007
Xanthobacteraceae	0.009	Phyllobacteriaceae	0.010	Veillonellaceae	0.008	Anaerolineaceae	0.007
Phyllobacteriaceae	0.009	Micromonosporaceae	0.009	Burkholderiales incertae sedis	0.008	Cytophagaceae	0.007

Table S9 Continued.

Endosphere (well-watered)		Endosphere (drought)		Endosphere T (well-watered)		Endosphere T (drought)	
Taxon	Relative abundance	Taxon	Relative abundance	Taxon	Relative abundance	Taxon	Relative abundance
Rhizobiaceae	0.141	Streptomycetaceae	0.244	Cystobacteraceae	0.154	Sinobacteraceae	0.141
Comamonadaceae	0.125	Rhizobiaceae	0.109	Cellulomonadaceae	0.070	Rhizobiaceae	0.103
Streptomycetaceae	0.070	Phyllobacteriaceae	0.101	Rhodocyclaceae	0.067	Hyphomicrobiaceae	0.094
Bradyrhizobiaceae	0.064	Chitinophagaceae	0.079	Comamonadaceae	0.059	Bradyrhizobiaceae	0.094
Phyllobacteriaceae	0.055	Comamonadaceae	0.058	Rhizobiaceae	0.055	Chitinophagaceae	0.088
Chitinophagaceae	0.055	Micromonosporaceae	0.039	Bradyrhizobiaceae	0.048	Comamonadaceae	0.084
Opitutaceae	0.049	Sinobacteraceae	0.036	Rhodospirillaceae	0.047	Caulobacteraceae	0.046
Rhodospirillaceae	0.044	Xanthomonadaceae	0.029	Caulobacteraceae	0.042	Xanthomonadaceae	0.041
Sinobacteraceae	0.040	Caulobacteraceae	0.023	Opitutaceae	0.039	Burkholderiaceae	0.039
Micromonosporaceae	0.035	Bradyrhizobiaceae	0.019	Ruminococcaceae	0.035	Sphingomonadaceae	0.033
Rhodocyclaceae	0.035	Opitutaceae	0.019	Desulfovibrionaceae	0.032	Rhodospirillaceae	0.023
Polyangiaceae	0.021	Sphingomonadaceae	0.017	Hyphomicrobiaceae	0.030	Polyangiaceae	0.020
Xanthomonadaceae	0.021	Pseudonocardiaceae	0.016	Sphingomonadaceae	0.026	Streptomycetaceae	0.018
Caulobacteraceae	0.020	Nocardioidaceae	0.015	Desulfobulbaceae	0.023	Planctomycetaceae	0.013
Sphingomonadaceae	0.019	Polyangiaceae	0.014	Sinobacteraceae	0.021	Erythrobacteraceae	0.013
Hyphomicrobiaceae	0.017	Hyphomicrobiaceae	0.012	Chitinophagaceae	0.020	Pseudomonadaceae	0.012
Planctomycetaceae	0.017	Burkholderiaceae	0.011	Burkholderiaceae	0.018	Micromonosporaceae	0.012
Enterobacteriaceae	0.014	Planctomycetaceae	0.009	Spirochaetaceae	0.017	Rhodocyclaceae	0.012
Burkholderiales incertae sedis	0.011	Cytophagaceae	0.009	Polyangiaceae	0.016	Cellulomonadaceae	0.010
Spirochaetaceae	0.009	Oxalobacteraceae	0.009	Anaerolineaceae	0.015	Oxalobacteraceae	0.010
Haliangiaceae	0.009	Rhodospirillaceae	0.009	Xanthomonadaceae	0.014	Haliangiaceae	0.010
Methylophilaceae	0.008	Burkholderiales incertae sedis	0.007	Oxalobacteraceae	0.014	Streptosporangiaceae	0.009
Pseudomonadaceae	0.008	Haliangiaceae	0.007	Erythrobacteraceae	0.012	Opitutaceae	0.008
Bdellovibrionaceae	0.007	Microbacteriaceae	0.005	Ignavibacteriaceae	0.011	Xanthobacteraceae	0.007
Cytophagaceae	0.007	Clostridiaceae 1	0.005	Veillonellaceae	0.010	Cytophagaceae	0.004
Burkholderiaceae	0.007	Rhodocyclaceae	0.005	Planctomycetaceae	0.009	Anaerolineaceae	0.004
Oxalobacteraceae	0.007	Conexibacteraceae	0.005	Haliangiaceae	0.009	Acetobacteraceae	0.003
Microbacteriaceae	0.005	Pseudomonadaceae	0.005	Pseudomonadaceae	0.009	Rhizobiales incertae sedis	0.003
Leptospiraceae	0.005	Thermomonosporaceae	0.005	Micromonosporaceae	0.006	Microbacteriaceae	0.003
Acidimicrobiaceae	0.005	Kofleriaceae	0.004	Enterobacteriaceae	0.005	Enterobacteriaceae	0.003

Dataset S1 | Bacterial taxa in the endosphere and rhizosphere found in all host plant species. Full-length V4 sequences and taxonomy associated with the ASVs found with all host plant species in the endosphere or rhizosphere. The prevalence column indicates how many individuals within each host plant species a particular bacterial ASV was found. For example "N ≥ 2 ind./host sp." indicates that the given bacterial ASV was found in at least two individuals of every host plant species. Red-shaded ASVs are core taxa found in both the endosphere and rhizosphere.

Dataset S2 | Bacterial taxa significantly associated with plant-soil feedback. Significant correlations between taxon $\log_2$ fold changes among focal and soil-conditioning host plant species and experimentally measured soil feedback. Positive correlations (blue-shaded rows), indicate that for the given bacterial taxon, focal species exhibit poor performance when abundance is greater in soil-conditioning versus focal plant species but exhibit increased performance when abundance is greater in focal versus soil-conditioning plant species. Negative correlations (unshaded rows) indicate that for the given bacterial taxon, focal species exhibit increased performance when the abundance is greater in soil-conditioning versus focal plant species but exhibit reduced performance when abundance is greater in focal versus soil-conditioning plant species. We used the false discovery rate to correct for multiple hypothesis testing. The prevalence column indicates whether or not a given ASV was found in every host plant species ("NA" indicates that the ASV was not found in all host plants; "N ≥ 1 ind./host sp." indicates that the ASV was found in at least oneindividual in every host plant). Shaded ASVs (orange, green, and purple) correspond to taxa found to be important in drought tolerance (see Dataset S4).

Dataset S3 | Drought-responsive taxa in the live root endosphere and root analogue endosphere. Endosphere bacterial taxa exhibiting significant $\log_2$ fold changes between watering treatments in living plant roots and in root anlogues.

Dataset S4 | Correlations between bacterial taxon enrichment and drought tolerance. Bacterial taxa whose $\log_2$ fold changes between watering treatments is significantly related to host plant species drought tolerance. Positive correlations indicate taxa whose enrichment was associated with increasing host plant drought tolerance, while negative estimates indicate taxa whose enrichment was associated with decreasing host plant drought tolerance. We used the false discovery rate to correct for multiple hypothesis testing. The prevalence column indicates whether a given ASV was found in every host plant species. Shaded ASVs (orange, green, and purple) correspond to taxa found to be important in plant-soil feedback (see Dataset S2).